arXiv:1510.02057v2 [math.PR] 30 Nov 2015

The Cusp-Airy Process

Erik Duse * Kurt Johansson † Anthony Metcalfe

December 1, 2015

Abstract

At a typical cusp point of the disordered region in a random tiling model we expect to see a determinantal process called the Pearcey process in the appropriate scaling limit. However, in certain situations another limiting point process appears that we call the Cusp-Airy process, which is a kind of two sided extension of the Airy kernel point process. We will study this problem in a class of random lozenge tiling models coming from interlacing particle systems. The situation was briefly studied previously by Okounkov and Reshetikhin under the name cuspidal turning point.

Contents

1 Introduction and Results **2**
1.1 The Cusp-Airy kernel . . . 2
1.2 Random Lozenge Tiling Model . . . 4
1.3 Interlacing Model . . . 6
1.4 Asymptotic Geometry of Discrete Interlaced Patterns . . . 7
1.5 Conditions for Cusps . . . 10
1.6 Rescaled Variables . . . 11
1.7 Integrand . . . 14
1.8 Main Theorem . . . 16
1.9 Random Top Line Measure . . . 18
1.10 Outline of the Paper . . . 24

2 Proof of Main Result **24**
2.1 Discrete Cancellation in the Correlation Kernel . . . 24
2.2 Change of Integration Contours . . . 25
2.3 Global Choice of Contours . . . 30
2.4 Estimates and localization . . . 33
2.5 Local Analysis . . . 37

3 Representations and Properties of The Cusp-Airy Kernel **40**
3.1 Symmetry Property of The Cusp-Airy Kernel . . . 40
3.2 Representation of The Cusp-Airy Kernel . . . 42

4 Derivation of the Correlation Kernel **45**
4.1 Integral Representation of the Correlation Kernel for the Yellow Particles . . . 45
4.2 Particle Transformation . . . 47

5 Appendix. Determinantal Point Processes **48**

*Supported the grant KAW 2010.0063 from the Knut and Alice Wallenberg Foundation
†Supported the grant KAW 2010.0063 from the Knut and Alice Wallenberg Foundation

1 Introduction and Results

1.1 The Cusp-Airy kernel

In this paper we will study random discrete interlacing particle systems which can also be interpreted as certain random lozenge tiling models. The particles, or lozenges, form a random point process which is determinantal. We are particularly interested in the limiting point process around the type of cusp point we see in the arctic curve in figure 1, see figure 1 in [16] or [17] for a simulation. Figure 1 illustrates the *liquid region* $\mathcal{L}$ and its boundary $\mathcal{E}$, the *arctic curve*. Inside the liquid region one expects to see the *extended sine-kernel* point process in the limit. At the tangency points of the polygon and the boundary $\mathcal{E}$ one expects to see the *GUE-corner* process. At all other points of the curve $\mathcal{E}$, except the cusp, one expects either the *Airy kernel* or *Id-Airy kernel* point processes in the appropriate scaling limit.

To clarify the situation around the cusp point consider figure 2. All possible tiling configurations of the polygon can be encoded by the red rhombi. This is illustrated in figure 3, where we see that the positions of the red rhombi form two interlacing regions that meet at the dashed line. The rhombi at the common line have been coloured in purple. The purple rhombi form a *discrete orthogonal polynomial ensemble*, DOPE, see Remark 1.5. The dashed line is also a symmetry line (coloured blue in figure 2). The fact that we have two symmetric interlacing systems meeting at common line, will imply that the frozen boundary has a reflection symmetry in the symmetry line. It will also imply that the particle system consisting of red rhombi will have no horizontal oscillations. Therefore, when considering a scaling limit at the cusp on the symmetry line of this determinantal point process, the correct scaling is discrete in the horizontal direction and continuous of size $n^{1/3}$ in the vertical direction, where n is the size of the hexagon. Going back to figure 2, we see that directly above the tip of the cusp the blue and yellow rhombi form a corner. This implies that the height function in [17] will have a jump above the tip of the cusp. This should be contrasted to the situation where one expects to find a Pearcey process in the scaling limit around a cusp point of the arctic curve. Then one has only one type of rhombi in the frozen configuration inside the cusp. This also implies that the height function is flat inside the cusp.

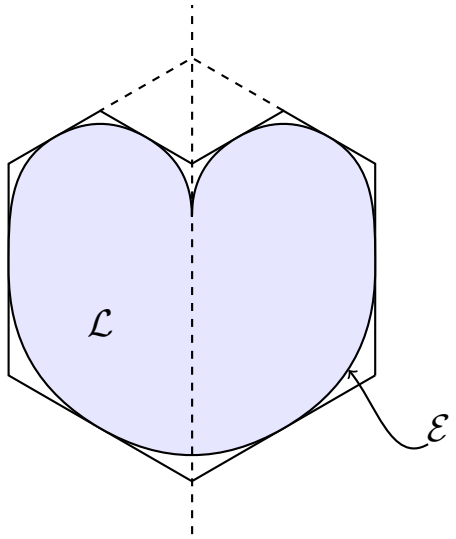

Figure 1: The *liquid region* $\mathcal{L}$ is coloured in blue. Its boundary is $\mathcal{E}$.

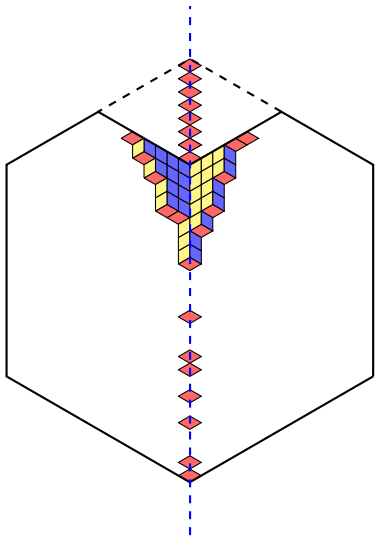

Figure 2:

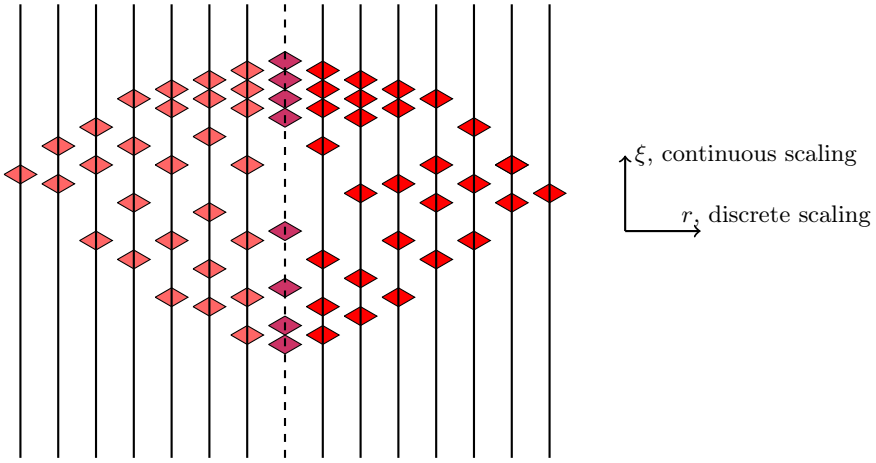

Figure 3:

At the cusp, in an appropriate scaling limit, we will see that the correlation kernel for the determinantal point process given by the red rhombi converges to a process with a kernel that we call the *Cusp-Airy kernel*. We will show this for the model corresponding to figure 1 up to certain natural technical conditions for a particular DOPE. In a simpler model of the type studied by Petrov in [20] we will give the full proof. This type of cusp situation in a random lozenge tiling model was discovered and discussed briefly by Okounkov and Reshetikhin in [18] who called it a *Cuspidal turning point*. The interpretation of their formula is however not completely clear, see remark 1.1 below.

Let us give the expression for the Cusp-Airy kernel.

Definition 1.1. For $r, s \in \mathbb{Z}$ and $\xi, \tau \in \mathbb{R}$ we define the *Cusp-Airy kernel* by

$$\mathcal{K}_{CA}((\xi, r), (\tau, s)) = -1_{\tau \geqslant \xi} 1_{s>r} \frac{(\tau - \xi)^{s-r-1}}{(s-r-1)!} + \frac{1}{(2\pi i)^2} \int_{\mathscr{L}_L + \mathscr{C}_{out}} dz \int_{\mathscr{L}_R + \mathscr{C}_{in}} dw \frac{1}{w - z} \frac{w^r}{z^s} e^{\frac{1}{3}w^3 - \frac{1}{3}z^3 - \xi w + \tau z}, \tag{1.1}$$

where the contours are defined in figure 4, and $1_{a<b}$ is the indicator function for $a < b$.

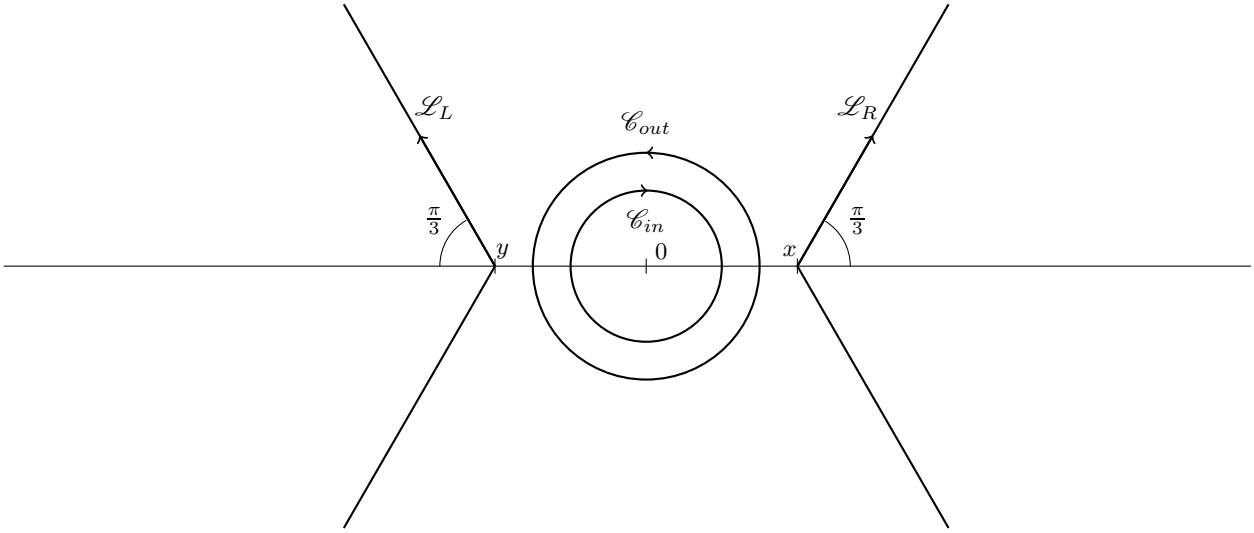

Figure 4: Integration contours for the Cusp-Airy kernel.

In section 3.2 we give a different formula for the kernel in terms of r-Airy integrals and some polynomials. When $r = s = 0$ we see that we get the Airy kernel. Hence, we expect the last red particle on the line $r = 0$ to have Tracy-Widom fluctuations. In the case $r = s \neq 0$ we interestingly get the *r-Airy kernel*, which has appeared in previous work, see [1] and [3].

Remark 1.1. In [18], Okounkov and Reshetikhin give a formula, without proof, for the correlation kernel in the appropriate scaling limit around the type of cusp point studied in the present paper, but in a different model. The definition of the kernel in [18] is somewhat formal due to the fact that the factor $\frac{1}{w-z}\frac{w^r}{z^s}$ in formula (1.1) above is interpreted via a "time-ordered expansion", see (13) in [18]. However, for the contours used in their formula (18) these expansions are not convergent. Similarly, in our formula (1.1) above we can not expand $\frac{1}{w-z}$ in a power series when $z \in \mathscr{L}_L$ and $w \in \mathscr{L}_R$. In this case it seems more natural to rewrite $\frac{1}{w-z}$ in a different way, see (3.9) in section 3.2 and compare with the formulas derived there, see Proposition 3.2.

1.2 Random Lozenge Tiling Model

Consider three different types of *lozenges* (rhombi with angles $\frac{\pi}{3}$ and $\frac{2\pi}{3}$) with sides of length 1. We label these as types Y, B, and R as shown in figure 5.

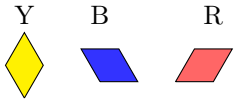

Figure 5: Three types of lozenges with sides of length 1.

Consider a 'half-hexagon' as shown in figure 6.

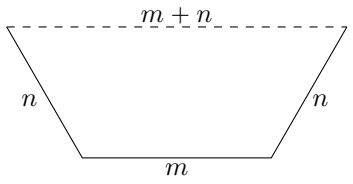

Figure 6: A 'half-hexagon' of height n and width $n + m$.

Suppose that we place n lozenge tiles of type Y on the top line of the 'half-hexagon' according to figure 7.

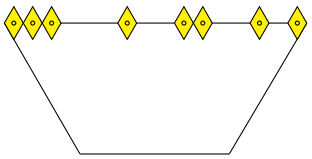

Figure 7: n tiles of type Y on the top line of the half-hexagon

Fix this configuration of n tiles of type Y on the top line, at say positions $\beta_1^{(n)}, \beta_2^{(n)}, ..., \beta_n^{(n)}$, and consider all possible tessellations of the 'half-hexagon' with uniform probability distribution. A possible such tessellation is shown in figure 8.

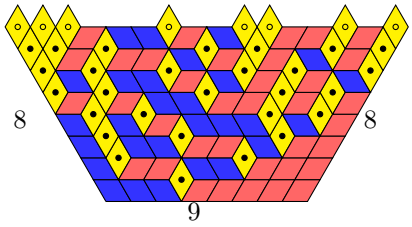

Figure 8: An example of a tiling and its equivalent interlaced particle configuration when $n = 8$ and $m = 9$. The unfilled circles represent the deterministic lozenges/particles.

By considering the positions of the yellow tiles, such a tessellation can be encoded as an interlaced particle system. More precisely, let $y_i^{(r)}$ denote the position of the i:th particle on the r:th row. Then the particles on row $r + 1$ will interlace with the particles on row r according to

$$y_1^{(r+1)} > y_1^{(r)} > y_2^{(r+1)} > y_2^{(r)} ... > y_r^{(r)} > y_{r+1}^{(r+1)},$$

for every $r = 1, ..., n - 1$, where $y_i^{(n)} = \beta_i^{(n)}$. It will be convenient to make a coordinate transformation according to figure 9. For more details see section 1.4 in [8] and section 2.1 in [20] .

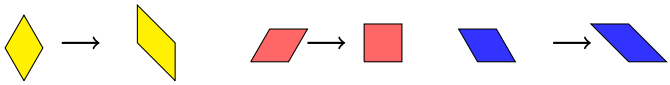

Figure 9: Coordinate transformation of lozenge tiles.

After the coordinate transformation, figure 8 becomes figure 10. Furthermore the interlacing condition between row $r + 1$ and row r has changed into

$$y_1^{(r+1)} \geqslant y_1^{(r)} > y_2^{(r+1)} \geqslant y_2^{(r)} ... \geqslant y_r^{(r)} > y_{r+1}^{(r+1)}.$$

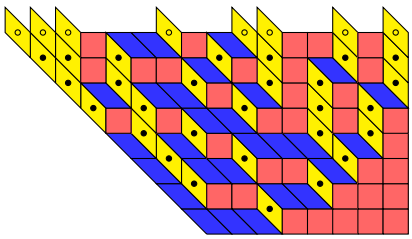

Figure 10: An example tiling and its equivalent interlaced particle configuration after the coordinate transformation. The unfilled circles represent the deterministic lozenges/particles.

1.3 Interlacing Model

We begin by briefly recalling the underlying probabilistic model described in [8]. A *discrete Gelfand-Tsetlin pattern* of depth n is an n-tuple, denoted $(y^{(1)}, y^{(2)}, \dots, y^{(n)}) \in \mathbb{Z} \times \mathbb{Z}^2 \times \cdots \times \mathbb{Z}^n$, which satisfies the interlacing constraint

$$y_1^{(r+1)} \geqslant y_1^{(r)} > y_2^{(r+1)} \geqslant y_2^{(r)} > \cdots \geqslant y_r^{(r)} > y_{r+1}^{(r+1)},$$

denoted $y^{(r+1)} \succ y^{(r)}$, for all $r \in \{1, \dots, n-1\}$. For each $n \geqslant 1$, fix $\beta^{(n)} \in \mathbb{Z}^n$ with $\beta_1^{(n)} > \beta_2^{(n)} > \cdots > \beta_n^{(n)}$, and consider the following probability measure on the set of patterns of depth n:

$$q_n(y^{(1)}, \dots, y^{(n)}) := \frac{1}{Z_n} \cdot \begin{cases} 1 & ; \quad \text{when } \beta^{(n)} = y^{(n)} \succ y^{(n-1)} \succ \cdots \succ y^{(1)}, \\ 0 & ; \quad \text{otherwise,} \end{cases}$$

where $Z_n > 0$ is a normalisation constant. This can equivalently be considered as a measure on configurations of interlaced particles in $\mathbb{Z} \times \{1, \dots, n\}$ by placing a particle at position $(x, r) \in \mathbb{Z} \times \{1, \dots, n\}$ whenever x is an element of $y^{(r)}$. The measure q_n is then the uniform probability measure on the set of all such interlaced configurations with the particles on the top row in the deterministic positions defined by $\beta^{(n)}$. This measure also arises naturally from tiling models as was indicated above. In [8] and [20] it was shown that this process is determinantal. Note that the fixed top row and the interlacing constraint implies that it is sufficient to restrict to those positions, $(x_1, y_1), (x_2, y_2) \in \mathbb{Z} \times \{1, \dots, n-1\}$, with $x_1 \geqslant \beta_n^{(n)} + n - y_1$ and $x_2 \geqslant \beta_n^{(n)} + n - y_2$. For all such (x_1, y_1) and (x_2, y_2), we give an integral representation of the correlation kernel $K_n((x_1, y_1), (x_2, y_2))$ in section 4.1.

In terms of tiling models, $K_n((x_1, y_1)(x_2, y_2))$ is equal to a correlation kernel for the yellow particles $K_{\mathcal{Y}}^{(n)}((x_1, y_1), (x_2, y_2))$. However at the cusp one should not consider the correlation kernel of the yellow particles, but the correlation kernel of the red particles instead. The correlation kernels of the different particle species are related according to Lemma 4.1 below, which we will prove in sec. 4.2.

Proposition 1.1. *The red tiles (particles) form a determinantal point process with correlation kernel*

$$K_{\mathcal{R}}^{(n)}((x_1, y_1), (x_2, y_2)) = -1_{x_1 < x_2} \frac{1}{(2\pi i)^2} \oint_{\mathscr{Z}_n} dz \oint_{\mathscr{W}_n} dw \frac{\prod_{k=x_2+y_2-n}^{x_2-1}(z-k)}{\prod_{k=x_1+y_1-n}^{x_1}(w-k)} \frac{1}{w-z} \prod_{i=1}^{n} \left(\frac{w - \beta_i^{(n)}}{z - \beta_i^{(n)}} \right) \tag{1.2}$$

$$+ 1_{x_1 \geqslant x_2} \frac{1}{(2\pi i)^2} \oint_{\mathscr{Z}_n'} dz \oint_{\mathscr{W}_n} dw \frac{\prod_{k=x_2+y_2-n}^{x_2-1}(z-k)}{\prod_{k=x_1+y_1-n}^{x_1}(w-k)} \frac{1}{w-z} \prod_{i=1}^{n} \left(\frac{w - \beta_i^{(n)}}{z - \beta_i^{(n)}} \right),$$

where $\mathscr{Z}_n$ is a counterclockwise oriented contour containing $\{\beta_j^{(n)} : \beta_j^{(n)} \geqslant x_2\}$ but not the set $\{\beta_j^{(n)} \leqslant x_2 - 1\}$, and $\mathscr{Z}_n'$ is a counterclockwise oriented contour containing $\{\beta_j^{(n)} : \beta_j^{(n)} < x_2\}$ but not the set $\{\beta_j^{(n)} \geqslant x_2 + 1\}$. In addition, $\mathscr{W}_n$ contains the set $\{x_1 + y_1 - n, ..., x_1\}$ and $\mathscr{Z}_n$ or $\mathscr{Z}_n'$. The integration contours are shown in figure 11. Here $A_n = \min_j\{\beta_j^{(n)} : j = 1, ..., n\}$ and $B_n = \max_j\{\beta_j^{(n)} : j = 1, ..., n\}$.

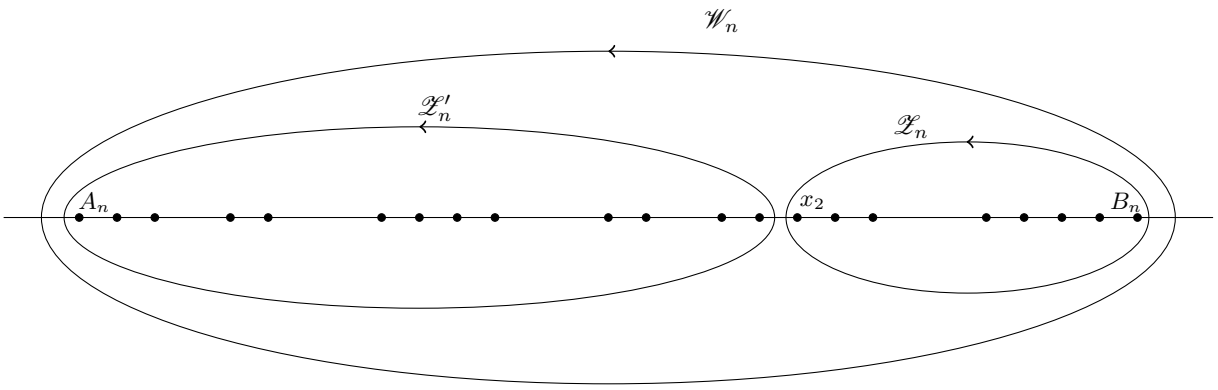

Figure 11: Integration contours

1.4 Asymptotic Geometry of Discrete Interlaced Patterns

It is natural to consider the asymptotic behaviour of the determinantal process introduced in the previous section as $n \to \infty$, under the assumption that the (rescaled) empirical distribution of the fixed particles on the top row converges weakly to a measure with compact support. More exactly:

Assumption 1. Assume that

$$\mu_n := \frac{1}{n}\sum_{i=1}^{n} \delta_{\beta_i^{(n)}/n} \rightharpoonup \mu$$

as $n \to \infty$, in the sense of weak convergence of measures, where μ is a positive Borel measure on $\mathbb{R}$.

We see that $\mu \leqslant \lambda$ where λ is Lebesgue measure (recall $\beta^{(n)} \in \mathbb{Z}^n$), $\|\mu\| = 1$, μ has compact support, and $b - a > 1$ where $[a, b]$ is the convex hull of $\mathrm{supp}(\mu)$. We write $\mu \in \mathcal{M}^{\lambda}_{c,1}(\mathbb{R})$. Additionally we note that μ admits a density w.r.t. λ, which is uniquely defined up to a set of zero Lebesgue measure. Denoting the density by φ, it satisfies $\varphi \in L^{\infty}(\mathbb{R})$, $\varphi(x) = 0$ for all $x \in \mathbb{R}\backslash[a, b]$, and $0 \leqslant \varphi(x) \leqslant 1$ for all $x \in [a, b]$. We write $\varphi \in \rho^{\lambda}_{c,1}(\mathbb{R})$. Note that $\mathbb{R}\backslash\mathrm{supp}(\mu)$ is the largest open set on which $\varphi = 0$ almost everywhere, and $\mathbb{R}\backslash\mathrm{supp}(\lambda - \mu)$ is the largest open set on which $\varphi = 1$ almost everywhere.

Note that, rescaling the vertical and horizontal positions of the particles of the Gelfand-Tsetlin patterns by $\frac{1}{n}$, the above assumption and the interlacing constraint imply that the rescaled particles lie asymptotically in the the following set:

$$\mathcal{P} = \{(\chi, \eta) \in \mathbb{R}^2 : a \leqslant \chi + \eta - 1 \leqslant \chi \leqslant b, 0 \leqslant \eta \leqslant 1\}. \tag{1.3}$$

Fixing $(\chi, \eta) \in \mathcal{P}$, the local asymptotic behaviour of particles near (χ, η) can be examined by considering the asymptotic behaviour of $K_n((x_1^{(n)}, y_1^{(n)}), (x_2^{(n)}, y_2^{(n)}))$ as $n \to \infty$, where $\{(x_1^{(n)}, y_1^{(n)})\}_{n \geqslant 1} \subset \mathbb{Z}^2$ and $\{(x_2^{(n)}, y_2^{(n)})\}_{n \geqslant 1} \subset \mathbb{Z}^2$ satisfy $\frac{1}{n}(x_j^{(n)}, y_j^{(n)}) \to (\chi, \eta)$ as $n \to \infty$, $j = 1, 2$. Assume this asymptotic behaviour, substitute $(x_1^{(n)}, y_1^{(n)})$ and $(x_2^{(n)}, y_2^{(n)})$ into the expression (1.2) for the correlation kernel, and rescale the contours by $\frac{1}{n}$ to get,

$$\begin{aligned} K^{(n)}_{\mathcal{R}}((x_1^{(n)}, y_1^{(n)}), (x_2^{(n)}, y_2^{(n)})) = &-1_{x_1 < x_2} \frac{1}{(2\pi i)^2} \oint_{\frac{1}{n}\mathscr{L}_n} dz \oint_{\frac{1}{n}\mathscr{W}_n} dw \, \frac{\exp(n f_n(w) - n\tilde{f}_n(z))}{w - z} \\ &+ 1_{x_1 \geqslant x_2} \frac{1}{(2\pi i)^2} \oint_{\frac{1}{n}\mathscr{L}'_n} dz \oint_{\frac{1}{n}\mathscr{W}_n} dw \, \frac{\exp(n f_n(w) - n\tilde{f}_n(z))}{w - z}, \end{aligned} \tag{1.4}$$

for all $n \in \mathbb{N}$. Here,

$$f_n(w) := \frac{1}{n}\sum_{i=1}^{n} \log\left(w - \frac{\beta_i^{(n)}}{n}\right) - \frac{1}{n}\sum_{j=x_1^{(n)}+y_1^{(n)}-n}^{x_1^{(n)}} \log\left(w - \frac{j}{n}\right),$$

$$\tilde{f}_n(z) := \frac{1}{n}\sum_{i=1}^{n} \log\left(z - \frac{\beta_i^{(n)}}{n}\right) - \frac{1}{n}\sum_{j=x_2^{(n)}+y_2^{(n)}-n+1}^{x_2^{(n)}-1} \log\left(z - \frac{j}{n}\right).$$

These expressions and assumption 1 leads us to define

$$f(w;\chi,\eta) := \int_{\mathbb{R}} \log(w-t)d\mu(t) - \int_{\chi+\eta-1}^{\chi} \log(w-t)dt, \tag{1.5}$$

for all $w \in \mathbb{C}\backslash\mathbb{R}$. Steepest descent analysis and equation (1.4) suggest that, as $n \to \infty$, the asymptotic behaviour of $K_{\mathcal{R}}^{(n)}((x_1^{(n)}, y_1^{(n)}), (x_2^{(n)}, y_2^{(n)}))$ depends on the behaviour of the roots of

$$f'(w;\chi,\eta) := \frac{df}{dw} = \int_{\mathbb{R}} \frac{d\mu(t)}{w-t} - \int_{\chi+\eta-1}^{\chi} \frac{dt}{w-t}, \tag{1.6}$$

for $w \in \mathbb{C}\backslash\mathbb{R}$. In [8], we define the *liquid region*, $\mathcal{L}$, as the set of all $(\chi,\eta) \in \mathcal{P}$ for which $f'_{(\chi,\eta)}$ has a unique root in the upper-half plane $\mathbb{H} := \{w \in \mathbb{C} : \mathrm{Im}(w) > 0\}$. Whenever $(\chi,\eta) \in \mathcal{L}$, one expects universal bulk asymptotic behaviour, i.e., that the local asymptotic behaviour of the particles near (χ,η) are governed by the *extended discrete sine kernel* as $n \to +\infty$. Also, one expects that the particles are not asymptotically densely packed. Moreover, when considering the corresponding tiling model and its associated height function, one would expect to see the Gaussian Free Field asymptotically. For a special case see [21].

Let $W_{\mathcal{L}} : \mathcal{L} \to \mathbb{H}$ map $(\chi,\eta) \in \mathcal{L}$ to the corresponding unique root of $f'_{(\chi,\eta)}$ in $\mathbb{H}$. In [8], we show that $W_{\mathcal{L}}$ is a homeomorphism with inverse $W_{\mathcal{L}}^{-1}(w) = (\chi_{\mathcal{L}}(w), \eta_{\mathcal{L}}(w))$ for all $w \in \mathbb{H}$, where

$$\chi_{\mathcal{L}}(w) := w + \frac{(w-\bar{w})(e^{C(\bar{w})}-1)}{e^{C(w)}-e^{C(\bar{w})}}, \tag{1.7}$$

$$\eta_{\mathcal{L}}(w) := 1 + \frac{(w-\bar{w})(e^{C(w)}-1)(e^{C(\bar{w})}-1)}{e^{C(w)}-e^{C(\bar{w})}}, \tag{1.8}$$

and $C : \mathbb{C}\backslash\mathrm{supp}(\mu) \to \mathbb{C}$ is the *Cauchy* transform of μ:

$$C(w) := \int_{\mathbb{R}} \frac{d\mu(t)}{w-t}, \tag{1.9}$$

Thus $\mathcal{L}$ is a non-empty, open (w.r.t to $\mathbb{R}^2$), simply connected subset of $\mathcal{P}$.

In [8] a subset of $\partial\mathcal{L}$ called *the edge* $\mathcal{E}$ was determined and its geometry classified. More precisely, the boundary behavior of $W_{\mathcal{L}}^{-1}$ for the open subset $R \subset \partial\mathbb{H} = \mathbb{R}$ was studied, where

$$R := (\mathbb{R}\backslash\mathrm{supp}(\mu)) \cup (\mathbb{R}\backslash\mathrm{supp}(\lambda-\mu)) \cup R_1 \cup R_2 = R_\mu \cup R_{\lambda-\mu} \cup R_0 \cup R_1 \cup R_2, \tag{1.10}$$

where

- $R_\mu := \{t \in \mathbb{R}\backslash\mathrm{supp}(\mu) : C(t) \neq 0\}$.
- $R_{\lambda-\mu} := \mathbb{R}\backslash\mathrm{supp}(\lambda-\mu)$.
- $R_0 := \{t \in \mathbb{R}\backslash\mathrm{supp}(\mu) : C(t) = 0\}$.

- R_1 is the set of all $t \in \partial(\mathbb{R}\backslash\text{supp}(\mu)) \cap \partial(\mathbb{R}\backslash\text{supp}(\lambda-\mu))$ for which there exists an $\epsilon > 0$ such that $(t, t+\epsilon) \subset \mathbb{R}\backslash\text{supp}(\mu)$ and $(t-\epsilon, t) \subset \mathbb{R}\backslash\text{supp}(\lambda-\mu)$.
- R_2 is the set of all $t \in \partial(\mathbb{R}\backslash\text{supp}(\mu)) \cap \partial(\mathbb{R}\backslash\text{supp}(\lambda-\mu))$ for which there exists an $\epsilon > 0$ such that $(t, t+\epsilon) \subset \mathbb{R}\backslash\text{supp}(\lambda-\mu)$ and $(t-\epsilon, t) \subset \mathbb{R}\backslash\text{supp}(\mu)$.

Note that $R_1 \cap R_2 = \varnothing$. $R_1 \cup R_2 := \partial(\mathbb{R}\backslash\text{supp}(\mu)) \cap \partial(\mathbb{R}\backslash\text{supp}(\lambda-\mu))$, the set of all common boundary points of the disjoint open sets $\mathbb{R}\backslash\text{supp}(\mu)$ and $\mathbb{R}\backslash\text{supp}(\lambda-\mu)$. Also $R_1 \cup R_2$ is a discrete subset of $[a,b]$. In words, $R_\mu \cup R_0$ is the interior of the set where the density $\varphi(x) = 0$ almost everywhere, and $R_{\lambda-\mu}$ is the interior of the set where $\varphi(x) = 1$ almost everywhere. We see that R_1 are the jumps from 1 to 0 and R_2 are the jumps from 0 to 1.

Definition 1.2. Let $t^* \in R_2$. We set

$$t_1 := \sup\{t \in \mathbb{R} : (t^*, t) \subset R_{\lambda-\mu}\} \tag{1.11}$$

and

$$t_2 := \inf\{t \in \mathbb{R} : (t, t^*) \subset R_\mu \cup R_0\}. \tag{1.12}$$

Then in particular $\varphi(t) = 0$ for all $t \in (t_2, t^*)$ and $\varphi(t) = 1$ for all $t \in (t^*, t_1)$. If $t = t^* \in R_1$ we interchange $R_{\lambda-\mu}$ and $R_\mu \cup R_0$ in (1.11) and (1.12)

It was shown in [8] that by considering a sequence $\{w_n\}_n \in \mathbb{H}$ such that $\lim_{n\to+\infty} w_n = t \in \mathbb{R} = \partial\mathbb{H}$ one gets a parametrization of the edge $\mathcal{E}$,

$$\lim_{n\to\infty} \chi(w_n) = t + \frac{1 - e^{-C(t)}}{C'(t)} := \chi_{\mathcal{E}}(t) \tag{1.13}$$

$$\lim_{n\to\infty} \eta(w_n) = 1 + \frac{e^{C(t)} + e^{-C(t)} - 2}{C'(t)} := \eta_{\mathcal{E}}(t) \tag{1.14}$$

for $t \in R_\mu$ and

$$\lim_{n\to\infty} \chi(w_n) = t + \frac{1 - (\frac{t-t_1}{t-t_2})e^{-C_I(t)}}{C_I'(t) + \frac{1}{t-t_2} - \frac{1}{t-t_1}} := \chi_{\mathcal{E}}(t) \tag{1.15}$$

$$\lim_{n\to\infty} \eta(w_n) = 1 + \frac{(\frac{t-t_2}{t-t_1})e^{C_I(t)} + (\frac{t-t_1}{t-t_2})e^{-C_I(t)}}{C_I'(t) + \frac{1}{t-t_2} - \frac{1}{t-t_1}} := \eta_{\mathcal{E}}(t) \tag{1.16}$$

for $t \in R_{\lambda-\mu}$, where $C_I(t) = \int_{\mathbb{R}\setminus I} \frac{d\mu(x)}{t-x}$, and I is any open interval such that $\mu\big|_I = \lambda$ and $t \in I$. Moreover the collection of these smooth parametrized curves has analytic extensions across the set $R_1 \cup R_2$. In particular,

$$(\chi_{\mathcal{E}}(t), \eta_{\mathcal{E}}(t)) = (t, 1 - (t-t_2)e^{C_I(t)}) \tag{1.17}$$

for $t \in R_1$ with $I = (t_2, t)$, and

$$(\chi_{\mathcal{E}}(t), \eta_{\mathcal{E}}(t)) = (t + (t_1 - t)e^{-C_I(t)}, 1 - (t_1 - t)e^{-C_I(t)}) \tag{1.18}$$

for $t \in R_2$, with $I = (t, t_1)$. Finally, it is proven in [8] that this gives a bijection $W_{\mathcal{E}} : \mathcal{E} \to R$, with inverse $W_{\mathcal{E}}^{-1}(t) = (\chi_{\mathcal{E}}(t), \eta_{\mathcal{E}}(t))$, where $\chi_{\mathcal{E}}(t)$ and $\eta_{\mathcal{E}}(t)$ are real analytic functions.

The importance of the *edge* $\mathcal{E}$ is that one expects universal edge fluctuations at $\mathcal{E}$. In particular one expects that the local asymptotics in a neighborhood of a generic point of $\mathcal{E}$ is either given by the *Airy* kernel or the $Id - Airy$ kernel. For a special case see [20], and more generally [9]. In this paper we will consider certain singular points on the curve $\mathcal{E}$. At these points the curve will have a cusp. Typically one would expect that the local fluctuations at these points in the limit $n \to \infty$ is a *Pearcey* process. However, for the situations considered in this paper this will not be the case. In fact we will show that at these points one gets the *Cusp-Airy process* given by the kernel (1.1).

1.5 Conditions for Cusps

One can rewrite the derivative given by (1.6) as

$$f'(w;\chi,\eta) = \int_a^{\chi+\eta-1} \frac{d\mu(x)}{w-x} - \int_{\chi+\eta-1}^{\chi} \frac{d(\lambda-\mu)(x)}{w-x} + \int_{\chi}^{b} \frac{d\mu(x)}{w-x}. \tag{1.19}$$

This implies that the function $f'(w;\chi,\eta)$ has an analytic extension to the set $\mathbb{C}\backslash(\text{supp}(\mu)\big|_{[a,\chi+\eta-1,\chi]} \bigcup \text{supp}(\lambda-\mu)\big|_{[\chi+\eta-1,\chi]} \bigcup \text{supp}(\mu)\big|_{[\chi,b]})$. It is shown in Lemma 2.6 in [8] that the *edge,* $\mathcal{E}$, is the disjoint union $\mathcal{E} := \mathcal{E}_\mu \cup \mathcal{E}_{\lambda-\mu} \cup \mathcal{E}_0 \cup \mathcal{E}_1 \cup \mathcal{E}_2$, where

- $\mathcal{E}_\mu$ is the set of all $(\chi,\eta) \in \mathcal{P}$ for which f' has a repeated root in $\mathbb{R}\backslash[\chi+\eta-1,\chi]$.
- $\mathcal{E}_{\lambda-\mu}$ is the set of all (χ,η) for which f' has a repeated root in $(\chi+\eta-1,\chi)$.
- $\mathcal{E}_0$ is the set of all (χ,η) for which $\eta = 1$ and f' has a root at χ $(= \chi+\eta-1)$. In particular, $\mathcal{E}$ is tangent to the line $\eta = 1$.
- $\mathcal{E}_1$ is the set of all (χ,η) for which $\eta < 1$ and f' has a root at χ. In particular, $\mathcal{E}$ is tangent to the line $\chi = t \in R_1$.
- $\mathcal{E}_2$ is the set of all (χ,η) for which $\eta < 1$ and f' has a root at $\chi+\eta-1$. In particular, $\mathcal{E}$ is tangent to the line $\chi+\eta-1 = t \in R_2$.

Moreover it is shown in Lemma 2.6 in [8] that one has following equivalent characterization of the behavior of the roots of $f'_t := f'(w;\chi_{\mathcal{E}}(t),\eta_{\mathcal{E}}(t))\big|_{w=t}$ whenever $(\chi,\eta) \in \mathcal{E}$:

(a) $(\chi_{\mathcal{E}}(t),\eta_{\mathcal{E}}(t)) \in \mathcal{E}_\mu$ if and only if $t \in R_\mu$. Moreover, in this case, t is a root of f'_t of multiplicity either 2 or 3.

(b) $(\chi_{\mathcal{E}}(t),\eta_{\mathcal{E}}(t)) \in \mathcal{E}_{\lambda-\mu}$ if and only $t \in R_{\lambda-\mu}$. Moreover, in this case, t is a root of f'_t of multiplicity either 2 or 3.

(c) $(\chi_{\mathcal{E}}(t),\eta_{\mathcal{E}}(t)) \in \mathcal{E}_0$ if and only if $t \in R_0$. Moreover, in this case, $f'_t = C$ and t is a root of f'_t of multiplicity 1.

(d) $(\chi_{\mathcal{E}}(t),\eta_{\mathcal{E}}(t)) \in \mathcal{E}_1$ if and only $t \in R_1$. Moreover, in this case, t is a root of f'_t of multiplicity either 1 or 2.

(e) $(\chi_{\mathcal{E}}(t),\eta_{\mathcal{E}}(t)) \in \mathcal{E}_2$ if and only $t \in R_2$. Moreover, in this case, t is a root of f'_t of multiplicity either 1 or 2.

If case (a) holds and t is a root of multiplicity 2 of f'_t one expects to see the *extended Airy kernel process.* If on the other hand t is a root of multiplicity 3 of f'_t one expects to see the *Pearcey process.* If case (b) holds and t is a root of multiplicity 2 of f'_t one expects to see the *Id-extended Airy kernel process.* What we mean by this is that we have to make a particle/hole transformation, i.e. change the type of tiles we are considering. If on the other hand t is a root of multiplicity 3 of f'_t one again expects to see the *Id-Pearcey process.* If case (c) holds one expects to see the *GUE corner process*, and similarly if case (d) and (e) holds and t is a root of multiplicity 1 of f'_t. In the remaining cases (d) and (e) when t is a root of multiplicity 2 of f'_t one will see the *Cusp-Airy process*, which will be shown in this paper.

In this article we will assume that $t = t_c \in R_1 \cup R_2$ and that t_c is a root of f'_t of multiplicity 2. If these conditions hold, then it is shown in Lemma 2.9 in [8] that the edge at $(\chi_{\mathcal{E}}(t),\eta_{\mathcal{E}}(t))$ is locally an algebraic cusp of first order, that is the curve locally looks like the algebraic curve $y^3 = x^2$ in a neighborhood of the origin. Moreover, if $t_c \in R_2$, then by Theorem 3.1 in [8] $\chi_c > t_1$. Then (1.18) together with the fact that $\chi_c + \eta_c - 1 = t_c$, where $\chi_c := \chi_{\mathcal{E}}(t_c)$ and $\eta_c := \eta_{\mathcal{E}}(t_c)$, gives

$$\begin{aligned} f'(t_c;\chi_c,\eta_c) &= C_I(t_c) - \int_{t_1}^{\chi_c} \frac{dx}{t_c - x} = C_I(t_c) + \log|t_c - \chi_c| - \log|t_c - t_1| \\ &= C_I(t_c) + \log|(t_c - t_1)e^{-C_I(t_c)}| - \log|t_c - t_1| = 0. \end{aligned}$$

A similar computation gives $f'(t_c;\chi_c,\eta_c)=0$ whenever $t_c\in R_1$. Therefore, $f'(t_c;\chi_c,\eta_c)\equiv 0$ whenever $t_c\in R_1\cup R_2$. This implies that that (χ_c,η_c) is a cusp of $\mathcal{E}$ for $t_c\in R_1\cup R_2$, if and only if $f''(t_c;\chi_c,\eta_c)=0$. However, a direct computation shows that if $t_c\in R_2$, then

$$f''(t_c;\chi_c,\eta_c)=C_I'(t_c)+\frac{e^{C_I(t_c)}-1}{t_c-t_1}$$

and if $t_c\in R_1$, then

$$f''(t_c;\chi_c,\eta_c)=C_I'(t_c)+\frac{1-e^{-C_I(t_c)}}{t_c-t_2}.$$

Therefore, $\mathcal{E}$ has a cups at (χ_c,η_c), if and only if

$$C_I'(t_c)=\frac{e^{C_I(t_c)}-1}{t_1-t_c} \tag{1.20}$$

if $t_c\in R_2$, and

$$C_I'(t_c)=\frac{1-e^{-C_I(t_c)}}{t_2-t_c}. \tag{1.21}$$

if $t_c\in R_1$. From now on we will consider only the case $t_c\in R_2$. The case when $t_c\in R_1$ can be treated analogously.

Assumption 2. Let $t_c\in R_2$ and let $(\chi_c,\eta_c):=(\chi_{\mathcal{E}}(t_c),\eta_{\mathcal{E}}(t_c))$. Assume that $f'(t_c;\chi_c,\eta_c)=f''(t_c;\chi_c,\eta_c)=0$ so that (χ_c,η_c) is the asymptotic cusp point.

Lemma 1.1. *If $t_c\in R_2$ and $f''(t_c;\chi_c,\eta_c)=0$, then $f'''(t_c;\chi_c,\eta_c)>0$.*

Proof. By Lemma 2.9 in [8], the signed extrinsic curvature $k_{\mathcal{E}}(t)$ is negative for all smooth points of the curve $\mathcal{E}$. From this it follows that all cusps point into the liquid region $\mathcal{L}$. Together with Lemma 2.9 case (9) and Lemma 2.8 formula (g) in [8] it follows that $f'''(t_c;\chi_c,\eta_c)>0$. □

In order to prove convergence to the Cusp-Airy kernel in our discrete model we will have to assume that μ_n will jump from empty to full not just asymptotically in terms of φ, but already at the discrete level. This is the content of the next assumption.

Assumption 3. Assume that for every $\varepsilon>0$ and n large enough we have for $t_c\in R_2$,

$$\mu_n\big|_{[t_2+\varepsilon,t_1-\varepsilon]}=\frac{1}{n}\sum_{\lfloor nt_c\rfloor\leqslant k\leqslant n(t_1-\varepsilon)}\delta_{k/n}. \tag{1.22}$$

where $\lfloor x\rfloor=\max\{m\in\mathbb{Z}:m\leqslant x\}$.

Remark 1.2. Assuming only weak convergence of the empirical measures $\{\mu_n\}_n$ to a limiting measure μ will not be sufficient when considering fluctuation of the *edge* $\mathcal{E}$. We will need better control of the convergence of sequence of empirical measures. More precisely, it is necessary to assume that their supports converge in an appropriate sense, see [9]. This will not be needed here since the other assumptions that we make are enough.

1.6 Rescaled Variables

Introduce the following notation

$$a_n:=n^{-1}\min\{t\in\operatorname{supp}(\mu_n)\}=n^{-1}\beta_n^{(n)}$$

and

$$b_n := n^{-1}\max\{t \in \mathrm{supp}(\mu_n)\} = n^{-1}\beta_1^{(n)}.$$

Furthermore, we write

$$t_c^{(n)} := n^{-1}\min\{\beta_i^{(n)} : \beta_i^{(n)} \geqslant \lfloor nt_c \rfloor\} = n^{-1}\min\{t \in \mathrm{supp}(\mu_n) : t \geqslant \lfloor nt_c \rfloor\}, \tag{1.23}$$

$$t_1^{(n)} + n^{-1} = n^{-1}\min\{t \in \mathrm{supp}(\lambda_n - \mu_n) : t > nt_c^{(n)}\}, \tag{1.24}$$

and

$$t_2^{(n)} = n^{-1}\max\{t \in \mathrm{supp}(\mu_n) : t < nt_c^{(n)}\}. \tag{1.25}$$

In words, $nt_1^{(n)}+1$ is the position of the first hole after $nt_c^{(n)}$, i.e., $nt_1^{(n)}$ is the position or the last particle in a densely packed block after $nt_c^{(n)}$, and $nt_2^{(n)}$ is the position of the last particle before $nt_c^{(n)}$. In particular $(nt_2^{(n)}, nt_c^{(n)})$ is an empty block and $[nt_c^{(n)}, nt_1^{(n)}]$ is a densely packed block. Finally, we define

$$x_c^{(n)} := n^{-1}\lfloor n\chi_c \rfloor \text{ and } y_c^{(n)} := 1 + t_c^{(n)} - x_c^{(n)}. \tag{1.26}$$

We note that by Assumption 3, it follows that $\lim_{n\to\infty} a_n = a$, $\lim_{n\to\infty} b_n = b$, $\lim_{n\to\infty} t_2^{(n)} = t_2$, $\lim_{n\to\infty} t_1^{(n)} = t_1$ and $\lim_{n\to\infty} t_c^{(n)} = t_c$. Let σ be a signed Borel measure on $\mathbb{R}$ and let

$$U^\sigma(x) = \int_{\mathbb{R}} \log|x-t| d\sigma(t) \tag{1.27}$$

denote the logarithmic potential of σ.

Remark 1.3. Note that sometimes the logarithmic potential is defined with opposite sign. We will however follow the convention in [22].

Consider the signed measure

$$d\nu(x) = (\chi_{[a,t_2]}(x) + \chi_{[\chi_c,b](x)})\varphi(x)dx - (1-\varphi(x))\chi_{[t_1,\chi_c]}(x)dx. \tag{1.28}$$

Then at the cusp $\chi_c + \eta_c - 1 = t_c$, and

$$\begin{aligned} f(w;\chi_c,\eta_c) = f(w;\chi_c) &= \int_a^{t_2} \log(w-x)d\mu(x) - \int_{t_1}^{\chi_c} \log(w-x)d(\lambda-\mu)(x) + \int_{\chi_c}^{b} \log(w-x)d\mu(x) \\ &= \int_{\mathbb{R}} \log(w-x)d\nu(x) = U^\nu(w) + i\int_{\mathbb{R}} \arg(w-t)d\nu(t), \end{aligned} \tag{1.29}$$

where log denotes the principal branch of the complex logarithm function.

In particular we note that f is independent of η_c. By assumption on μ we have a complete cancelation of the measures μ and λ on $[t_c, t_1]$, that is $\lambda - \mu\big|_{[t_c,t_1]} = 0$. For the exact kernel however, the cancelation of factors is not necessarily complete. Moreover due to the rigidity of the interlacing system, as shown in figure 3, their will be no fluctuations around the frozen boundary at the cusp in the orthogonal direction to the tangential direction of the cusp. It is therefore natural to assume a discrete variation in the orthogonal direction. We therefore assume the following scaling:

Definition 1.3. Introduce the fixed limiting variables $r, s \in \mathbb{Z}$, and $\xi, \tau \in \mathbb{R}$. Let

$$c_0 = \frac{2(\chi_c - t_c)}{d_0}, \tag{1.30}$$

where

$$d_0 = \left(\frac{2}{f'''(t_c)}\right)^{1/3}. \tag{1.31}$$

Define the rescaled variables $\xi_n, \tau_n \in \mathbb{R}$, by

$$\begin{cases} x_1 = nx_c^{(n)} + \frac{1}{2}\big(r - c_0 n^{1/3}\xi_n\big) \\ y_1 = ny_c^{(n)} + \frac{1}{2}\big(r + c_0 n^{1/3}\xi_n\big) \\ x_2 = nx_c^{(n)} + \frac{1}{2}\big(s - c_0 n^{1/3}\tau_n\big) \\ y_2 = ny_c^{(n)} + \frac{1}{2}\big(s + c_0 n^{1/3}\tau_n\big) \end{cases}. \tag{1.32}$$

We assume that

$$\lim_{n\to\infty} \xi_n = \xi, \quad \lim_{n\to\infty} \tau_n = \tau. \tag{1.33}$$

When taking limits of the correlation kernel we will always use the scaling (1.32). Note that by (1.26), the rescaled variables satisfy

$$\begin{cases} y_1 + x_1 = n + nt_c^{(n)} + r \\ y_1 - x_1 = ny_c^{(n)} - nx_c^{(n)} + c_0 n^{1/3}\xi_n \\ y_2 + x_2 = n + nt_c^{(n)} + s \\ y_2 - x_2 = ny_c^{(n)} - nx_c^{(n)} + c_0 n^{1/3}\tau_n \end{cases}. \tag{1.34}$$

It will be convenient to introduce the notation

$$\Delta x_1^{(n)} = \frac{1}{2}(r - c_0 n^{1/3}\xi_n), \quad \Delta x_2^{(n)} = \frac{1}{2}(s - c_0 n^{1/3}\tau_n). \tag{1.35}$$

The rescaled coordinate system is depicted in figure 12.

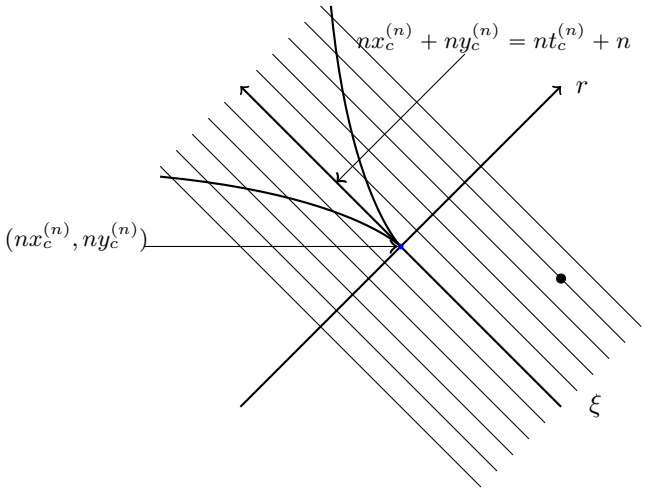

Figure 12: Rescaled coordinate system at the cusp.

1.7 Integrand

In order to write the integrand in (1.2) in a convenient way we introduce some notation. Let

$$q_n(w;r) = \frac{\prod_{k=nt_c^{(n)}}^{x_1}(w-k)}{\prod_{k=x_1+y_1-n}^{x_1}(w-k)} \tag{1.36}$$
$$= 1_{r>0}\prod_{k=nt_c^{(n)}}^{nt_c^{(n)}+r-1}(w-k) + 1_{r=0} + 1_{r<0}\prod_{k=nt_c^{(n)}+r}^{nt_c^{(n)}-1}(w-k)^{-1},$$

and

$$Q_n(w;\Delta x_1^{(n)}) = \frac{\prod_{k=nt_c^{(n)}}^{nx_c^{(n)}}(w-k)}{\prod_{k=nt_c^{(n)}}^{x_1}(w-k)} \tag{1.37}$$
$$= 1_{\Delta x_1^{(n)}>0}\prod_{k=nx_c^{(n)}+1}^{nx_c^{(n)}+\Delta x_1^{(n)}}(w-k)^{-1} + 1_{\Delta x_1^{(n)}=0} + 1_{\Delta x_1^{(n)}<0}\prod_{k=nx_c^{(n)}+\Delta x_1^{(n)}+1}^{nx_c^{(n)}}(w-k).$$

We see that $q_n(w;r)$ only depends on the parameters through r. Also, since $x_1 = nx_c^{(n)} + \Delta x_1^{(n)}$, $Q_n(w;\Delta x_1^{(n)})$ only depends on the parameters through $\Delta x_1^{(n)}$.

Furthermore, let

$$E_n(w) = \frac{\prod_{\beta_i^{(n)}\leqslant nt_2^{(n)}}(w-\beta_i^{(n)})\prod_{nt_1^{(n)}<\beta_i^{(n)}}(w-\beta_i^{(n)})}{\prod_{k=nt_1^{(n)}+1}^{nx_c^{(n)}}(w-k)}. \tag{1.38}$$

Lemma 1.2. *We have that*

$$K_{\mathcal{R}}^{(n)}((x_1,y_1),(x_2,y_2)) = -1_{x_1<x_2}\frac{1}{(2\pi i)^2}\oint_{\Gamma_n}dz\oint_{\gamma_n}dw\frac{1}{(w-z)(z-n^{-1}x_2)}\frac{q_n(nw;r)Q_n(nw,\Delta x_1^{(n)})E_n(nw)}{q_n(nz;s)Q_n(nz;\Delta x_2^{(n)})E_n(nz)}$$
$$+ 1_{x_1\geqslant x_2}\frac{1}{(2\pi i)^2}\oint_{\tilde{\Gamma}_n}dz\oint_{\tilde{\gamma}_n}dw\frac{1}{(w-z)(z-n^{-1}x_2)}\frac{q_n(nw;r)Q_n(nw,\Delta x_1^{(n)})E_n(nw)}{q_n(nz;s)Q_n(nz;\Delta x_2^{(n)})E_n(nz)}, \tag{1.39}$$

where where Γ_n is a counterclockwise oriented contour that contains the set $\{n^{-1}\beta_i^{(n)} \geqslant t_1^{(n)}\}$ but not the set $\{\beta_i^{(n)} \leqslant t_c^{(n)}+s\}$, and $\tilde{\Gamma}_n$ is a counterclockwise oriented contour containing the set $\{n^{-1}\beta_i^{(n)} \leqslant t_c^{(n)}+s\}$ but not the set $\{n^{-1}\beta_i^{(n)} \geqslant t_1^{(n)}\}$. In addition, γ_n is the counterclockwise oriented contour that contains the set $n^{-1}\{x_1+y_1-n,...,x_1\}$ and Γ_n and $\tilde{\gamma}_n$ is the counterclockwise oriented contour that contains the set $n^{-1}\{x_1+y_1-n,...,x_1\}$ and $\tilde{\Gamma}_n$. See figure 13 and 14.

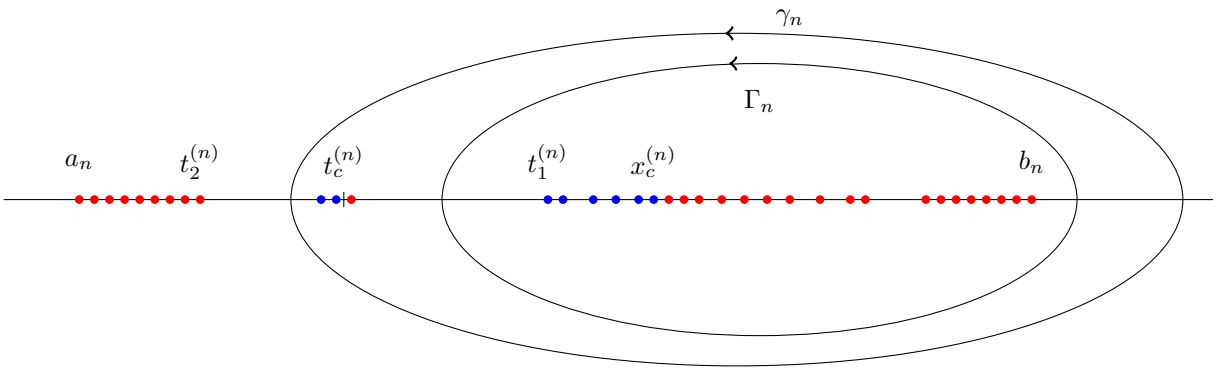

Figure 13: Integration contours for the correlation kernel. Blue dots indicate the positions of poles and red dots indicate the position of zeroes of the function $q_n(nw;r)E_n(nw)$.

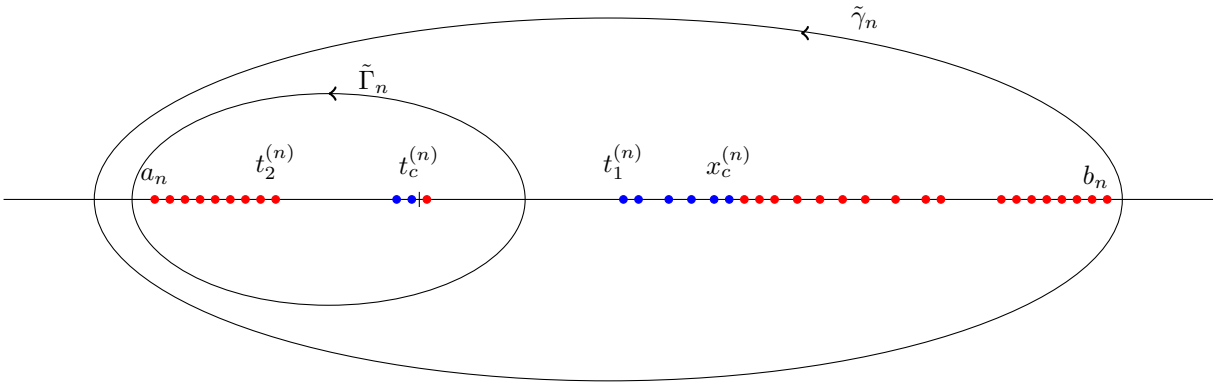

Figure 14: Integration contours for the correlation kernel. Blue dots indicate the positions of poles and red dots indicate the position of zeroes of the function $q_n(nw;r)E_n(nw)$.

The lemma will be proven in section 2.1.
Let ν_n and $\nu_{n,j}$, $j = 1, 2$, be the signed measures

$$\nu_n(t) = \frac{1}{n}\sum_{\beta_i^{(n)} \leqslant nt_2^{(n)}} \delta_{\beta_i^{(n)}/n} - \frac{1}{n}\left(\sum_{k=nt_1^{(n)}+1}^{nx_c^{(n)}} \delta_{k/n} - \sum_{nt_1^{(n)} < \beta_i^{(n)} \leqslant nx_c^{(n)}} \delta_{\beta_i^{(n)}/n} \right) + \frac{1}{n}\sum_{nx_c^{(n)} < \beta_i^{(n)}} \delta_{\beta_i^{(n)}/n}, \quad (1.40)$$

$$\nu_{n,j}(t) = \frac{1}{n}\sum_{\beta_i^{(n)} \leqslant nt_2^{(n)}} \delta_{\beta_i^{(n)}/n} - \frac{1}{n}\left(\sum_{k=nt_1^{(n)}+1}^{x_j^{(n)}} \delta_{k/n} - \sum_{nt_1^{(n)} < \beta_i^{(n)} \leqslant x_j^{(n)}} \delta_{\beta_i^{(n)}/n} \right) + \frac{1}{n}\sum_{x_c^{(n)} < \beta_i^{(n)}} \delta_{\beta_i^{(n)}/n}. \quad (1.41)$$

Furtheremore, define f_n, $g_{n,j}$ and $h_{n,j}$ by

$$f_n(w) = \frac{1}{n}\log E_n(nw) = \int_{\mathbb{R}} \log(w-t)d\nu_n(t), \quad (1.42)$$

$$g_{n,j}(w) = \frac{1}{n}\log Q_n(nw; \Delta x_j^{(n)}) + f_n(w) := \frac{1}{n}h_{n,j}(w) + f_n(w). \quad (1.43)$$

In particular, $\mathrm{Re}[g_{n,j}(w)] = \int_{\mathbb{R}} \log|w-t| d\nu_{n,j}(t) = U^{\nu_{n,j}}(w)$. Here, we let log be the principal branch of the logaritm for $f_n(w)$. For $h_{n,j}(w)$, we let the branch cut of log lie along the the *positive* real axis.

With these choices of branch cuts, it follows that f_n is analytic on $\mathbb{C}\backslash(-\infty, b_n]$, and $h_{n,j}$ is analytic in $\mathbb{C}\backslash[t_1^{(n)}, +\infty)$. In particular we note that $f_n(w)$ has a jump discontinuity over the real line at t_c. However $\mathrm{Re}[f_n]$ is real analytic on $\mathbb{C}\backslash([a_n, t_2^{(n)}] \cup [t_1^{(n)}, b_n])$, and f_n' is homolorphic on $\mathbb{C}\backslash([a_n, t_2^{(n)}] \cup [t_1^{(n)}, b_n])$. Moreover, $\lim_{t_c \pm i\varepsilon \to t_c} f(t_c \pm i\varepsilon) := f_n^{\pm}(t_c) = \mathrm{Re}[f_n(t_c)] \pm i\pi k/n$, where k is an integer. Therefore $\exp(n(f_n^+(t_c) - f_n^-(t_c))) = \exp(2\pi i k) = 1$. Thus the jump discontinuity in the imaginary part of f_n does not matter when we perform a steepest descent analysis in a neighborhood of t_c. From now on it will be understood that when we Taylor expand f_n at $w = t_c$, we look at the branch

$$f_n^+(t_c) + \sum_{n=1}^{\infty} \frac{f^{(n)}(t_c)}{n!}(w - t_c)^n.$$

It follows from our assumptions that f_n and $g_{n,j}$ converge uniformly to f on compact subsets of $\mathbb{C}\backslash([a, t_2] \cup [t_1, b])$, see Lemma 2.1

We need one more assumption which will enable us to replace the non-asymptotic function $f_n(z)$ by the asymptotic function $f(z)$ in a neighbourhood of the critical point t_c.

Assumption 4. There is a neighbourhood U of t_c such that

$$\lim_{n\to\infty} n^{2/3}(f_n'(z) - f'(z)) = 0 \tag{1.44}$$

uniformly in U.

1.8 Main Theorem

We can now give the main theorem about convergence to the Cusp-Airy kernel for our system of red particles in the interlacing model.

Theorem 1.1. *Assume that the sequence of empirical measures $\{\mu_n\}_n$ satisfies Assumptions 1-4, and assume the scaling in Definition 1.3. Then*

$$\lim_{n\to\infty} \frac{p_n(x_2, y_2)}{p_n(x_1, y_1)} \frac{c_0}{2} n^{1/3} K_{\mathcal{R}}^{(n)}((x_1, y_1), (x_2, y_2)) = \mathcal{K}_{CA}((\xi, r), (\tau, s)) \tag{1.45}$$

uniformly for ξ and τ in some fixed compact subset of $\mathbb{R}$, where

$$p_n(x_1, y_1) = \left(d_0 n^{\frac{2}{3}}\right)^{x_1 + y_1 - n - nt_c^{(n)}} Q_n(nt_c; x_1 - nx_c^{(n)}). \tag{1.46}$$

Let (ξ_j^r, r) be the rescaled coordinates for particles on line r. Fix $r_1, \ldots, r_M \in \mathbb{Z}$ and let $\phi : \mathbb{R} \times \{r_1, \ldots, r_M\} \to [0, 1]$ be a bounded measurable function with compact support. Let $\mathbb{E}_{\beta^{(n)}}$ denote the expectation with respect to the determinantal point process with kernel $K_{\mathcal{R}}^{(n)}$. Then,

$$\lim_{n\to\infty} \mathbb{E}_{\beta^{(n)}}\left[\prod_{r\in\{r_1,\ldots,r_m\}} \prod_j (1 - \phi(\xi_j^r, r))\right] = \det(I - \phi\mathcal{K}_{CA})_{L^2(\mathbb{R}\times\{r_1,\ldots,r_M\})}. \tag{1.47}$$

Example 1.1. Let the limiting measure $d\mu(t) = \chi_{[-1-a,-1]}(t)dt + \chi_{[0,a]}(t)dt + \chi_{[2a,1]}(t)dt$ where $a = \frac{-3+\sqrt{17}}{4} \approx 0.28$. In particular $\|\mu\| = 1$ and $t_c = 0 \in R_2$. Let $t_1 = a$. Then, with $I = (0, a)$,

$$C_I(t) = \log\left|\frac{t + 1 + a}{t + 1}\right| + \log\left|\frac{t - 2a}{t - 1}\right|.$$

From equation (1.18) we then get $(\chi_{\mathcal{E}}(0), \eta_{\mathcal{E}}(0)) = \left(\frac{1}{2(1+a)}, 1 - \frac{1}{2(1+a)}\right)$. Using that $a < \frac{1}{2(1+a)} < 2a$ and (1.19), we obtain

$$f''(0; \chi_{\mathcal{E}}(0), \eta_{\mathcal{E}}(0)) = \int_{-1-a}^{-1} \frac{ds}{s^2} - \int_{a}^{\chi_{\mathcal{E}}(0)} \frac{ds}{s^2} + \int_{2a}^{1} \frac{ds}{s^2} = \frac{1 - a - 8a^2 - 4a^3}{2a(1+a)} = 0,$$

since a is a root of the polynomial $1 - x - 8x^2 - 4x^3$. Thus Assumption 2 is satisfied. We will now construct a sequence of empirical measures $\{\mu_n\}_n$ that satisfies Assumptions 1,3 and 4. Let

$$\mu_n = \frac{1}{n} \sum_{k=\lfloor -n(1-a) \rfloor}^{-n+d_n} \delta_{k/n} + \frac{1}{n} \sum_{k=0}^{\lfloor na \rfloor} \delta_{k/n} + \frac{1}{n} \sum_{k=\lfloor 2na \rfloor}^{n} \delta_{k/n}$$

where d_n is chosen so that $-n + d_n - \lfloor -n(1-a) \rfloor + \lfloor na \rfloor + n - \lfloor 2na \rfloor + 3 = n$. Clealy, $\mu_n \rightharpoonup \mu$, so Assumption 1 is satisfied. Now,

$$\mathrm{supp}(\mu_n) = \frac{1}{n}\{\lfloor -n(1-a) \rfloor, ..., -n + d_n\} \bigcup \frac{1}{n}\{0, ..., \lfloor na \rfloor\} \bigcup \frac{1}{n}\{\lfloor 2na \rfloor, ..., n\},$$

so by construction $\{\mu_n\}_n$ satisfies Assumption 3. Now,

$$\nu_n = \frac{1}{n} \sum_{k=\lfloor -n(1-a) \rfloor}^{-n+d_n} \delta_{k/n} - \frac{1}{n} \sum_{k=\lfloor na \rfloor + 1}^{\left\lfloor \frac{n}{2(1+a)} \right\rfloor} \delta_{k/n} + \frac{1}{n} \sum_{k=\lfloor 2na \rfloor}^{n} \delta_{k/n},$$

and thus

$$f_n'(w) = \int_{\mathbb{R}} \frac{d\nu_n(t)}{w - t} = \frac{1}{n} \sum_{k=\lfloor -n(1-a) \rfloor}^{-n+d_n} \frac{1}{w - k/n} - \frac{1}{n} \sum_{k=\lfloor na \rfloor + 1}^{\left\lfloor \frac{n}{2(1+a)} \right\rfloor} \frac{1}{w - k/n} + \frac{1}{n} \sum_{k=\lfloor 2na \rfloor}^{n} \frac{1}{w - k/n}, \tag{1.48}$$

and

$$f_n''(w) = -\int_{\mathbb{R}} \frac{d\nu_n(t)}{(w-t)^2} = -\frac{1}{n} \sum_{k=\lfloor -n(1-a) \rfloor}^{-n+d_n} \frac{1}{w - k/n} + \frac{1}{n} \sum_{k=\lfloor na \rfloor + 1}^{\left\lfloor \frac{n}{2(1+a)} \right\rfloor} \frac{1}{(w - k/n)^2} - \frac{1}{n} \sum_{k=\lfloor 2na \rfloor}^{n} \frac{1}{(w - k/n)^2}. \tag{1.49}$$

Choose $r < a$. Then for n large enough, $\frac{1}{w-t}$ and $-\frac{1}{(w-t)^2}$ are continuously differentiable in $B(0, r)$. Hence (1.48) and (1.49) are Riemann sums of smooth functions with equidistant partitions. Thus, there exists a constant $C > 0$, such that

$$|f_n'(z) - f'(z)| \leqslant \frac{C}{n},$$

holds uniformly in $B(0, r)$ for n large enough. In particular Assumption 4 is satisfied. This example shows that we indeed can get the Cusp-Airy limit in a natural model of the type considered in [20].

Remark 1.4. The regularity assumption on the sequence of empirical measures made in Assumption 3 are necessary for Theorem 1 to hold, and cannot be substantially relaxed. If one in particular try to perform the cancellation of factors as in Lemma 1.2 without Assumption 3, one immediately sees that $q_n(w; r) \neq 1_{r>0} \prod_{k=nt_c^{(n)}+1}^{nt_c^{(n)}+r} (w-k)^{-1} + 1_{r=0} + 1_{r<0} \prod_{k=nt_c^{(n)}+r+1}^{nt_c^{(n)}} (w-k)$, in general, and that $q_n(w; r)$ would also depend on the sequence $\{\beta_i^{(n)}\}_n$. In particular the limit in Theorem 1.1 need not exist.

1.9 Random Top Line Measure

Up to now we have assumed that the top line configuration of *yellow* particles is fixed. However, for many models it is natural not to assume that the top line configuration is fixed, but instead is a random particle process.

Let $\Sigma \subset \mathbb{R}$ be finite union of closed, bounded intervals and write $\Sigma_n = \mathbb{Z} \cap n\Sigma$. Let $\mathcal{X}^{(n)}$ denote the set

$$\mathcal{X}^{(n)} = \{\beta^{(n)} \in \Sigma_n^n \,;\, \beta_1^{(n)} < \cdots < \beta_n^{(n)}\}.$$

We will call $\mathcal{X}^{(n)}$ the set of all admissible top line configurations. Note that $\mathcal{X}^{(n)}$ is a finite set. We will now assume that we have a probability distribution $p^{(n)}(\beta_1^{(n)}, ..., \beta_n^{(n)})$ on $\mathcal{X}^{(n)}$. Extended to Σ_n^n, we assume that $p^{(n)}(\beta_1^{(n)}, ..., \beta_n^{(n)})$ is a symmetric function which vanishes if $\beta_i^{(n)} = \beta_j^{(n)}$ for some $i \neq j$. Let $\mathbf{P}^{(n)}$ denote the probability and $\mathbf{E}^{(n)}$ the corresponding expectation given by $p^{(n)}$. Also, let $\mathbb{E}_{\beta^{(n)}}$ denote the expectation with respect to the red particles in the uniform interlacing with fixed top line $\beta^{(n)}$ that we studied above.

Let μ with $\operatorname{supp}\mu \subseteq \Sigma$ be given and let f be defined by (1.5) as previously. We assume that Assumption 2 holds with this f. In order to transfer the Main theorem to the case with a random top line we will use the following assumption.

Assumption 5. For each $n \geqslant 1$ there is a set $\mathcal{X}_{reg}^{(n)} \subseteq \mathcal{X}^{(n)}$ of regular top line configurations such that the following holds:

(i) $\mathbf{P}^{(n)}[\mathcal{X}_{reg}^{(n)}] \to 1$ as $n \to \infty$,

(ii) If $\beta^{(n)} \in \mathcal{X}_{reg}^{(n)}$, $n \geqslant 1$ is any sequence of regular top line configurations, we define μ_n and f_n as previously. Then μ_n and f_n satisfy Assumptions 1, 3 and 4 above.

We now can now give a version of Theorem 1.1 when we have a random top line measure.

Theorem 1.2. *Consider uniform interlacing with a random top line given by $p^{(n)}$ as above, and consider the red particle point process. Let (ξ_j^r, r) be the rescaled coordinates for particles on line r. Fix $r_1, \ldots, r_M \in \mathbb{Z}$ and let $\phi : \mathbb{R} \times \{r_1, \ldots, r_M\} \to [0, 1]$ be a bounded measurable function with compact support. Assume that Assumption 5 holds. Then*

$$\lim_{n\to\infty} \mathbf{E}_n\left[\mathbb{E}_{\beta^{(n)}}\left[\prod_{r\in\{r_1,\ldots,r_M\}}\prod_j (1-\phi(\xi_j^r, r))\right]\right] = \det(I - \phi\mathcal{K}_{CA})_{L^2(\mathbb{R}\times\{r_1,\ldots,r_M\})}. \tag{1.50}$$

Proof. We can write

$$\begin{aligned}
&\mathbf{E}_n\left[\mathbb{E}_{\beta^{(n)}}\left[\prod_{r\in\{r_1,\ldots,r_M\}}\prod_j (1-\phi(\xi_j^r, r))\right]\right] \\
&= \mathbf{E}_n\left[1_{\mathcal{X}_{reg}^{(n)}}\mathbb{E}_{\beta^{(n)}}\left[\prod_{r\in\{r_1,\ldots,r_M\}}\prod_j (1-\phi(\xi_j^r, r))\right]\right] + \mathbf{E}_n\left[1_{\mathcal{X}^{(n)}\setminus\mathcal{X}_{reg}^{(n)}}\mathbb{E}_{\beta^{(n)}}\left[\prod_{r\in\{r_1,\ldots,r_M\}}\prod_j (1-\phi(\xi_j^r, r))\right]\right].
\end{aligned} \tag{1.51}$$

By Assumption 5 the second term in the right hand side of (1.51) goes to 0 as $n \to \infty$. There is a $\tilde{\beta}^{(n)}$ such that

$$\max_{\beta^{(n)}\in\mathcal{X}_{reg}^{(n)}} \mathbb{E}_{\beta^{(n)}}\left[\prod_{r\in\{r_1,\ldots,r_M\}}\prod_j (1-\phi(\xi_j^r, r))\right]$$

is assumed at $\beta^{(n)} = \tilde{\beta}^{(n)}$, since the maximum is over a finite set. By Assumption 5 we can apply the Main theorem to the sequence $\tilde{\beta}^{(n)}$ and thus

$$\limsup_{n\to\infty} \mathbf{E}_n\left[1_{\mathcal{X}_{reg}^{(n)}} \mathbb{E}_{\beta^{(n)}}\left[\prod_{r\in\{r_1,\ldots,r_M\}}\prod_j (1-\phi(\xi_j^r, r))\right]\right] \leqslant \limsup_{n\to\infty} \mathbb{E}_{\tilde{\beta}^{(n)}}\left[\prod_{r\in\{r_1,\ldots,r_M\}}\prod_j (1-\phi(\xi_j^r, r))\right]$$
$$= \det(I - \phi\mathcal{K}_{CA})_{L^2(\mathbb{R}\times\{r_1,\ldots,r_M\})}.$$

We can do the analogous argument for the lower limes, and in this way we obtain the desired result. □

Remark 1.5. Interlacing particle systems with a random top line occur in certain types of lozenge tiling models. More precisely, we are interested in those tiling models that can be decomposed into two regions, such that after possibly adding *virtual particles*, these the regions become interlacing regions of the type describe in section 1.2, glued together along a common line as depicted in figure 15.

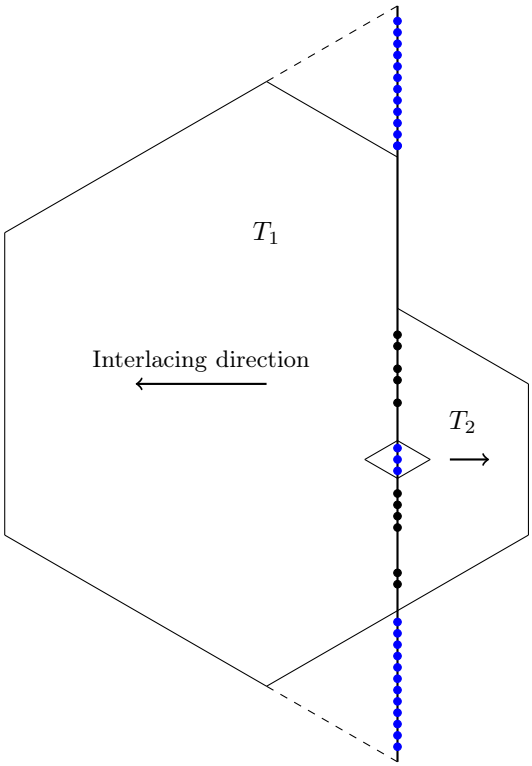

Figure 15: Decomposition of a polygon into two interlacing regions T_1 and T_2 glued together along the thick black line. The blue dots indicate the positions of *virtual* particles/tiles and the black dots indicate the positions of ordinary particles/tiles.

Recall that the number of interlacing configurations with a given top line configuration $(y_1, y_2, ..., y_N) \in \mathbb{Z}^N$ is given by Weyl's dimension formula in [24] for the irreducible characters of the unitary group $U(n)$,

$$\mathcal{N}^\sharp(y_1, ..., y_N) = \frac{\prod_{1\leqslant i<j\leqslant N} |y_i - y_j|}{\prod_{1\leqslant i<j\leqslant N} |i-j|} := \frac{1}{2C_N} \prod_{\substack{1\leqslant i,j\leqslant N \\ i\neq j}} |y_i - y_j|. \tag{1.52}$$

Let $(y_1, y_2, ..., y_N)$ be the positions of the particles/tiles on the intersecting thick black line as in figure 15. Let $\mathcal{V}$ be the index set for the *virtual* or *frozen* particles and let $\mathcal{F}$ be the index set for the *free* particles,

so that $|\mathcal{V}| + |\mathcal{F}| = N$, and y_i is a *virtual* particle if $i \in \mathcal{V}$ and *free* otherwise. Assume that $|\mathcal{F}| = n$, and let $g : \{1, ..., n\} \to \mathcal{F}$ be a set bijection such that $x_i := y_{g(i)}$, and $x_1 < x_2 < ... < x_n$. Furthermore, the *virtual* particles are densely packed, which implies that they vill form wedge shaped frozen regions. However, the fact that the two interlacing regions T_1 and T_2 need not be symmetrical implies that we need not have frozen regions on both sides of the intersecting black line. Let $\mathcal{V}_L \subseteq \mathcal{V}$ be the index set of those *virtual* particles such that they form a frozen region to the left, and let $\mathcal{V}_R \subseteq \mathcal{V}$ be the index set of those *virtual* particles such that they form a frozen region to the right. Then by (1.52), the number of interlacing configuration with a given fixed configuration of free particles at positions $(x_1, ..., x_n)$ is given by

$$\begin{aligned}
\mathcal{M}^\sharp(x_1, ..., x_n) &= \frac{1}{2C_N} \prod_{1 \leqslant i < j \leqslant N} |y_i - y_j| \\
&= \frac{1}{2C_N} \prod_{\substack{i,j \in \mathcal{F} \\ i \neq j}} |y_i - y_j|^2 \prod_{\substack{i \in \mathcal{F} \\ j \in \mathcal{V}_L}} |y_i - y_j| \prod_{\substack{i \in \mathcal{F} \\ j \in \mathcal{V}_R}} |y_i - y_j| \prod_{\substack{i,j \in \mathcal{V}_L \\ i \neq j}} |y_i - y_j| \prod_{\substack{i,j \in \mathcal{V}_R \\ i \neq j}} |y_i - y_j| \\
&= \frac{1}{2C_N} \prod_{\substack{1 \leqslant k,l \leqslant n \\ k \neq l}} |x_k - x_l|^2 \prod_{k=1}^{n} \prod_{j \in \mathcal{V}_L} |x_k - y_j| \prod_{k=1}^{n} \prod_{j \in \mathcal{V}_R} |x_k - y_j| \prod_{\substack{i,j \in \mathcal{V}_L \\ i \neq j}} |y_i - y_j| \prod_{\substack{i,j \in \mathcal{V}_R \\ i \neq j}} |y_i - y_j|.
\end{aligned}$$

Now, consider the set of all possible lozenge tessellations of the the original polygon. One easily sees that each such tessellation is in a bijective correspondence with two interlacing configurations on T_1 and T_2 with the same configuration of *free* particles $x^{(n)} = (x_1, x_2, ..., x_n)$ on their common top line. In particular, $x_i \in \Sigma_n$ for each $i = 1, ..., n$, where Σ is a finite union of intervals. The set $\mathcal{X}_n$ then denotes the set of all configurations of *free* particles. Consider the set of all lozenge tessellations of the polygon with uniform distribution. Then this induces a probability distribution on $\mathcal{X}_n$, given by

$$p^{(n)}(x_1, ..., x_n) = \mathbb{P}[\text{particles at positions } x_1, x_2, ..., x_n] = \frac{\mathcal{M}^\sharp(x_1, ..., x_n)}{\sum\limits_{(x_1,...,x_n) \in \mathcal{X}_n} \mathcal{M}^\sharp(x_1, ..., x_n)}.$$

Let

$$w_n(x) := \prod_{j \in \mathcal{V}_L} |x - y_j| \prod_{j \in \mathcal{V}_R} |x - y_j|.$$

Then

$$p^{(n)}(x_1, ..., x_n) = \frac{1}{Z_n} \prod_{1 \leqslant i < j \leqslant n} (x_i - x_j)^2 \prod_{i=1}^{n} w_n(x_i) = \frac{1}{Z_n} \Delta_n(x)^2 \prod_{i=0}^{n} w_n(x_i), \tag{1.53}$$

where Z_n is a normalization constant, and $\Delta_n(x)$ is the Vandermonde determinnat. Associated with a particular weight function $w_n(x)$ is a class of discrete orthogonal polynomials $\{p_{n,k}(x)\}_k$ satisfying

$$\sum_{x \in \Sigma_n} p_{n,k}(x) p_{n,l}(x) w_n(x) = \delta_{kl}. \tag{1.54}$$

Such particle processes are called *discrete orthogonal polynomial ensembles*, DOPE, and have been studied e.g. in [4]. In particular if one considers the random empirical measure $\mu_n = \frac{1}{n} \sum_{i=1}^{n} \delta_{x_i}$, then $\mu_n \rightharpoonup \mu_V^\lambda$, where the measure $\mu_V^\lambda \in \mathcal{M}_1^\lambda(\Sigma)$ is the unique solution of the constrained variational problem

$$\min_{\nu \in \mathcal{M}_1^\lambda(\Sigma)} \{I_V[\nu]\} = \min_{\nu \in \mathcal{M}_1^\lambda(\Sigma)} \left\{ \int_{\Sigma \times \Sigma} \log |x - y|^{-1} d\nu(x) d\nu(y) + \int_\Sigma V(x) d\nu(x) \right\}, \tag{1.55}$$

where $V(x) = \lim_{n\to\infty} -n^{-1}\log(w_n(x))$. In the case of those problems originating from a random tiling model as above, the potential will be of the form

$$V(x) = U^{\chi_{I^r}}(x) + U^{\chi_{I^l}}(x), \tag{1.56}$$

where I^r and I^l are finite unions of closed intervals of $\mathbb{R}$, such that $(I^r \cup I^l)^\circ \cap \Sigma^\circ = \varnothing$. In particular $\lim_{n\to\infty} -n^{-1}\log(w_n(x)) = V(x)$ uniformly on compact subsets of Σ not containing the subset $\partial\Sigma \cap \partial(I^r \cup I^l)$. It follows from Theorem 2.1 in [7] that the minimizer μ_V^λ of the variational problem (1.55) has a unique the characterization in terms of the following variational inequalities.

There exists a constant F_V^λ such that

$$2U^{\mu_V^\lambda}(x) + V(x) \geqslant F_V^\lambda \quad \text{for all } x \in \Sigma\backslash\text{supp}(\mu_V^\lambda) := I_V \tag{1.57}$$

$$2U^{\mu_V^\lambda}(x) + V(x) = F_V^\lambda \quad \text{for all } x \in \text{supp}(\mu_V^\lambda) \cap \text{supp}(\lambda - \mu_V^\lambda) := I_B \tag{1.58}$$

$$2U^{\mu_V^\lambda}(x) + V(x) \leqslant F_V^\lambda \quad \text{for all } x \in \Sigma\backslash(\text{supp}(\mu_V^\lambda) \cap \text{supp}(\lambda - \mu_V^\lambda)) := I_S. \tag{1.59}$$

It follows from general *large deviation estimates* for DOPE that we can define $\mathcal{X}_{reg}^{(n)}$ so that Assumption 3 is satisfied for large classes of potentials, see [11]. In particular, in the class of potentials of the form (1.56) and associated weights w_n coming from certain tiling models, this is proved in the upcoming review article [10].

It is shown in [10] that if $R_1 \cup R_2 \neq \varnothing$, with $\mu = \mu_V^\lambda$, then for $t_c \in R_1 \cup R_2$, we must have $t_c \in \partial\Sigma$. Thus, if in particular $t_c \in R_2$, then there exists an interval $[t_2, t_c]$, such that $[t_2, t_c] \cap \text{supp}(\mu_n) = \varnothing$. This implies that the sequence of empirical measures $\{\mu_n\}_n$ automatically satisfies the left-sided part of regularity assumption in Assumption 3. Let

$$R_m^{(n)}(x_1, ..., x_m) = \mathbb{P}[\text{there are particles at each of the nodes } x_1, ..., x_m] \tag{1.60}$$

be the m:th correlation kernel with $1 \leqslant m \leqslant n$. If the potential $V(x)$ is analytic in a complex convex neighbourhood of Σ, then it is proven in Theorem 3.3 and Theorem 3.5 in [4] that for all subsets $V \in I_V$ and $S \in I_S$ such that $d_H(V, I_B) > 0$ and $d_H(S, I_B) > 0$ there exists constants $K = K(d_H(V, I_B)) > 0$ and $L = L(d_H(S, I_B)) > 0$, such that

$$\max_{x_1,...,x_m \in V} |R_m^{(n)}(x_1, ..., x_m)| \leqslant C_V \frac{e^{-mnK_V}}{n^m} \tag{1.61}$$

and

$$\max_{x_1,...,x_m \in S} |1 - R_m^{(n)}(x_1, ..., x_m)| \leqslant C_S \frac{e^{-mnL_S}}{n^m} \tag{1.62}$$

for some positive constants C_V and C_S. In particular this implies that we can define $\mathcal{X}_{reg}^{(n)}$ so that Assumption 3 holds. Unfortunately, the class of potentials given by (1.56) need not be analytic in a neighborhood of Σ due to the fact that we may have $\partial\Sigma \cap \partial(I^r \cup I^l) \neq 0$. However, the we believe that by additional local arguments around such points, one may generalize the methods used in the book [4] to prove that Theorem 3.3 and Theorem 3.5 in [4] also hold in this case. In particular, the effect of non-analyticity should only matter on a very small neighborhood around the points of $\partial\Sigma \cap \partial(I^r \cup I^l)$. Since $t_c \notin \partial\Sigma \cap \partial(I^r \cup I^l)$, and therefore is a macroscopic distance away from $\partial\Sigma \cap \partial(I^r \cup I^l)$, the effects of non-analyticity should not matter.

Finally, let $A \subset \mathbb{R}$ be an interval and let K be a compact subset of $\{z \in \mathbb{C} : d_H(z, A \cap \text{supp}(\mu_n)) > 0\}$. Then, for a "generic" potential V, and a sequence of weight functions $\{w_n(x)\}_n$, such that $\lim_{n\to\infty} -n^{-1}\log(w_n(x)) = V(x)$ uniformly on compact subsets of Σ, we should have for every $\varepsilon > 0$ and every $z \in K$ that

$$\lim_{n\to\infty} \mathbb{P}\left[\left|\int_{\mathbb{R}} \frac{\chi_A(t) d(\mu_n - \mu)(t)}{z - t}\right| > \frac{1}{n^{1-\varepsilon}}\right] = 0. \tag{1.63}$$

In particular, this implies that we can define $\mathcal{X}_{reg}^{(n)}$ so that Assumption 4 holds. This result should also follow from Riemann-Hilbert methods adapted to the class of potentials derived from tiling models, with the caveat that some of the local arguments need to be modified due to the possible non-analyticity of $V(x)$ at some of the points of $\partial\Sigma$. This questions has also been studied in [5] for very similar models by means of *discrete loop equations*, though the assumptions in [5] are not satisfied in our models, and can therefore not be applied directly. However, in the special case when Σ is an interval, the results in [5] do apply. In particular they apply to the model in Example 1.2.

Remark 1.6. Let $z^{(r)} = (y_1^{(r)}, ..., y_r^{(r)}, x_n + n - r - 1, x_n + n - r - 2, ..., x_n)$. Then, using (1.53) the total probability distribution is given by

$$\nu_{tot}[(y^1, ..., y^{(n-1)}, x^{(n)})] = \frac{1}{Z_{n,tot}} \Delta_n(x)^2 \prod_{i=0}^{n} w_n(x_i) \prod_{r=0}^{n-1} \det\left(1_{z_j^{(r+1)} \geqslant z_i^{(r)}}\right).$$

Hence, by the Eynard-Mehta theorem, the total process is also a determinantal process. One could therefore try to derive the correlation kernel for the total process instead of the conditional process. However, the Eynard-Mehta formula for the kernel of this process seems very difficult to analyze. In particular, we can not expect to get such a simple formula for the kernel as (1.2), as it would necessarily need to contain all the information about the DOPE, which is highly non-trivial.

Example 1.2. Consider now the example discussed briefly in section 1.1 see fig 2. This can be approached via the tiling model illustrated in figure 16. Elementary geometry gives $\delta = \frac{2}{\sqrt{3}} - 2\kappa$, where $\kappa \in (0, 1/\sqrt{3})$. In the figure we have added densely packed virtual particles in the intervals $[0, \kappa]$ and $[2\kappa + 2\delta, 3\kappa + 2\delta]$. Moreover, the particles contained in the interval $[\kappa + \delta, 2\kappa + 2\delta]$ are distributed according to a *discrete orthogonal polynomial ensemble*, DOPE, as is shown above. The fraction of particles contained in this interval as $n \to \infty$ equals $1 - \sqrt{3}\kappa$. We will now make the symmetric parameter choice $\kappa = \delta = \frac{2}{3\sqrt{3}}$. Associated to the DOPE, there is an equilibrium measure with respect to an external field as above. See also Proposition 2.2 in [5]. Solving the minimization problem gives the density of the measure μ,

$$\rho(t) = \chi_{[0, \frac{2}{3\sqrt{3}}]}(t) + \chi_{[\frac{8}{3\sqrt{3}}, \frac{10}{3\sqrt{3}}]}(t) + \phi(3t)\chi_{[\frac{4}{3\sqrt{3}}, \frac{8}{3\sqrt{3}}]}(t), \tag{1.64}$$

where

$$\begin{aligned}\phi(x) = &-\frac{\sqrt{(b-x)(x-a)}}{2\pi} \int_0^{2/\sqrt{3}} \frac{dt}{\sqrt{(t-a)(t-b)}(t-x)} - \frac{\sqrt{(b-x)(x-a)}}{\pi} \int_{4/\sqrt{3}}^{a} \frac{dt}{\sqrt{(t-a)(t-b)}(t-x)} \\ &+ \frac{\sqrt{(b-x)(x-a)}}{2\pi} \int_{8/\sqrt{3}}^{10/\sqrt{3}} \frac{dt}{\sqrt{(t-a)(t-b)}}.\end{aligned} \tag{1.65}$$

Here (a, b) is the unique solution of

$$-\frac{1}{2} \int_0^{2/\sqrt{3}} \frac{dt}{\sqrt{(t-a)(t-b)}} - \int_{4/\sqrt{3}}^{a} \frac{dt}{\sqrt{(t-a)(t-b)}} + \frac{1}{2} \int_{8/\sqrt{3}}^{10/\sqrt{3}} \frac{dt}{\sqrt{(t-a)(t-b)}} = 0 \tag{1.66}$$

and

$$-\frac{1}{2} \int_0^{2/\sqrt{3}} \frac{tdt}{\sqrt{(t-a)(t-b)}} - \int_{4/\sqrt{3}}^{a} \frac{tdt}{\sqrt{(t-a)(t-b)}} + \frac{1}{2} \int_{8/\sqrt{3}}^{10/\sqrt{3}} \frac{tdt}{\sqrt{(t-a)(t-b)}} = 1 \tag{1.67}$$

satisfying $\frac{4}{\sqrt{3}} < a < b < \frac{8}{\sqrt{3}}$. In particular it follows that $\rho\big|_{[\frac{4}{3\sqrt{3}}, a]} \equiv 1$. A direct verification that the Cauchy transform of ρ satisfies Assumption 2 for $t_c = \frac{4}{3\sqrt{3}}$ is very difficult using (1.65)-(1.67) even in the case when the original polygon has an apparent symmetry. This is due to the artificial decomposition of the polygon into two interlacing regions which are glued together along a common boundary. After this

decomposition has been done, the original symmetry is no longer apparent in the parametrization of the *edge* $\mathcal{E}$. We will therefore prove that the asymptotic cusp condition holds by an indirect symmetry argument. Instead of considering figure 16, we consider figure 17. We see the yellow dashed line corresponds to the decomposition in figure 16 into two interlacing regions glued together along the yellow dashed line. However, we may equally well decompose our hexagon into two interlacing regions in blue particles glued together along the dashed blue line instead. Moreover there is bijective correspondence between each configuration of blue and yellow particles given by a reflection in the dashed black symmetry line. This implies in particular that the *edge* $\mathcal{E}$ must posses a reflection symmetry in the dashed black line. Now, the parametrization of the *edge* $\mathcal{E}$, given by the density (1.65) and (1.13)-(1.16) is smooth by Remark 2.1 in [8], in fact real analytic. Since the density ρ of the limit measure μ satisfies $\rho\big|_{[\frac{4}{3\sqrt{3}},a]} = 1$, it follows from Lemma 2.7 in [8], that $\mathcal{E}$, is tangent to the line $\chi + \eta - 1 = \frac{4}{3\sqrt{3}}$. However, by Theorem 2.3 in [8], the parametrization is injective. This together with the fact that the only singularities of the *edge* $\mathcal{E}$ are cusps implies the *edge* $\mathcal{E}$ has a cusp at the tangent point with the line $\chi + \eta - 1 = \frac{4}{3\sqrt{3}}$. Lemma 2.8 and Lemma 2.9 in [8], implies that $f''(\frac{4}{3\sqrt{3}}; \chi_{\mathcal{E}}(\frac{4}{3\sqrt{3}}), \eta_{\mathcal{E}}(\frac{4}{3\sqrt{3}})) = 0$. Hence, modulo the technical issues discussed above about how to construct $\mathcal{X}_{reg}^{(n)}$, we get a cusp-point where the scaling limit is given by the Cusp-Airy process.

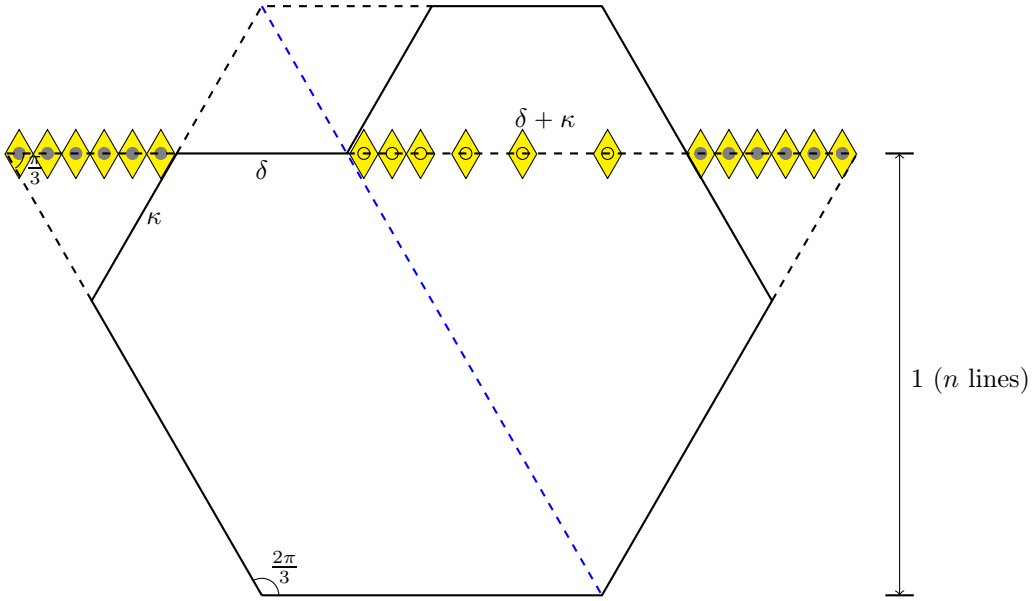

Figure 16:

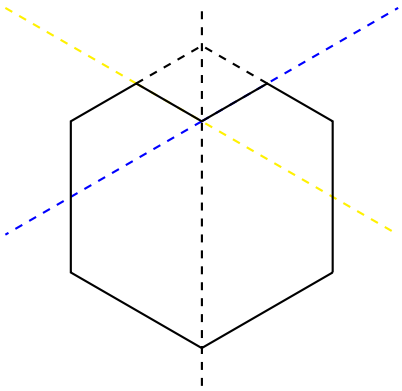

Figure 17:

1.10 Outline of the Paper

We now give a brief outline of the paper. In section 2.1 we prove Lemma 1.2. Due to the fact that $f'''(t_c, \chi_c, \eta_c) > 0$, it will be necessary to change the integration contours of the correlation kernel given in Proposition 1.2 to be able to deform the contours to the local steepest ascent/descent contours. This is done section 2.1. In section 2.3 we prove the existence of global ascent/descent contours and finally in sections 2.4 and 2.5 we perform the local asymptotic analysis to arrive at the final result

In section 3.1 we prove a certain reflection symmetry of the Cusp-Airy kernel in the axis $r = 0$. In section 3.2 we proceed to prove an alternative representation of the the Cusp-Airy kernel in terms of r-Airy integrals and certain polynomials. In section 4 we derive the integral representation of the kernel for the interlacing particle system, or the yellow particles and prove Proposition 1.1.

2 Proof of Main Result

2.1 Discrete Cancellation in the Correlation Kernel

In this section we will perform the discrete cancellation of factors in the correlation kernel (1.2). In the continuum limit, this corresponds to the cancellation between the measures μ and λ on the interval $[t_c, t_1]$, where $\mu\big|_{[t_c,t_1]} = \lambda$. The difference is that on the discrete level, the cancellation need no longer be exact.

We now prove Lemma 1.2

Proof. Using Assumption 3 and the definition of $t_c^{(n)}, t_1^{(n)}$ and $t_2^{(n)}$ we have

$$\begin{aligned}
\frac{\prod_{i=1}^{n}(w-\beta_i^{(n)})}{\prod_{k=x_1+y_1-n}^{x_1}(w-k)} &= \frac{\prod_{\beta_i^{(n)}\leqslant nt_2^{(n)}}(w-\beta_i^{(n)})\prod_{k=nt_c^{(n)}}^{nt_1^{(n)}}(w-k)\prod_{nt_1^{(n)}<\beta_i^{(n)}}(w-\beta_i^{(n)})}{\prod_{k=x_1+y_1-n}^{x_1}(w-k)} \\
&= \frac{\prod_{k=nt_c^{(n)}}^{nx_c^{(n)}}(w-k)}{\prod_{k=x_1+y_1-n}^{x_1}(w-k)}\frac{\prod_{\beta_i^{(n)}\leqslant nt_2^{(n)}}(w-\beta_i^{(n)})\prod_{nt_1^{(n)}<\beta_i^{(n)}}(w-\beta_i^{(n)})}{\prod_{k=nt_1^{(n)}+1}^{nx_c^{(n)}}(w-k)} \\
&= \frac{\prod_{k=nt_c^{(n)}}^{x_1}(w-k)}{\prod_{k=x_1+y_1-n}^{x_1}(w-k)}\frac{\prod_{k=nt_c^{(n)}}^{nx_c^{(n)}}(w-k)}{\prod_{k=nt_c^{(n)}}^{x_1}(w-k)}\frac{\prod_{\beta_i^{(n)}\leqslant nt_2^{(n)}}(w-\beta_i^{(n)})\prod_{nt_1^{(n)}<\beta_i^{(n)}}(w-\beta_i^{(n)})}{\prod_{k=nt_1^{(n)}+1}^{nx_c^{(n)}}(w-k)} \\
&= q_n(w;r)Q_n(w;\Delta x_1^{(n)})E_n(w),
\end{aligned}$$

where we have used the definitions of q_n, Q_n and E_n. Similarly, we get

$$\frac{\prod_{i=1}^{n}(z-\beta_i^{(n)})}{\prod_{k=x_2+y_2-n}^{x_2-1}(z-k)} = (z-x_2)q_n(z;r)Q_n(z;\Delta x_1^{(n)})E_n(z).$$

Finally we rescale the integration variables according to $w \to \frac{1}{n}w$ and $z \to \frac{1}{n}z$. Set $\Gamma_n = \frac{1}{n}\mathscr{Z}_n$, $\tilde{\Gamma}_n = \frac{1}{n}\tilde{\mathscr{Z}}_n$, and $\gamma_n = \tilde{\gamma}_n = \frac{1}{n}\mathscr{W}_n$. Since we have cancelled out poles we may deform Γ_n to be a contour that contains the set $\{n^{-1}\beta_i^{(n)} \geqslant t_1^{(n)}\}$ but not the set $\{n^{-1}\beta_i^{(n)} \leqslant t_c^{(n)} + s\}$. Similarly, we may deform Γ'_n to contain the set $\{n^{-1}\beta_i^{(n)} \leqslant t_c^{(n)} + s\}$ but not the set $\{n^{-1}\beta_i^{(n)} \geqslant n^{-1}t_1^{(n)}\}$. □

2.2 Change of Integration Contours

In order to perform a steepest descent analysis in a later section, it will be necessary to change the integration contours so that they may be suitably deformed around the critical point.

Proposition 2.1. *The correlation kernel can be rewritten as*

$$K_{\mathcal{R}}^{(n)}((\xi_n, r)(\mu_n, s)) = -1_{x_1 \geqslant x_2} B_n((x_1, y_1), (x_2, y_2)) + \tilde{K}_{\mathcal{R}}^{(n)}((x_1, y_1), (x_2, y_2)), \tag{2.1}$$

where

$$\tilde{K}_{\mathcal{R}}^{(n)}((x_1, y_1), (x_2, y_2)) = \frac{1}{(2\pi i)^2}\oint_{\Gamma_n^1+\Gamma_n^2} dz \oint_{\gamma_n^1+\gamma_n^2} dw \frac{1}{z - n^{-1}x_2}\frac{q(nw;r)}{q(nz;s)}\frac{e^{n(f_n(w)-f_n(z))+n(h_{n,1}(w)-h_{n,2}(z)}}{w-z} \tag{2.2}$$

and

$$B_n((x_1, y_1), (x_2, y_2)) = \frac{1}{2\pi i}\oint_{\Gamma_n^2} dz \frac{1}{z - n^{-1}x_2}\frac{q(nz;r)}{q(nz;s)} e^{n(h_{n,1}(z)-h_{n,2}(z))}. \tag{2.3}$$

Here the contours are as in figure 18; more precisely:

- Γ_n^1 *is a counter-clockwise oriented contour that contains the interval* $[t_c^{(n)} - \max\{|r|, |s|\}, b_n]$ *and nothing else of the support of* ν_n. *Furthermore,* Γ_n^1 *contains the contours* Γ_n^2, γ_n^2 *and* γ_n^3

- Γ_n^2 *is a clockwise oriented contour that contains* γ_n^2 *and the interval* $[t_c^{(n)} - \max\{|r|, |s|\}, t_c^{(n)} + \max\{|r|, |s|\}]$ *and nothing else of the support of* ν_n.

- γ_n^1 *is a clockwise oriented contour that contains the interval* $[t_1^{(n)}, b_n]$ *and nothing else of the support of* ν_n.

- γ_n^2 *is a clockwise oriented contour that contains the interval* $[t_c^{(n)} - \max\{|r|, |s|\}, t_c^{(n)} + \max\{|r|, |s|\}]$ *and nothing else of the support of* ν_n.

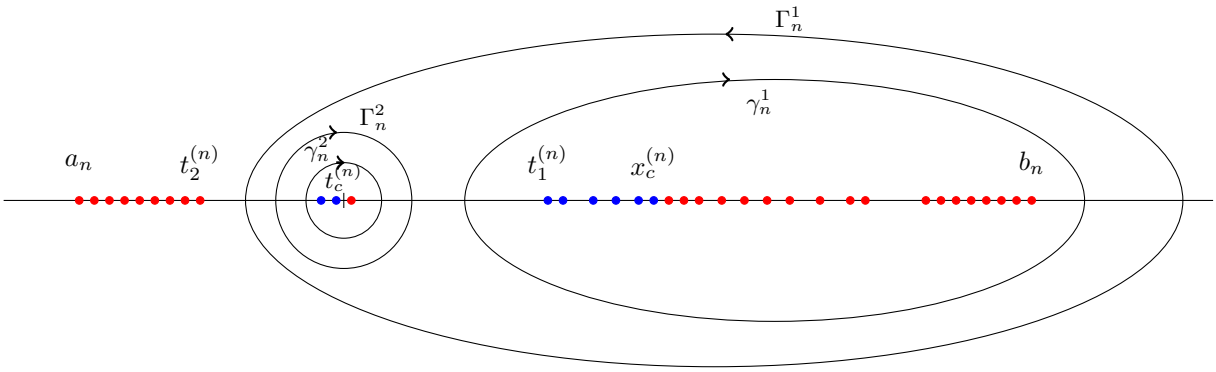

Figure 18: Integration contours

Proof. The starting point is lemma 1.2. The proof will consist of a series of deformations of the contours. It will be convenient to introduce the notation

$$J^{(n)}_{\Gamma,\gamma} := \frac{1}{(2\pi i)^2}\oint_{\Gamma} dz \oint_{\gamma} dw \frac{1}{z - n^{-1}x_2}\frac{q_n(nw;r)}{q_n(nz;s)}\frac{Q_n(nw;\Delta x_1^{(n)})}{Q_n(nz;\Delta x_2^{(n)})}\frac{E_n(nw)E_n(nz)^{-1}}{w-z}$$

for some contours Γ, γ. First assume that $x_1 < x_2$ and consider the deformation of γ_n in figure 13 into two contours γ_n^2 and γ_n^0 as shown in figure 19. Next consider adding the contour γ_n^1. This is shown in figure 20. Consider the contour $\gamma_n^0 + \gamma_n^1$. Then the integrand of $K_{\mathcal{R}}^{(n)}$ in (1.39) has one residue inside the domain bounded by γ_n^1 and γ_n^0. Computing this residue gives

$$\begin{aligned}
&\frac{1}{(2\pi i)^2}\oint_{\Gamma_n} dz \oint_{\gamma_n^0\cup\gamma_n^1} dw \frac{1}{z - n^{-1}x_2}\frac{q_n(nw;r)}{q_n(nz;s)}\frac{Q_n(nw;\Delta x_1^{(n)})}{Q_n(nz;\Delta x_2^{(n)})}\frac{E_n(nw)E_n(nz)^{-1}}{w-z}\\
&= \frac{1}{2\pi i}\oint_{\Gamma_n}\frac{\prod_{k=x_2+y_2-n}^{x_2-1}(nz-k)}{\prod_{k=x_1+y_1-n}^{x_1}(nz-k)}dz = \frac{1}{2\pi i}\oint_{\Gamma_n}\frac{\prod_{k=nt_c^{(n)}+s}^{x_2-1}(nz-k)}{\prod_{k=nt_c^{(n)}+r}^{x_1}(nz-k)}dz\\
&= \frac{1}{2\pi i}\oint_{\Gamma_n}\frac{q_n(nz;r)}{q_n(nz;s)}\prod_{k=x_1+1}^{x_2-1}(nz-k)dz = 0,
\end{aligned}$$

since Γ_n contains no poles. Hence

$$J^{(n)}_{\Gamma_n\gamma_n^0} = -J^{(n)}_{\Gamma_n\gamma_n^1} \tag{2.4}$$

Next, we deform the contour Γ_n into the contours Γ_n^1 and Γ_n^2 according to Figure 21. This gives us

$$\begin{aligned}
J_{\Gamma_n\gamma_n} &= J_{\Gamma_n\gamma_n^0} + J_{\Gamma_n\gamma_n^2}\\
&= -J_{\Gamma_n\gamma_n^1} + J_{\Gamma_n\gamma_n^2} \quad \text{by (2.4)}\\
&= -(J_{\Gamma_n^1\gamma_n^1} + J_{\Gamma_n^2\gamma_n^1}) + (J_{\Gamma_n^1,-\gamma_n^2} + J_{\Gamma_n^2,-\gamma_n^2}).
\end{aligned}$$

We now instead assume that $x_1 \geqslant x_2$. We then deform deform the contour $\tilde{\Gamma}_n$ into the contours $\tilde{\Gamma}_n^1$ and $\tilde{\Gamma}_n^2$ according to figure 22. Finally, we deform the contour $\tilde{\gamma}_n$ into the contours $\tilde{\gamma}_n^0$, $\tilde{\gamma}_n^2$ and $\tilde{\gamma}_n^1$, according to figure 23. However, using that the only residue contained in $\tilde{\gamma}_n^0$ is the pole $(w-z)^{-1}$, we get

$$J^{(n)}_{\tilde{\Gamma}_n^1\tilde{\gamma}_n^0} = \frac{1}{2\pi i}\oint_{\tilde{\Gamma}_n^1}\frac{q_n(nz;r)}{q_n(nz;s)}\prod_{k=x_1+1}^{x_2-1}(nz-k)dz = 0,$$

since the contour $\tilde{\Gamma}_n^1$ contains no poles in z. Similarly, we get that

$$J^{(n)}_{\tilde{\Gamma}_n^2\tilde{\gamma}_n^0} = 0$$

since $\tilde{\gamma}_n^0$ contains no poles in w. This gives

$$J^{(n)}_{\tilde{\Gamma}_n\tilde{\gamma}_n} = J^{(n)}_{\tilde{\Gamma}_n^1\tilde{\gamma}_n^2} + J^{(n)}_{\tilde{\Gamma}_n^1\tilde{\gamma}_n^1} + J^{(n)}_{\tilde{\Gamma}_n^2\tilde{\gamma}_n^2} + J^{(n)}_{\tilde{\Gamma}_n^2\tilde{\gamma}_n^1},$$

where the contours are shown in figure 24. We now deform the contour $\tilde{\Gamma}_n^1$ into $\tilde{\Gamma}_n^3 + C_R$ according to figure 25. Clearly the contribution along ℓ vanish and to prove that the contribution from C_R vanishes as $R \to \infty$ we observe that that $g_{n,2}(z) = \nu_{n,2}(\mathbb{R}) \log|z| + O(|z|^{-1})$ and $\lim_{n\to\infty} \nu_{n,2}(\mathbb{R}) = \nu(\mathbb{R}) > 0$. From this it is not difficult to see that $\lim_{R\to\infty} |J^{(n)}_{C_R\tilde{\gamma}_n^i}| = 0$.

We now have the contours as shown in figure 26. Using that $\tilde{\Gamma}_n^3 = -\Gamma_n^1$, $\tilde{\gamma}_n^1 = -\gamma_n^1$and $\tilde{\Gamma}_n^2 = -\Gamma_n^2$, where the minus sign means orientation reversion, we get

$$\begin{aligned} J^{(n)}_{\tilde{\Gamma}_n\tilde{\gamma}_n} &= J^{(n)}_{\tilde{\Gamma}_n^3\tilde{\gamma}_n^1} + J^{(n)}_{\tilde{\Gamma}_n^3\tilde{\gamma}_n^2} + J^{(n)}_{\tilde{\Gamma}_n^2\tilde{\gamma}_n^1} + J^{(n)}_{\tilde{\Gamma}_n^2\tilde{\gamma}_n^2} \\ &= J^{(n)}_{\Gamma_n^1\gamma_n^1} - J^{(n)}_{\Gamma_n^1\tilde{\gamma}_n^2} + J^{(n)}_{\Gamma_n^2\gamma_n^1} - J^{(n)}_{\Gamma_n^2\tilde{\gamma}_n^2}. \end{aligned}$$

We see that γ_n^2 is inside Γ_n^2 which is inside $\tilde{\gamma}_n^2$. Using the residue theorem we find

$$\begin{aligned} J^{(n)}_{\Gamma_n^2\tilde{\gamma}_n^2} - J^{(n)}_{\Gamma_n^2,-\gamma_n^2} &= \frac{1}{(2\pi i)^2}\oint_{\Gamma_n^2} dz \frac{1}{z - n^{-1}x_2}\frac{q_n(nz;r)}{q_n(nz;s)}\frac{Q_n(nz;\Delta x_1^n)}{Q_n(nz;\Delta x_2^{(n)})} \\ &= \frac{1}{(2\pi i)^2}\oint_{\Gamma_n^2} dz \frac{1}{z - n^{-1}x_2}\frac{q_n(nz;r)}{q_n(nz;s)} e^{n(h_{n,1}(w) - h_{n,2}(z))} \\ &:= B_n((x_1,y_1),(x_2,y_2)). \end{aligned}$$

Furthermore, $J^{(n)}_{\Gamma_n^1\tilde{\gamma}_n^2} = J^{(n)}_{\Gamma_n^1,-\gamma_n^2}$. Together, this gives

$$J^{(n)}_{\tilde{\Gamma}_n\tilde{\gamma}_n} = J^{(n)}_{\Gamma_n^1\gamma_n^1} - J^{(n)}_{\Gamma_n^1,-\gamma_n^2} + J^{(n)}_{\Gamma_n^2\gamma_n^1} - J^{(n)}_{\Gamma_n^2,-\gamma_n^2} - B_n.$$

Hence, by lemma 1.2, we get

$$\begin{aligned} &K^{(n)}_{\mathcal{R}} = -1_{x_1<x_2} J^{(n)}_{\Gamma_n\gamma_n} + 1_{x_1\geqslant x_2} J^{(n)}_{\tilde{\Gamma}_n\tilde{\gamma}_n} \\ &= -1_{x_1<x_2}(-J^{(n)}_{\Gamma_n^1\gamma_n^1} - J^{(n)}_{\Gamma_n^2\gamma_n^1} + J^{(n)}_{\Gamma_n^1,-\gamma_n^2} + J^{(n)}_{\Gamma_n^2,-\gamma_n^2}) + 1_{x_1\geqslant x_2}(J^{(n)}_{\Gamma_n^1\gamma_n^1} - J^{(n)}_{\Gamma_n^1,-\gamma_n^2} + J^{(n)}_{\Gamma_n^2\gamma_n^1} - J^{(n)}_{\Gamma_n^2,-\gamma_n^2} - B_n) \\ &= -1_{x_1\geqslant x_2} B_n + J^{(n)}_{\Gamma_n^1\gamma_n^1} + J^{(n)}_{\Gamma_n^2\gamma_n^1} - J^{(n)}_{\Gamma_n^1,-\gamma_n^2} - J^{(n)}_{\Gamma_n^2,-\gamma_n^2} \\ &= -1_{x_1\geqslant x_2} B_n + J^{(n)}_{\Gamma_n^1\gamma_n^1} + J^{(n)}_{\Gamma_n^2\gamma_n^1} + J^{(n)}_{\Gamma_n^1\gamma_n^2} + J^{(n)}_{\Gamma_n^2\gamma_n^2} \end{aligned}$$

This gives us finally,

$$\begin{aligned} &K^{(n)}_{\mathcal{R}}((x_1,y_1),(x_2,y_2)) = -1_{x_1\geqslant x_2} B_n((x_1,y_1),(x_2,y_2)) + J^{(n)}_{(\Gamma_n^1+\Gamma_n^2)(\gamma_n^1+\gamma_n^2)} \\ &= -1_{x_1\geqslant x_2}\frac{1}{2\pi i}\oint_{\Gamma_n^2} dz \frac{1}{z - n^{-1}x_2}\frac{q_n(nz;r)}{q_n(nz;s)} e^{n(h_{n,1}(w) - h_{n,2}(z))} \\ &+ \frac{1}{(2\pi i)^2}\oint_{\Gamma_n^1+\Gamma_n^2} dz \oint_{\gamma_n^1+\gamma_n^2} dw \frac{1}{z - n^{-1}x_2}\frac{q_n(nw;r)}{q_n(nz;s)}\frac{e^{n(f_n(w) - nf_n(z)) + n(h_{n,1}(w) - h_{n,2}(z))}}{w - z} \end{aligned}$$

by the definitions of f_n, $h_{n,1}$ and $h_{n,2}$. □

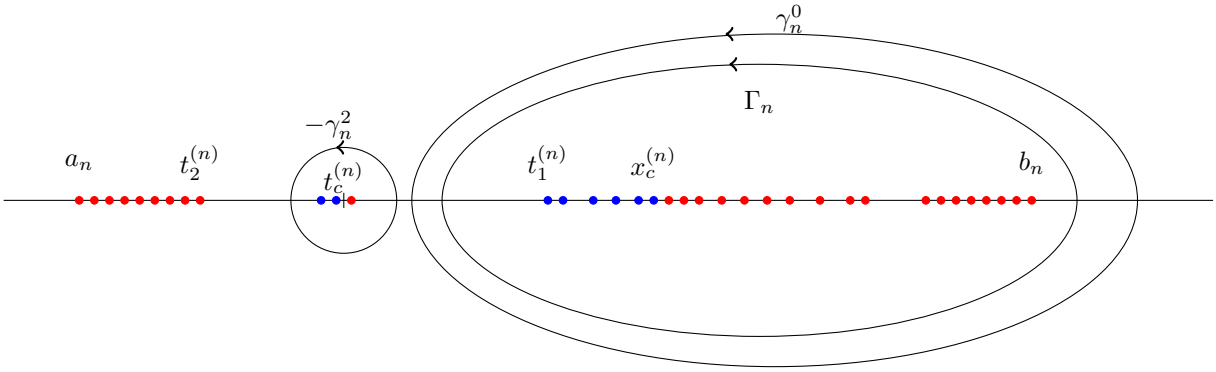

Figure 19: Integration contours

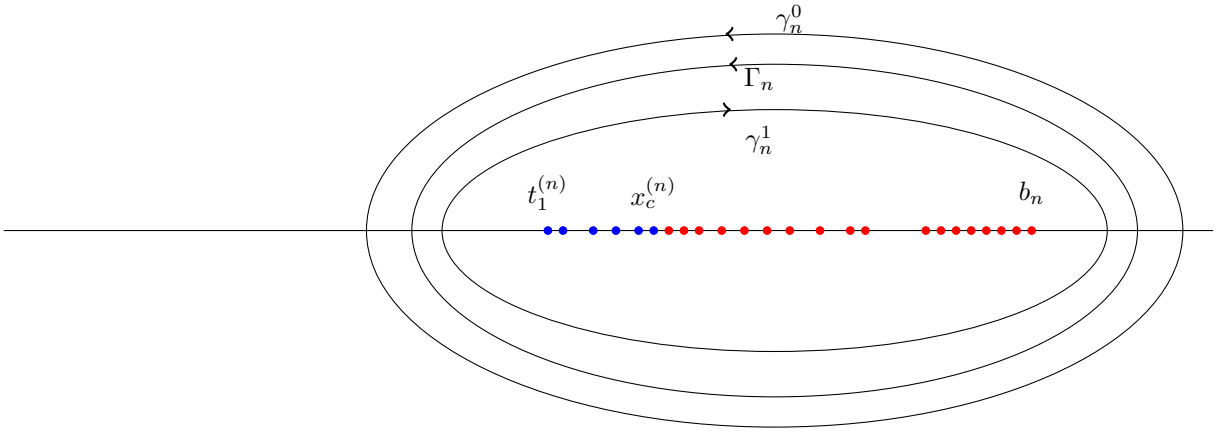

Figure 20: Integration contours

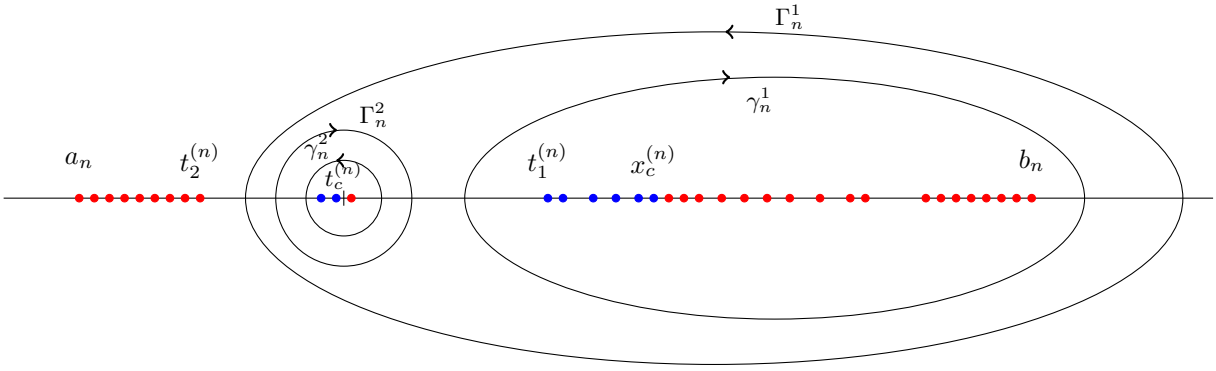

Figure 21: Integration contours

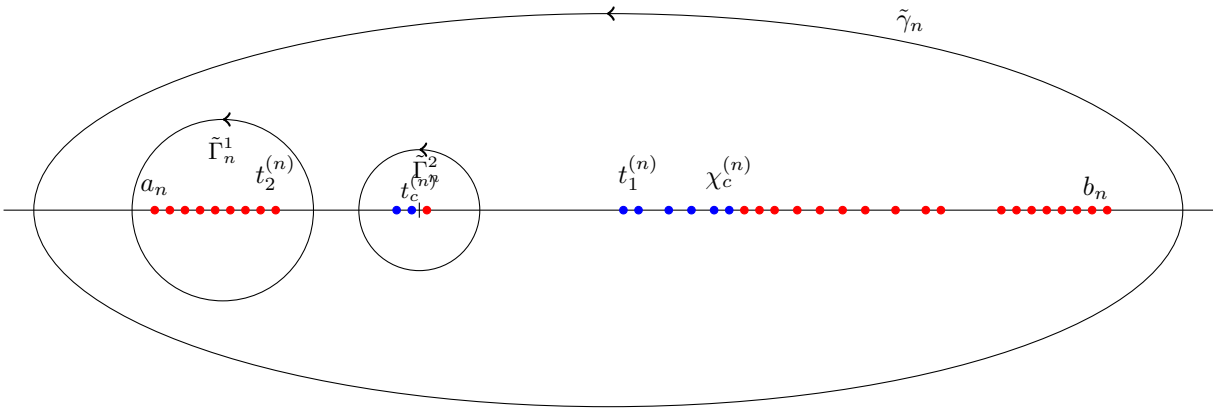

Figure 22: Integration contours

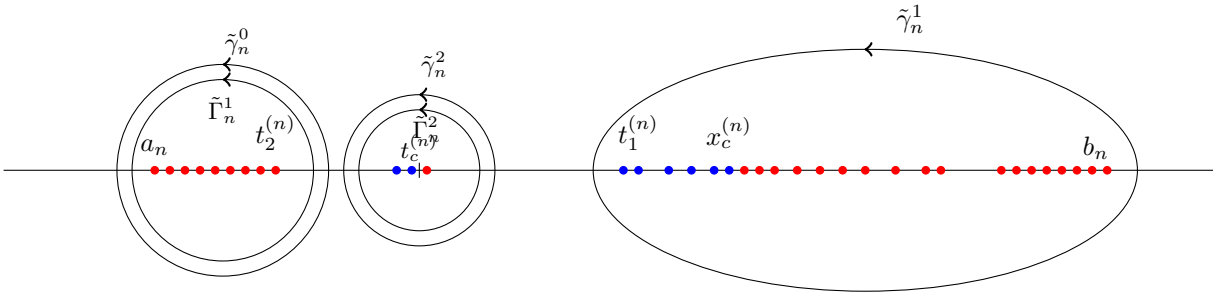

Figure 23: Integration contours

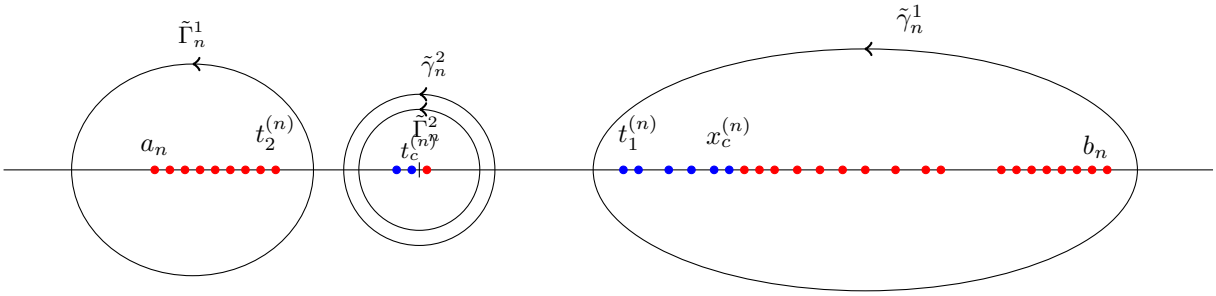

Figure 24: Integration contours

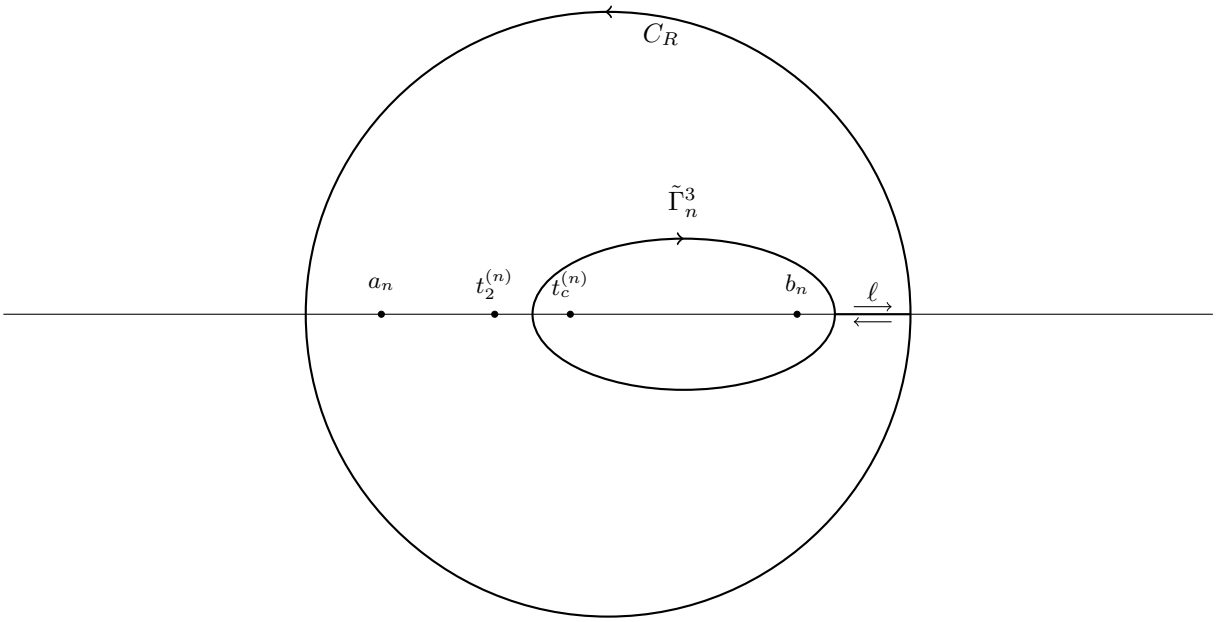

Figure 25: Integration contours

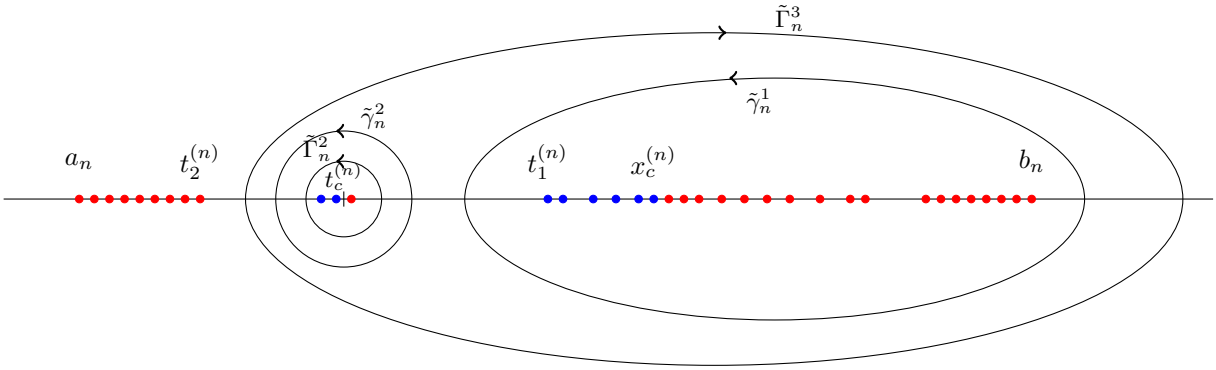

Figure 26: Integration contours

2.3 Global Choice of Contours

Recall the asymptotic function $f(w;\chi_c)$ given by (1.29),

$$f(w;\chi_c) = \int_{\mathbb{R}} \log(w-t)d\nu(t) = U^{\nu}(w) + i\int_{\mathbb{R}} \arg(w-t)d\nu(t).$$

For every $\delta > 0$ we let $\Omega_\delta := \{w \in \mathbb{C} : d(w, \mathrm{supp}(\nu)) > \delta\}$.

Lemma 2.1. *The functions $f_n(w), g_{n,1}(w)$ and $g_{n,2}(w)$ converge uniformly to $f(w;\chi_c)$ on $\overline{\Omega}_\delta \bigcap \overline{B(0,R)}$, for any $\delta > 0$ and any $R > 0$.*

Proof. This is a standard consequence of the weak convergence of μ_n and Vitali's theorem, (see [23] page 157). □

Lemma 2.2. *Consider the function $\nu([x,+\infty))$, where the measure ν is as defined in (1.28). Then $\nu([x,+\infty))$ is monotonically decreasing on $(-\infty,t_2)$, constant in (t_2,t_1), monotonically increasing on (t_1,χ_c), and monotonically decreasing on $(\chi_c,+\infty)$. More precisely,*

$$\nu([x,+\infty)) = \begin{cases} \eta_c & \text{if } x \leqslant a \\ \mu([x,+\infty)) - (\chi_c - t_c) & a < x < t_2 \\ \mu([t_c,+\infty)) - (\chi_c - t_c) & t_2 < x < t_1 \\ \mu([\chi_c,+\infty)) - \int_x^{\chi_c}(1-\varphi(t))dt & t_1 \leqslant x \leqslant \chi_c \\ \mu([x,+\infty)) & \chi_c < x < b \\ 0 & x \in (b,+\infty) \end{cases} . \tag{2.5}$$

Proof. By definition of ν we have

$$\begin{aligned} \nu([x,+\infty)) &= \int_x^\infty (\chi_{[a,t_2]}(t) + \chi_{[t_1,\chi_c]}(t) + \chi_{[\chi_c,b]}(t))\varphi(t)dt - \int_x^\infty \chi_{[t_1,\chi_c]}dt \\ &= \int_x^\infty (\chi_{[a,t_2]}(t) + \chi_{[t_c,\chi_c]}(t) + \chi_{[\chi_c,b]}(t))\varphi(t)dt - \int_x^\infty \chi_{[t_c,\chi_c]}dt \\ &= \mu([x,+\infty)) - \int_x^\infty \chi_{[t_c,\chi_c]}(t)dt, \end{aligned}$$

from which (2.5) follows. The monotonicity properties are immediate from these formulas. □

Since $f(\overline{w};\chi_c) = \overline{f(w;\chi_c)}$ it is sufficient to prove the existence of the contours in the upper-half plane $\mathbb{H}$.

Lemma 2.3. *The asymptotic function $f(w;\chi_c)$ has global steepest ascent/descent contours in the upper half plane as shown in figure 27.*

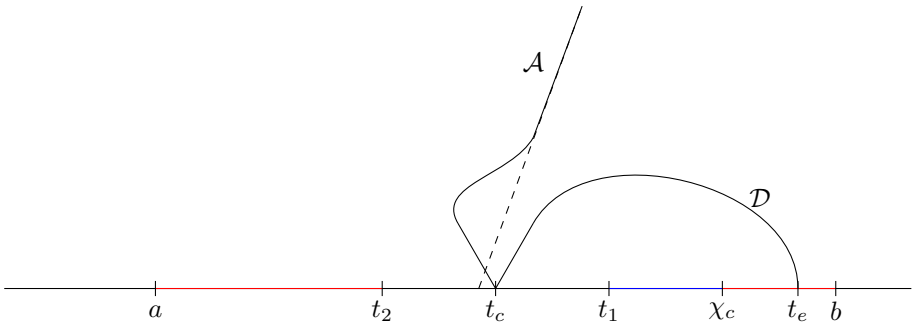

Figure 27: Steepest ascent and descent paths for the asymptotic function $f(w;\chi_c)$. The support of ν^+ is indicated by a red line and the support of ν^- by a blue line.

Proof. Since $f(\overline{w};\chi_c) = \overline{f(w;\chi_c)}$ it is sufficient to prove the existence of the contours in the upper-half plane $\mathbb{H}$. We note that U^ν is real analytic in $\mathbb{C}\backslash\text{supp}(\nu)$ and that $\int_{\mathbb{R}} \arg(w-t)d\nu(t)$ is real analytic in $\mathbb{C}\backslash(-\infty,b]$. Moreover, the boundary values on the real axis are given by

$$\lim_{\substack{w\to x\in\mathbb{R} \\ w\in\mathbb{H}}} U^\nu(w) = U^\nu(x)$$

and

$$\lim_{\substack{w\to x\in\mathbb{R} \\ w\in\mathbb{H}}} \int_{\mathbb{R}} \arg(x-t)d\nu(t) = \pi\nu([x,+\infty)).$$

In particular, $U^\nu(w)$ has a continuous extension to all of $\mathbb{C}$.

Since $f'''(t_c;\chi_c,\eta_c) > 0$ the local steepest ascent/descent structure around t_c is as in figure 28.

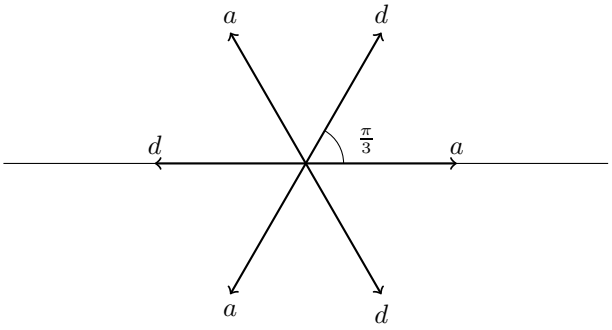

Figure 28: Local steepest ascent/descent contours of the asymptotic function $f(\omega,\chi_c)$, where a denotes ascent contour and d denotes descent contour.

Recall that the contours of steepest ascent/descent are those for which $\operatorname{Im} f(w) = \operatorname{Im} f(t_c) = \pi\mu([t_c,b])$. Note that $U^\nu(w) = \nu(\mathbb{R})\log|w| + O(|w|^{-1})$ as $|w|\to\infty$. Therefore $\lim_{\substack{w\to\infty\\ w\in\mathbb{H}}} U^\nu(w) = +\infty$. This implies that the descent contour have to be contained in some ball $B(0,R)$, R sufficiently large. On the other hand since the function $\operatorname{Im} f(w)$ is real analytic, the curve $\operatorname{Im} f(w) = \operatorname{Im} f(t_c)$ has to be either a closed curve in $B(0,R)\backslash\operatorname{supp}(\nu)$ or end somewhere in $\operatorname{supp}(\nu)$. Assume the first case. Then, clearly there has to be a point $t_p \neq t_c$ on the curve such that $f'(t_p) = 0$. By Theorem 3.1 in [8], we must for such a t_p have $t_p \in \mathbb{R}\backslash\operatorname{supp}(\nu)$ and $f''(t_p) \neq 0$. At such a point we have descent contour exiting at angle $\pm\pi/2$ and ascent contours exiting at 0 and π. This gives a contradiction. We may therefore assume the second case holds

It follows from Lemma 2.2 that if $\pi\nu([t_c,\infty)) < 0$ then the equation $\pi\nu([x,\infty)) = \pi\mu([t_c,+\infty))$ has no solution and the steepest descent contour from t_c has to go to infinity, which is impossible. If $\pi\nu([t_c,\infty)) = 0$, then we have to be in the first case above which is impossible. Thus, $\pi\nu([t_c,\infty)) > 0$ and Lemma 2.2 implies that the equation $\pi\nu([x,\infty)) = \pi\mu([t_c,+\infty))$ has at least one solution t_e for $x \in (\chi_c, b)$ and no solution for $x \in (-\infty,t_2)\cup(t_1,\chi_c)\cup[b,\infty)$. In figure 29 we give a plot of what the function $\pi\nu([x,+\infty))$ may look like. If $\nu([x,\infty))$ is strictly monotonically decreasing at t_e, then t_e is the unique solution to the equation above. Otherwise, by the monotonicity of $\nu([x,\infty))$, there exists an interval $[t_e^-,t_e^+]$ such that $\pi\nu([x,\infty)) = \pi\mu([t_c,+\infty))$ for all $x \in [t_e^-,t_e^+]$. In particular, $(t_e^-,t_e^+)\cap\operatorname{supp}(\mu) = \varnothing$.

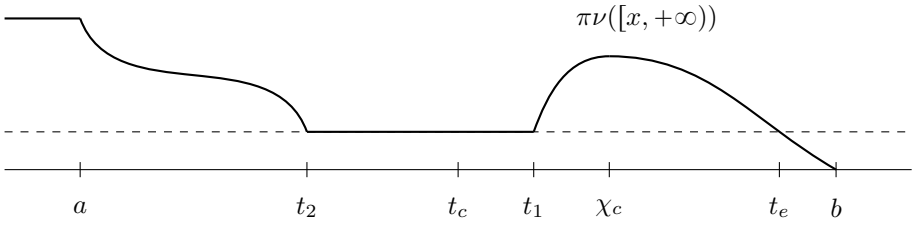

Figure 29: An example of a plot of the function $\int \arg(x-t)d\nu(t)$ for some possible ν.

By Lemma 2.2 and the discussion above, the only possible end points are t_2, t_1 and t_e or t_2, t_1, t_e^- and t_e^+. Assume that it ends at t_1. Then we get a closed contour in $\overline{\mathbb{H}}$ containing the interval $[t_c,t_1]$, and such that the boundary value of $\operatorname{Im}[f(w)]$ equals $\operatorname{Im}[f(t_c)] = \pi\mu([t_c,b])$ everywhere on the curve. However, since $\operatorname{Im}[f(w)]$ is harmonic inside the domain bounded by the curve, this implies that $\operatorname{Im}[f(w)]$ is constant, a contradiction. Similarly, the descent contour cannot end in t_2. Thus it has to end either at t_e or one of t_e^- and t_e^+.

This proves the existence of the global steepest descent path of $f(w,\chi_c)$. We now consider the ascent path. Recall that the ascent and descent paths cannot intersect. By considering the local ascent and descent contours we know it cannot end at t_1. Suppose that it ends a t_2. However, by a similar argument as before, this is not possible. Moreover, by the continuity of $U^\nu(w)$ it cannot end at t_e. Thus, the ascent contour will become an asymptote of the line $\{te^{i\theta} : t \in [0,+\infty), \theta = \pi\mu([t_c,b])\}$ since $\int_{\mathbb{R}} \arg(w-t)d\nu(t) = \nu(\mathbb{R})\arg(w) + O(|w|^{-1})$ as $|w| \to \infty$. Now assume that the decent path ends at t_e^- and that the ascent path ends at t_e^+. Again by forming a closed contour containing the interval $[t_e^-, t_e^+]$ and exploiting the harmonicity of $\mathrm{Im}[f(w)]$, we get a contradiction. Thus as before, contour will become an asymptote of the line $\{te^{i\theta} : t \in [0,+\infty), \theta = \pi\mu([t_c,b])\}$.

□

2.4 Estimates and localization

We start with some preliminary results that we will need. By lemma 2.1 and Assumption 4, if we take δ_0 small enough, then $|g_{n,i}(w)| \leqslant C$ for $|w - t_c| \leqslant \delta_0$, where C is a constant. We have the Taylor expansion

$$g_{n,i}(z) = g_{n,i}(t_c) + g'_{n,i}(t_c)(z-t_c) + \frac{1}{2}g''_{n,i}(t_c)^2(z-t_c)^2 + \frac{1}{6}g'''_{n,i}(t_c)^3(z-t_c)^3 + r_{n,i}(z)(z-t_c)^4, \quad (2.6)$$

where

$$r_{n,i}(z) = \frac{1}{2\pi i}\int_{|w-t_c|=\delta_3} \frac{g_{n,i}(w)}{(w-t_c)^5(1-\frac{z-t_c}{w-t_c})}dw. \quad (2.7)$$

From (2.7) we see that, if we take $\delta_1 \leqslant \delta_0/2$, then there is a constant $C(\delta_0)$ so that

$$|r_{n,i}(z)| \leqslant C(\delta_0), \quad (2.8)$$

for all $z \in B(t_c,\delta_1)$. Consider a curve

$$z(t) = t_c + \zeta(t), \quad (2.9)$$

$t \in I$, such that $|\zeta(t)| \leqslant Ct \leqslant \delta_1$ for all $t \in I$, I an interval. From (2.6) we obtain

$$\begin{aligned}\mathrm{Re}[g_{n,i}(z(t)) - g_{n,i}(t_c)] = g'_{n,i}(t_c)\mathrm{Re}[\zeta(t)] + \frac{1}{2}g''_{n,i}(t_c)\mathrm{Re}[\zeta(t)^2] + \frac{1}{6}g'''_{n,i}(t_c)\mathrm{Re}[\zeta(t)^3] \\ + \mathrm{Re}[r_{n,i}(z(t))\zeta(t)^4].\end{aligned} \quad (2.10)$$

Note that, by the assumption on $\zeta(t)$,

$$|\mathrm{Re}[\zeta(t)]| \leqslant Ct, \quad |\mathrm{Re}[\zeta(t)^2]| \leqslant Ct^2, \quad |\mathrm{Re}[r_{n,i}(z(t))\zeta(t)^4]| \leqslant Ct^4, \quad (2.11)$$

for all $t \in I$, where the constant C is independent of δ_1.

By the definition (1.43), we have that

$$h_{n,i}(z) = \sum_{k=\Delta x_i^{(n)}}^{-1} \log\left(z - \left(\frac{x_c^{(n)}}{n} + \frac{k}{n}\right)\right)$$

if $\Delta x_i^{(n)} < 0$, $h_{n,i}(z) = 0$ if $\Delta x_i^{(n)} = 0$ and

$$h_{n,i}(z) = -\sum_{k=1}^{\Delta x_i^{(n)}} \log\left(z - \left(\frac{x_c^{(n)}}{n} + \frac{k}{n}\right)\right),$$

if $\Delta x_i^{(n)} > 0$. Write $\kappa_i = \operatorname{sgn}(\Delta x_i^{(n)})$ ($= 0$ if $\Delta x_i^{(n)} = 0$). Then,

$$h'_{n,i}(z) = -\kappa_i \sum_{k=1}^{|\Delta x_i^{(n)}|} \frac{1}{z - \left(\frac{x_c^{(n)}}{n} + \kappa_i \frac{k}{n}\right)}. \tag{2.12}$$

From this, and (1.35), it follows that, if $|z - t_c| \leqslant \delta_1$, with δ_1 small enough, then

$$|h'_{n,i}(z)| = Cn^{1/3}, \quad |h''_{n,i}(z)| \leqslant Cn^{1/3}. \tag{2.13}$$

Similarly to (2.6), we get

$$h_{n,i}(z(t)) = h_{n,i}(t_c) + h'_{n,i}(t_c)\zeta(t) + s_{n,i}(z(t))\zeta(t)^2, \tag{2.14}$$

where

$$|s_{n,i}(z(t))| \leqslant Cn^{1/3}, \tag{2.15}$$

and $z(t)$ is given by (2.9).

We will now discuss the localization of the asymptotic analysis of the kernel to a neighbourhood of t_c. Let $\delta_1 > 0$ and let $B_2 = B(t_c, \delta_1)$ be a (small) ball around t_c. The descent contour $\mathcal{D}$ from Lemma 2.3 intersects $\partial B_2 \cap \mathbb{H}$ at the point D_2, se figure 30

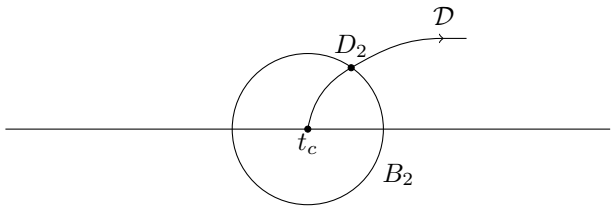

Figure 30: The global descent path $\mathcal{D}$ close to t_c

We now formulate a lemma that will allow us to neglect the contribution from $\mathcal{D}$ outside B_2.

Lemma 2.4. *If we choose δ_1 sufficiently small, there is a constant $b_0(\delta_1) > 0$ such that for n large enough*

$$Re\,[g_{n,i}(D_2) - g_{n,i}(t_c)] \leqslant -b_0(\delta_1). \tag{2.16}$$

Proof. We take $\zeta(t) = te^{i\theta(\delta_1)}$, $0 \leqslant t \leqslant \delta_1$, where $\theta(\delta_1)$ is chosen so that $\zeta(\delta_1) = D_2$. It follows from Lemma 2.1, $f'(t_c) = f''(t_c) = 0$, and $f'''(t_c) > 0$ that, given $\varepsilon_1 > 0$, we have

$$|g'_{n,i}(t_c)| \leqslant \varepsilon_1, \quad |g''_{n,i}(t_c)| \leqslant \varepsilon_1 \tag{2.17}$$

for large n, and there is a $c_1 > 0$ so that

$$g'''_{n,i}(t_c) \geqslant c_1 \tag{2.18}$$

for all sufficiently large n. Also, since $f'(t_c) = f''(t_c) = 0$ and $f'''(t_c) > 0$, a local Taylor expansion of f shows that $\theta(\delta_1) \to \pi/3$ as $\delta_1 \to 0$. Consequently,

$$\operatorname{Re}\zeta(t)^3 = t^3 \cos 3\theta(\delta_1) \leqslant -\frac{1}{2}t^3 \tag{2.19}$$

for $0 \leqslant t \leqslant \delta_1$ if δ_1 is sufficiently small. From (2.10), (2.11), (2.17), and (2.18) we see that

$$\begin{aligned}\operatorname{Re}\left[g_{n,i}(D_2) - g_{n,i}(t_c)\right] &\geqslant -\frac{1}{12}c_1\delta_1^3 + C\varepsilon_1(\delta_1 + \delta_1^2) + C\delta_1^4 \\ &= c_1\delta_1^3\Big[-\frac{1}{12} - C'\varepsilon_1(\delta_1^{-2} + \delta_1^{-1}) + C'\delta_1\Big]. \end{aligned} \tag{2.20}$$

We can now choose δ_1 so that $C'\delta_1 \leqslant 1/48$ and then ϵ_1 so that $C'\varepsilon_1(\delta_1^{-2} + \delta_1^{-1}) \leqslant 1/48$. We then get (2.16) with $b_0(\delta_1) = c_1\delta_1^3/24$ and the lemma is proved. □

Let $B_3 = B(t_e, \delta_2)$ be a small ball around t_e. The descent contour $\mathcal{D}$ intersects $\partial B_3 \cap \mathbb{H}$ at the point D_3. Let $\mathcal{C}$ be as in figure 31 and $\mathcal{D}'$ be the part of $\mathcal{D}$ outside B_2 and B_3, so that $\mathcal{D}'$ lies strictly in $\mathbb{H}$. Hence, from Lemma 2.1, it follows that $g_{n,i}(z) \to f(z)$ uniformly on $\mathcal{D}'$ as $n \to \infty$.

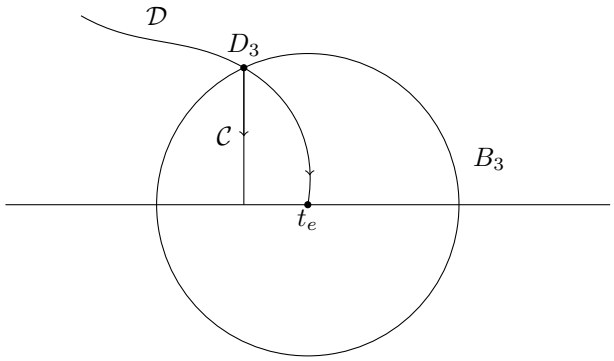

Figure 31: The global descent path $\mathcal{D}$ and $\mathcal{C}$ close to t_e

The next lemma gives the estimate we need on $\mathcal{C}$.

Lemma 2.5. *There is a constant $b_1(\delta_2)$ such that $b_1(\delta_2) \to 0$ as $\delta_2 \to 0$ and*

$$Re\left[g_{n,i}(z) - g_{n,i}(D_3)\right] \leqslant b_1(\delta_2) \tag{2.21}$$

for all $z \in \mathcal{C}$ if n is sufficiently large.

Proof. Let $D_3 = x_0 + iy_0$ and set

$$z(t) = x_0 + i(y_0 - t), \quad 0 \leqslant t \leqslant y_0 \leqslant \delta_2.$$

We have chosen δ_2 so small that $x_0 > \chi_c$. From (1.42) we see that

$$\begin{aligned}\frac{d}{dt}\mathrm{Re}[f_n(z(t))] &= \frac{d}{dt}\bigg(\frac{1}{n}\sum_{\beta_i^{(n)} \leqslant t_2^{(n)}} \log|z(t) - n^{-1}\beta_i^{(n)}| + \frac{1}{n}\sum_{\beta_i^{(n)} > t_1^{(n)}} \log|z(t) - n^{-1}\beta_i^{(n)}|\bigg) \\ &\quad - \frac{d}{dt}\frac{1}{n}\sum_{k=t_1^{(n)}+1}^{x_c^{(n)}} \log|z(t) - n^{-1}k| = u_1^{(n)}(t) + u_2^{(n)}(t).\end{aligned}$$

Note that $u_1^{(n)}(t) \leqslant 0$ and

$$\begin{aligned}u_2^{(n)}(t) &= -\frac{d}{dt}\frac{1}{2n}\sum_{k=t_1^{(n)}+1}^{x_c^{(n)}} \log\left(\left(x_0 - \frac{k}{n}\right)^2 - (y_0 - t)^2\right) \\ &= \frac{1}{n}\sum_{k=t_1^{(n)}+1}^{x_c^{(n)}} \frac{y_0 - t}{\left(x_0 - \frac{k}{n}\right)^2 + (y_0 - t)^2} \leqslant \frac{\delta_2}{n}\sum_{k=t_1^{(n)}+1}^{x_c^{(n)}} \frac{1}{\left(x_0 - \frac{k}{n}\right)^2} \leqslant C\delta_2,\end{aligned}$$

since $x_c^{(n)}/n \to \chi_c < x_0$ as $n \to \infty$. Thus,

$$\operatorname{Re}\left[f_n(z) - f_n(D_3)\right] \leqslant C\delta_2$$

for all $z \in \mathcal{C}$ if n is sufficiently large. It remains to estimate $\frac{1}{n}\operatorname{Re}[h_{n,i}(z(t))]$. Consider $h_{n,1}$ and assume $\Delta x_1^{(n)} > 0$, the other cases are similar. From (1.43) and (1.37) we obtain

$$\frac{1}{n}\left|\operatorname{Re}\left[h_{n,1}(z(t))\right]\right| \leqslant \frac{\log n}{n}\Delta x_1^{(n)} + \frac{1}{2n}\sum_{k=nx_c^{(n)}+1}^{nx_c^{(n)}+\Delta x_1^{(n)}} \log\left|\left(x_0 - \frac{k}{n}\right)^2 + (y_0 - t)^2\right| \leqslant \frac{C\log n}{n^{2/3}} \leqslant \delta_2$$

if n is sufficiently large. Here we used again the fact that $x_c^{(n)}/n \to \chi_c < x_0$. This proves the lemma. □

From Proposition 2.1 and (1.46) we see that

$$\begin{aligned}&\frac{p_n(x_2,y_2)}{p_n(x_1,y_1)}\frac{c_0 n^{1/3}}{2}\tilde{K}_{\mathcal{R}}^{(n)}((x_1,y_1),(x_2,y_2))\\ &= \frac{1}{(2\pi i)^2}\oint_{\Gamma_n^1+\Gamma_n^2} dz \oint_{\gamma_n^1+\gamma_n^2} dw \frac{c_0 n^{1/3}}{z - n^{-1}x_2}\frac{(d_0 n^{2/3})^r q(nw;r)}{(d_0 n^{2/3})^s q(nz;s)}\frac{e^{n(g_{n,1}(w)-g_{n,1}(t_c))-n(g_{n,2}(z)-g_{n,2}(t_c))}}{w-z}. \quad (2.22)\end{aligned}$$

Note also that

$$(d_0 n^{2/3})^r q_n(nw;r) = \prod_{k=0}^{r-1}\left(\frac{n^{1/3}(w-t_c) - k/n^{1/3}}{d_0}\right) \quad (2.23)$$

if $r > 0$; there is an analogous formula if $r < 0$ and if $r = 0$ the expression is $= 1$.

By uniform convergence we have that $|g_{n,i}(z) - f(z)| \leqslant \frac{1}{4}b_0(\delta_1)$ for all $z \in \mathcal{D}'$ if n is large enough. Thus, if $z \in \mathcal{D}'$ we have

$$\operatorname{Re}[g_{n,i}(z) - g_{n,i}(D_2)] \leqslant \operatorname{Re}[g_{n,i}(z) - f(z)] + \operatorname{Re}[f(D_2) - g_{n,i}(D_2)] + \underbrace{\operatorname{Re}[f(z) - f(D_2)]}_{\leqslant 0} \leqslant \frac{1}{2}b_0(\delta_1),$$

where we have used that $\mathcal{D}'$ is a descent curve. Combining this with Lemma 2.4, we obtain

$$\operatorname{Re}[g_{n,i}(z) - g_{n,i}(t_c)] \leqslant -\frac{1}{2}b_0(\delta_1). \quad (2.24)$$

for all $z \in \mathcal{D}'$. Given δ_1 we choose δ_2 so small that $b_1(\delta_2) \leqslant b_0(\delta_1)/4$. Since $D_3 \in \mathcal{D}'$ we find, using Lemma 2.5 and (2.24) that

$$\operatorname{Re}[g_{n,i}(z) - g_{n,i}(t_c)] \leqslant -\frac{1}{4}b_0(\delta_1). \quad (2.25)$$

for all $z \in \mathcal{C}$ if n is sufficiently large.

Note that

$$\operatorname{Re} g_{n,2}(z) = \nu_{n,2}(\mathbb{R})\log|z| + O(|z|^{-1}) \quad (2.26)$$

as $|z| \to \infty$, and $\nu_{n,2}(\mathbb{R}) \to \nu(\mathbb{R}) > 0$ as $n \to \infty$. In (2.22) we can let Γ_n^2 and γ_n^2 be small circles around t_c inside B_2 and deform γ_n^1 to the descent contour $\mathcal{D}' + \mathcal{C}$ (and its reflection image in the lower half plane). Using (2.26) we see that we can deform Γ_n^1 to the ascent contour $\mathcal{A}$. We can now use the estimates (2.24), (2.25) and (2.26) to see that in the integral (2.22) we can ignore $\mathcal{D}' + \mathcal{C}$ and the part of $\mathcal{A}$ outside B_2 in the limit. More precisely, we also have to combine this estimate with the estimates and computations inside B_2 that we will do in the next section. We leave out the details.

2.5 Local Analysis

Let $\{M_n\}_{n\geqslant 1}$ be a sequence satisfying

$$M_n \to \infty, \quad \frac{M_n}{n^{1/12}} \to 0, \quad n^{2/3} M_n |f_n'(t_c)| \to 0 \tag{2.27}$$

as $n \to \infty$, which exists by Assumption 4. Consider the ball $B_1 = B(t_c, M_n n^{-1/3})$. Again we will only discuss the descent contour; the ascent case is analogous. As above, we take $\zeta(t) = te^{i\theta(\delta_1)}$ in (2.9) with $M_n/n^{1/3} \leqslant t \leqslant \delta_1$, so that $z(\delta_1) = t_c + \zeta(\delta_1) = D_2$, see figure 32.

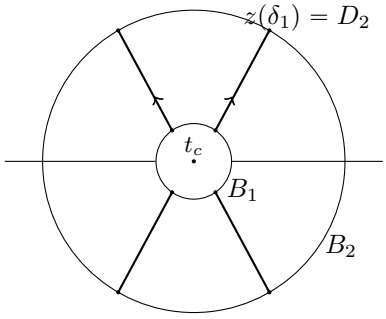

Figure 32: Local contours in the region $B_2 \backslash B_1$

It follows from (2.10),(2.11) and (2.18) that there is a constant C so that

$$\mathrm{Re}[g_{n,i}(z(t)) - g_{n,i}(t_c)] \leqslant -t^3 \left[\frac{1}{12} c_1 - \frac{C|g_{n,i}'(t_c)|}{t^2} - \frac{C|g_{n,i}''(t_c)|}{t} - Ct \right]. \tag{2.28}$$

It follows from Assumption 4 that $n^{2/3} f_n'(t_c) \to 0$ and $n^{2/3} f_n''(t_c) \to 0$ as $n \to \infty$. Combining this with (2.13) we see that, for $t \in [M_n/n^{1/3}, \delta_1]$,

$$\frac{|g_{n,i}'(t_c)|}{t^2} \leqslant C \frac{n^{2/3}}{M_n^2} (|f_n'(t_c)| + Cn^{-2/3}) \tag{2.29}$$

and

$$\frac{|g_{n,i}''(t_c)|}{t} \leqslant C \frac{n^{2/3}}{M_n} (|f_n''(t_c)| + Cn^{-2/3}). \tag{2.30}$$

Using (2.27) we see that the right hand sides of (2.29) and (2.30) are $\leqslant c_1/72$ if n is large enough. Also, we can assume that δ_1 has been chosen so small that Ct in (2.28) satisfies $Ct \leqslant C\delta_1 \leqslant c_1/72$. It then follows from (2.28) that

$$\mathrm{Re}\left[g_{n,i}(z(t)) - g_{n,i}(t_c)\right] \leqslant -\frac{1}{24} c_1 t^3 \tag{2.31}$$

for $t \in [M_n/n^{1/3}, \delta_1]$. If we let

$$z(t) = t_c + d_0 n^{-1/3} t e^{i\theta(\delta_1)},$$

$t \in [M_n, \delta_1 n^{1/3}]$, then (2.31) gives the estimate

$$n\mathrm{Re}\left[g_{n,i}(t_c + d_0 n^{-1/3} t e^{i\theta(\delta_1)}) - g_{n,i}(t_c)\right] \leqslant -\frac{d_0^3 c_1}{24} t^3. \tag{2.32}$$

This estimate can be used together with the corresponding estimate for the ascent contour to control, in the limit, the contribution from the parts of the descent and ascent contours that lie in $B_2 \backslash B_1$. We find that we can neglect the contributions from $B_2 \backslash B_1$.

We now define the local contours that will be used in B_1. Let $D_1 = t_c + M_n n^{-1/3} e^{i\theta(\delta_1)}$. Fix $x > 0$ and $y < 0$. We define $\overline{\gamma}_n^1$ in the upper half plane by

$$z(t) = t_c + d_0 n^{-1/3} u_n(t) := t_c + d_0 n^{-1/3}(x + te^{i\theta_n(\delta_1)}), \tag{2.33}$$

where $0 \leqslant t \leqslant M_n'$. Here $\theta_n(\delta_1)$ and M_n' are such that $z(M_n') = D_1$. Note that $M_n'/M_n \to 1$ as $n \to \infty$. I the lower half plane we just take the mirror image. We define $\overline{\Gamma}_n^1$ analogously corresponding to the ascent contour, see figure 33. Also, we define $\overline{\Gamma}_n^2$ by $z(t) = t_c + d_0 n^{-1/3} r_1 e^{it}$, $0 \leqslant t \leqslant 2\pi$ and $\overline{\gamma}_n^2$ by $z(t) = t_c + d_0 n^{-1/3} r_2 e^{-it}$, $0 \leqslant t \leqslant 2\pi$, where $0 < r_2 < r_1 < \min(x, -y)$, see figure 33.

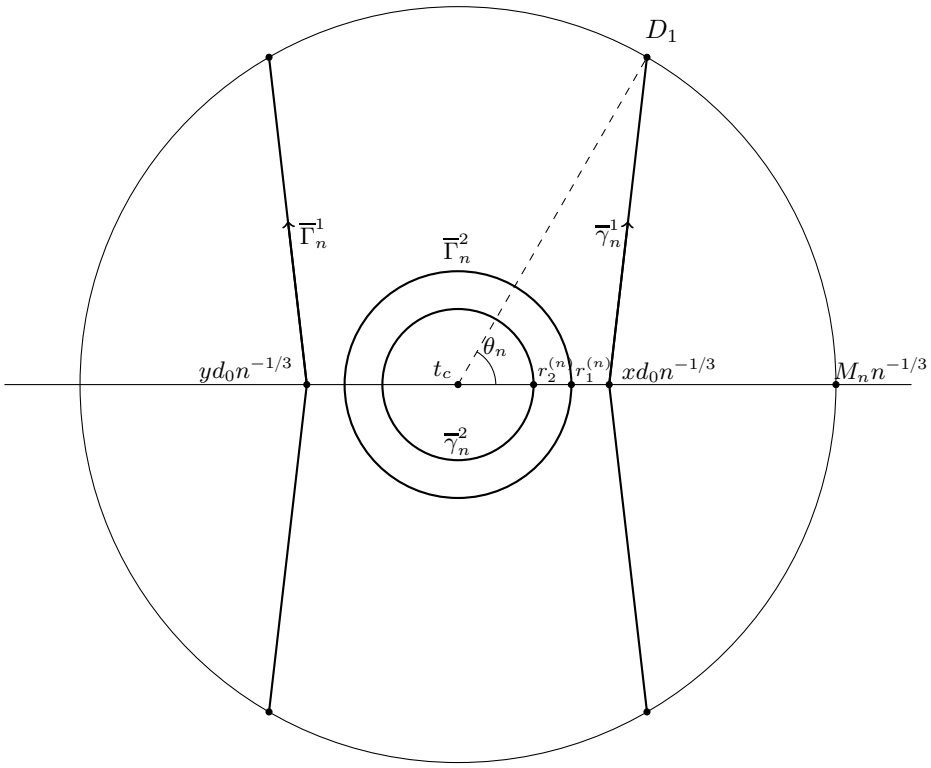

Figure 33: Local contours in B_1. Here $r_i^{(n)} = n^{-1/3} r_i$ for $i = 1, 2$.

Write

$$\begin{aligned}&\tilde{L}_{\mathcal{R}}^{(n)}((x_1, y_1), (x_2, y_2)) \\ &= \frac{1}{(2\pi i)^2} \oint_{-\overline{\Gamma}_n^1 - \overline{\Gamma}_n^2} dz \oint_{\gamma_n^1 + \gamma_n^2} dw \frac{c_0 n^{1/3}}{z - n^{-1} x_2} \frac{(d_0 n^{2/3})^r q(nw; r)}{(d_0 n^{2/3})^s q(nz; s)} \frac{e^{n(g_{n,1}(w) - g_{n,1}(t_c)) - n(g_{n,2}(z) - g_{n,2}(t_c))}}{w - z}.\end{aligned} \tag{2.34}$$

From (2.22) and the discussion above it follows that

$$\lim_{n\to\infty} \frac{p_n(x_2, x_1)}{p_n(x_1, y_1)} \frac{c_0 n^{1/3}}{2} \tilde{L}_{\mathcal{R}}^{(n)}((x_1, y_1), (x_2, y_2)) = \lim_{n\to\infty} \tilde{K}_{\mathcal{R}}^{(n)}((x_1, y_1), (x_2, y_2)).$$

Consider the contribution from $\overline{\gamma}_n^1$. Write

$$n(g_{n,1}(w) - g_{n,1}(t_c)) = n(f_n(w) - f_n(t_c)) + h_{n,1}(w) - h_{n,1}(t_c).$$

In analogy with (2.6) we have, with $z(t)$ given by (2.33),

$$n(f_n(z(t)) - f(t_c)) = n^{2/3} f_n'(t_c) d_0 u_n(t) + \frac{1}{2} n^{1/3} f_n''(t_c) d_0^2 u_n(t)^2 + \frac{1}{6} f_n'''(t_c) d_0^3 u_n(t)^3 + n^{-1/3} \tilde{r}_n(z(t)) d_0^4 u_n(t)^4, \tag{2.35}$$

where $|\tilde{r}_n(z(t))| \leqslant C$ for $0 \leqslant t \leqslant M_n'$. Since $|u_n(t)| \leqslant C M_n$,

$$|n^{-1/3} \tilde{r}_n(z(t)) d_0^4 u_n(t)^4| \leqslant C n^{-1/3} M_n^4 \to 0, \tag{2.36}$$

as $n \to \infty$ for $0 \leqslant t \leqslant M_n$, by (2.27). Also,

$$\begin{aligned} |n^{2/3} f_n'(t_c) d_0 u_n(t)| &\leqslant C M_n n^{2/3} |f_n'(t_c)| \\ |n^{1/3} f_n''(t_c) d_0^2 u_n(t)^2| &\leqslant C M_n^2 n^{1/3} |f_n''(t_c)|. \end{aligned} \tag{2.37}$$

By (2.27) and Assumption 4 it follows that the right hand sides of (2.37) go to 0 as $n \to \infty$. Furthermore it follows from Assumption 4 that $n^{2/3}|f_n'''(t_c) - f'''(t_c)| \to 0$ as $n \to \infty$. Hence, we have shown that

$$n(f_n(t_c) - f(t_c)) = \frac{d_0^3}{6} f'''(t_c) u_n(t)^3 + o(1) = \frac{1}{3} u_n(t)^3 + o(1) \tag{2.38}$$

uniformly for $t \in [0, M_n']$ as $n \to \infty$, by our choice (1.31). From the definition of $\theta_n(\delta_1)$ it follows that $n^{1/3}|\theta_n(\delta_1) - \theta(\delta_1)|$ is bounded, and thus $M_n^3 |\theta_n(\delta_1) - \theta(\delta_1)| \to 0$ as $n \to \infty$ by (2.27). From this we see that

$$n(f_n(z(t)) - f(t_c)) = \frac{1}{3}(x + t e^{i\theta(\delta_1)})^3 + o(1), \tag{2.39}$$

uniformly for $t \in [0, M_n']$ as $n \to \infty$. From (2.14) we obtain

$$h_{n,1}(z(t)) - h_{n,1}(t_c) = h_{n,1}'(t_c) d_0 n^{-1/3} u_n(t) + s_{n,1}(z(t)) d_0^2 n^{-2/3} u_n(t)^2, \tag{2.40}$$

and by (2.15),

$$|n^{-2/3} d_0^2 s_{n,1}(z(t)) u_n(t)^2| \leqslant C n^{-1/3} M_n^2 \to 0, \tag{2.41}$$

uniformly for $0 \leqslant t \leqslant M_n'$ as $n \to \infty$ by (2.27). Recall (2.12) and consider the case when $\Delta x_1^{(n)} > 0$. From (2.12) we see that

$$\begin{aligned} \left| n^{-1/3} h_{n,1}'(t_c) + \frac{\Delta x_1^{(n)}}{(t_c - \chi_c) n^{1/3}} \right| &\leqslant \frac{1}{n^{1/3}} \left| \sum_{k=1}^{\Delta x_1^{(n)}} - \frac{1}{t_c - \frac{x_c^{(n)}}{n} - \frac{k}{n}} + \frac{1}{t_c - \chi_c} \right| \\ &\leqslant \frac{C}{n^{1/3}} \sum_{k=1}^{\Delta x_1^{(n)}} \left| \frac{\frac{k}{n} + \frac{x_c^{(n)}}{n} - \chi_c}{t_c - \frac{t_c - x_c^{(n)}}{n} - \frac{k}{n}} \right| \leqslant \frac{C}{n^{2/3}} \end{aligned}$$

since $|\Delta x_1^{(n)}| \leqslant |r/2 - c_0 n^{1/3} \xi_n| \leqslant C n^{1/3}$, $|x_c^{(n)}/n - \chi_c| \leqslant 1/n$, $\xi_n \to \xi$ as $n \to \infty$ and $\chi_c > t_c$. It follows that

$$n^{-1/3} h_{n,1}'(t_c) - \frac{c_0 \xi}{2(t_c - \chi_c)} \to 0 \tag{2.42}$$

as $n \to \infty$. Using this and the control on $\theta_n(\delta_1)$, it follows from (2.40), (2.41) and (2.42) that

$$h_{n,1}(z(t)) - h_{n,1}(t_c) = -\frac{c_0 d_0 \xi}{2(t_c - \chi_c)} (x + t e^{i\theta(\delta_1)}) + o(1), \tag{2.43}$$

uniformly for $0 \leqslant t \leqslant M_n$ as $n \to \infty$. We have chosen c_0, (1.30), so that

$$\frac{c_0 d_0}{2(t_c - \chi_c)} = -1. \tag{2.44}$$

Thus

$$h_{n,1}(z(t)) - h_{n,1}(t_c) = -\xi(x + te^{i\theta(\delta_1)}) + o(1), \tag{2.45}$$

uniformly for $0 \leqslant t \leqslant M_n$ as $n \to \infty$. Now, by (2.23), for $r > 0$,

$$(d_0 n^{2/3})^r q_n(nz(t); r) = \prod_{k=0}^{r-1} \frac{n^{1/3}(d_0 n^{-1/3}(x + te^{i\theta_n(\delta_1)}) + n^{1/3}(t_c - t_c^{(n)}) - k/n^{2/3}}{d_0} = \left(x + te^{i\theta(\delta_1)}\right)^r e^{o(1)}$$

uniformly for $0 \leqslant t \leqslant M_n$ as $n \to \infty$.

We can do the same type of computations for $\overline{\Gamma}_n^1$, $\overline{\Gamma}_n^2$ and $\overline{\gamma}_n^2$. This gives us

$$\begin{aligned}
&\lim_{n\to\infty} \frac{c_0 d_0}{2(t_c - \chi_c)(2\pi i)^2} \tilde{L}_{\mathcal{R}}^{(n)}((x_1, y_1), (x_2, y_2)) \\
&= \frac{c_0 d_0}{2(t_c - \chi_c)(2\pi i)^2} \int_{-\mathscr{L}_L - \mathscr{C}_{out}} dz \int_{\mathscr{L}_R + \mathscr{C}_{in}} dw \frac{1}{w - z} \frac{w^r}{z^s} e^{\frac{1}{3}w^3 - \frac{1}{3}z^3 - \xi w + \tau z} \\
&= \frac{1}{(2\pi i)^2} \int_{\mathscr{L}_L + \mathscr{C}_{out}} dz \int_{\mathscr{L}_R + \mathscr{C}_{in}} dw \frac{1}{w - z} \frac{w^r}{z^s} e^{\frac{1}{3}w^3 - \frac{1}{3}z^3 - \xi w + \tau z}.
\end{aligned} \tag{2.46}$$

It remains to consider the asymptotics of B_n in (2.2).

$$\begin{aligned}
&\lim_{n\to\infty} \frac{p_n(x_2, y_2)}{p_n(x_1, y_1)} \frac{c_0 n^{1/3}}{2} B_n((x_1, y_1), (x_2, y_2)) \\
&= \lim_{n\to\infty} 1_{x_1 \geqslant x_2} \frac{1}{2\pi i} \int_{-\overline{\Gamma}_n^2} dz \frac{c_0 n^{1/3}}{z - x_2/n} \frac{(d_0 n^{2/3})^r q_n(nz; r)}{(d_0 n^{2/3})^s q_n(nz; s)} e^{h_{n,1}(z) - h_{n,1}(t_c) - (h_{n,2}(z) - h_{n,2}(t_c)}
\end{aligned} \tag{2.47}$$

since $\overline{\Gamma}_n^2$ has the opposite orientation to Γ_n^2. Using the same asymptotics for q_n and h_n as above we get

$$-1_{-\xi \geqslant -\tau} \frac{1}{2\pi i} \int_{-\mathscr{C}_{out}} z^{r-s} e^{(\tau - \xi)z} \, dz = 1_{\tau \geqslant \xi} 1_{s>r} \frac{(\tau - \xi)^{s-r-1}}{(s - r - 1)!}.$$

This gives us finally the complete *Cusp-Airy* kernel

$$\mathcal{K}_{CA}((\xi, r), (\tau, s)) = -1_{\tau \geqslant \xi} 1_{s>r} \frac{(\tau - \xi)^{s-r-1}}{(s - r - 1)!} + \frac{1}{(2\pi i)^2} \int_{\mathscr{L}_L + \mathscr{C}_{out}} dz \int_{\mathscr{L}_R + \mathscr{C}_{in}} dw \frac{1}{w - z} \frac{w^r}{z^s} e^{\frac{1}{3}w^3 - \frac{1}{3}z^3 - \xi w + \tau z}. \tag{2.48}$$

It is not difficult to check that the asymptotics above is uniform for ξ, τ in compact subsets of $\mathbb{R}$. A standard argument using the Hadamard inequality then proves (1.47). This completes the proof of the Main Theorem.

3 Representations and Properties of The Cusp-Airy Kernel

3.1 Symmetry Property of The Cusp-Airy Kernel

From the geometry of the problem we expect that the Cusp-Airy process should be symmetric around the line $r = 0$. This is indeed seen in the kernel as the next proposition shows.

Proposition 3.1. *The Cusp-Airy kernel satisfies*

$$\mathcal{K}_{CA}((\xi,-r),(\tau,-s)) = (-1)^{s-r}\mathcal{K}_{CA}((\tau,s),(\xi,r)). \tag{3.1}$$

In particular, this implies that the correlation functions satisfies the reflection symmetry

$$\rho_n((\xi_1,-r_1),(\xi_2,-r_2),...,(\xi_n,-r_n)) = \rho_n((\xi_1,r_1),(\xi_2,r_2),...,(\xi_n,r_n)) \tag{3.2}$$

for all n.

Proof. First note that under the change of variables $z \to -z$ and $w \to -w$ the contours transform according to: $\mathscr{L}_L \to -\mathscr{L}_R$, $\mathscr{L}_R \to -\mathscr{L}_L$, $\mathscr{C}_{in} \to \mathscr{C}_{in}$, and $\mathscr{C}_{out} \to \mathscr{C}_{out}$. Thus we see that

$$\begin{aligned}
&\mathcal{K}_{CA}((\xi,-r),(\tau,-s)) = -1_{\tau\geqslant\xi}1_{-s>-r}\frac{(\tau-\xi)^{-s+r-1}}{(-s+r-1)!}\\
&+\frac{1}{(2\pi i)^2}\int_{\mathscr{L}_L\cup\mathscr{C}_{out}}dz\int_{\mathscr{L}_R\cup\mathscr{C}_{in}}dw\frac{1}{w-z}\frac{w^{-r}}{z^{-s}}e^{\frac{1}{3}w^3-\frac{1}{3}z^3-\xi w+\tau z} = \{z\to -z, w\to -w\}\\
&= 1_{\tau\geqslant\xi}1_{r>s}(-1)^{r-s}\frac{(\xi-\tau)^{r-s-1}}{(r-s-1)!}+\frac{(-1)^{s-r}}{(2\pi i)^2}\int_{-\mathscr{L}_R\cup\mathscr{C}_{out}}dz\int_{-\mathscr{L}_L\cup\mathscr{C}_{in}}dw\frac{1}{z-w}\frac{z^s}{w^r}e^{\frac{1}{3}z^3-\frac{1}{3}w^3-\tau z+\xi w} = \{z\leftrightarrow w\}\\
&= 1_{\tau\geqslant\xi}1_{r>s}(-1)^{r-s}\frac{(\xi-\tau)^{r-s-1}}{(r-s-1)!}+\frac{(-1)^{s-r}}{(2\pi i)^2}\int_{-\mathscr{L}_L\cup\mathscr{C}_{in}}dz\int_{-\mathscr{L}_R\cup\mathscr{C}_{out}}dw\frac{1}{w-z}\frac{w^s}{z^r}e^{\frac{1}{3}w^3-\frac{1}{3}z^3-\tau w+\xi z}.
\end{aligned}$$

Let $\mathscr{C}$ be a negatively oriented circular contour around the origin which is contained inside $\mathscr{C}_{in}$. The residue theorem implies that

$$\begin{aligned}
&\frac{1}{(2\pi i)^2}\int_{-\mathscr{L}_L\cup\mathscr{C}_{in}}dz\int_{-\mathscr{L}_R\cup\mathscr{C}_{out}}dw\frac{1}{w-z}\frac{w^s}{z^r}e^{\frac{1}{3}w^3-\frac{1}{3}z^3-\tau w+\xi z}\\
&=\frac{1}{2\pi i}\int_{\mathscr{C}_{in}}dz z^{s-r}e^{(\xi-\tau)z}+\frac{1}{(2\pi i)^2}\int_{-\mathscr{L}_L+\mathscr{C}_{in}}dz\int_{-\mathscr{L}_R-\mathscr{C}}dw\frac{1}{w-z}\frac{w^s}{z^r}e^{\frac{1}{3}w^3-\frac{1}{3}z^3-\tau w+\xi z}\\
&=-1_{r>s}\frac{(\xi-\tau)^{r-s-1}}{(r-s-1)!}+\frac{1}{(2\pi i)^2}\int_{-\mathscr{L}_L+\mathscr{C}_{in}}dz\int_{-\mathscr{L}_R-\mathscr{C}}dw\frac{1}{w-z}\frac{w^s}{z^r}e^{\frac{1}{3}w^3-\frac{1}{3}z^3-\tau w+\xi z}.
\end{aligned}$$

This gives

$$\begin{aligned}
\mathcal{K}_{CA}((\xi,-r),(\tau,-s)) &= 1_{\tau\geqslant\xi}1_{r>s}(-1)^{s-r}\frac{(\xi-\tau)^{r-s-1}}{(r-s-1)!}-(-1)^{s-r}1_{r>s}\frac{(\xi-\tau)^{r-s-1}}{(r-s-1)!}\\
&+\frac{(-1)^{r-s}}{(2\pi i)^2}\int_{-\mathscr{L}_L+\mathscr{C}_{in}}dz\int_{-\mathscr{L}_R-\mathscr{C}_{in}}dw\frac{1}{w-z}\frac{w^s}{z^r}e^{\frac{1}{3}w^3-\frac{1}{3}z^3-\tau w+\xi z},
\end{aligned}$$

We can now change $\mathscr{C}\to\mathscr{C}_{out}$ and $\mathscr{C}_{in}\to-\mathscr{C}_{out}$. This finally gives

$$\begin{aligned}
&\mathcal{K}_{CA}((\xi,-r),(\tau,-s))\\
&=(-1)^{s-r}1_{r>s}\frac{(\xi-\tau)^{r-s-1}}{(r-s-1)!}\big[1_{\tau\geqslant\xi}-1\big]+\frac{(-1)^{s-r}}{(2\pi i)^2}\int_{\mathscr{L}_L\cup\mathscr{C}_{out}}dz\int_{\mathscr{L}_R\cup\mathscr{C}_{in}}dw\frac{1}{w-z}\frac{w^s}{z^r}e^{\frac{1}{3}w^3-\frac{1}{3}z^3-\tau w+\xi z}\\
&=-(-1)^{s-r}1_{\xi>\tau}1_{r>s}\frac{(\xi-\tau)^{r-s-1}}{(r-s-1)!}+\frac{(-1)^{s-r}}{(2\pi i)^2}\int_{\mathscr{L}_L\cup\mathscr{C}_{out}}dz\int_{\mathscr{L}_R\cup\mathscr{C}_{in}}dw\frac{1}{w-z}\frac{w^s}{z^r}e^{\frac{1}{3}w^3-\frac{1}{3}z^3-\tau w+\xi z}\\
&=(-1)^{s-r}\mathcal{K}_{CA}((\tau,s)(\xi,r)).
\end{aligned}$$

□

3.2 Representation of The Cusp-Airy Kernel

In this section we will derive an alternative representation of the Cusp-Airy kernel involving the so called r-Airy integrals and certain polynomials. Define the *r-Airy integrals*,

$$A_r^{\pm}(u) = \frac{1}{2\pi}\int_{\ell} e^{\frac{1}{3}ia^3+iua}(\mp ia)^{\pm r}\,da,$$

where $r \geqslant 0$ and ℓ is a contour from $\infty e^{5\pi i/6}$ to $\infty e^{\pi i/6}$ such that 0 lies above the contour, see [1]; compare also with the functions $s^{(m)}$ and $t^{(m)}$ in [3]. Note that $A_0^{\pm}(u) = \mathrm{Ai}\,(u)$, the standard Airy function. Let $\mathscr{L}_L^*$ be the contour $\mathscr{L}_L$ shifted to the right so that 0 lies to the left of it, see figure 35; define $\mathscr{L}_R^*$ analogously by shifting $\mathscr{L}_R$ to the left so that 0 is to the right of it. It is straightforward to check that

$$\frac{1}{2\pi i}\int_{\mathscr{L}_R^*} e^{\frac{1}{3}w^3-uw}w^r\,dw = \frac{(-1)^r}{2\pi i}\int_{\mathscr{L}_L^*} e^{-\frac{1}{3}z^3+uz}z^r\,dz = A_r^+(u), \tag{3.3}$$

and

$$\frac{(-1)^r}{2\pi i}\int_{\mathscr{L}_R^*} e^{\frac{1}{3}w^3-uw}\frac{1}{w^r}\,dw = \frac{1}{2\pi i}\int_{\mathscr{L}_L^*} e^{-\frac{1}{3}z^3+uz}\frac{1}{z^r}\,dz = A_r^-(u), \tag{3.4}$$

for $r \geqslant 0$.

Define the polynomials $P_n(w,\xi)$ and $p_n(\xi)$ through

$$P_n(w,\xi) := e^{-\frac{1}{3}w^3+uw}\frac{d^n}{dw^n}e^{\frac{1}{3}w^3-uw} \tag{3.5}$$

and

$$p_n(u) := P_n(0,u). \tag{3.6}$$

By Cauchy's integral formula, we have for $r \geqslant 0$,

$$\frac{1}{2\pi i}\int_{\mathscr{C}_{out}} e^{\frac{1}{3}w^3-uw}w^r\,dw = \frac{(-1)^{r-1}}{2\pi i}\int_{\mathscr{C}_{out}} e^{-\frac{1}{3}z^3+uz}z^r\,dz = p_{r-1}(u). \tag{3.7}$$

Note that $\mathscr{L}_L + \mathscr{C}_{out} = \mathscr{L}_L^*$, see figure 34. Thus,

$$\frac{(-1)^r}{2\pi i}\int_{\mathscr{L}_R} e^{\frac{1}{3}w^3-uw}\frac{1}{w^r}\,dw = \frac{1}{2\pi i}\int_{\mathscr{L}_L} e^{-\frac{1}{3}z^3+uz}\frac{1}{z^r}\,dz = A_r^-(u) + (-1)^r p_{r-1}(u). \tag{3.8}$$

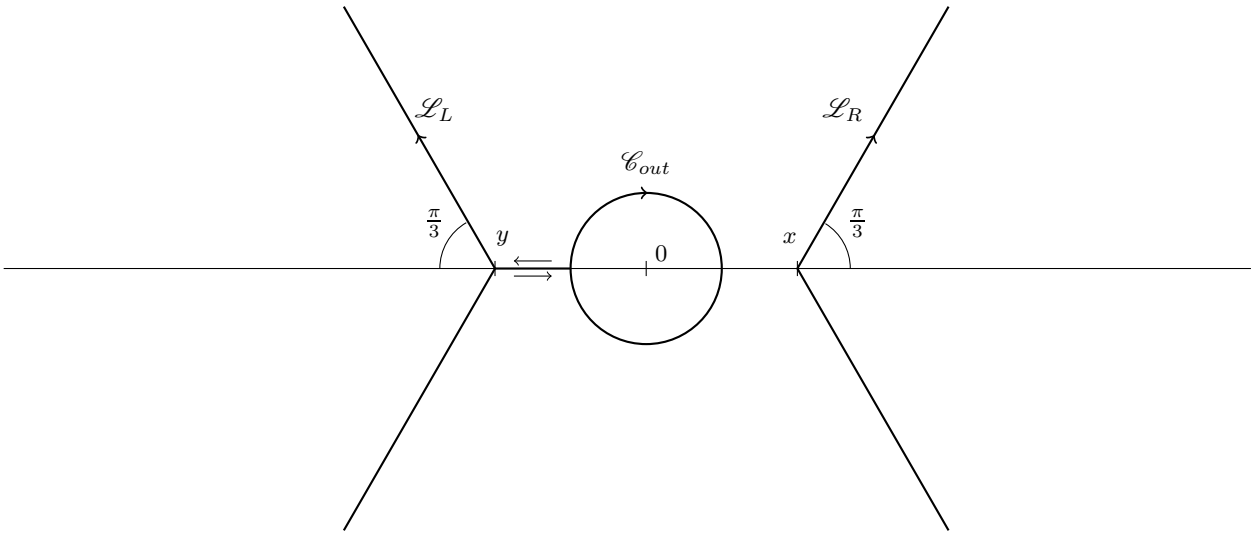

Figure 34: Deformation of the contours $\mathscr{L}_L$ and $\mathscr{C}_{out}$ so that $\mathscr{L}_L$ can be moved to the right of 0.

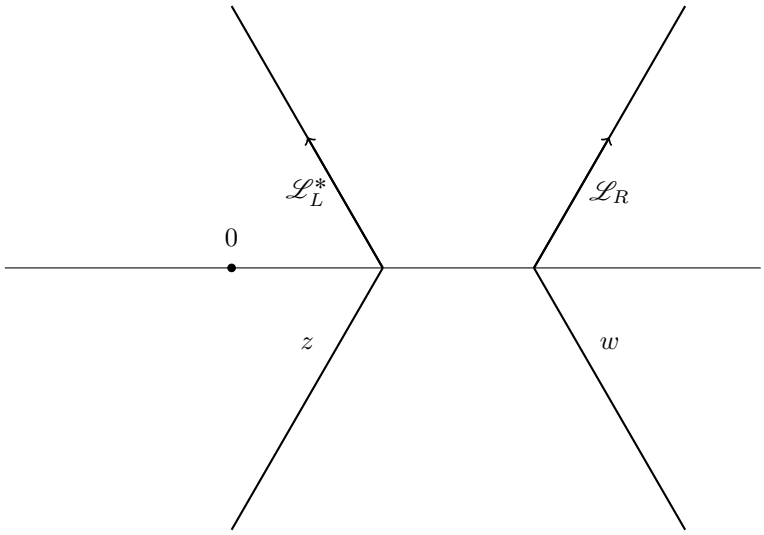

Figure 35: Integration contours moved to the right of 0.

We can now give a different formula for the Cusp-Airy kernel in terms of the r-Airy integrals.

Proposition 3.2. *The Cusp-Airy kernel can be written as*

$$\mathcal{K}_{CA}((\xi,r),(\tau,s)) = -1_{\tau\geqslant\xi}1_{s>r}\frac{(\tau-\xi)^{s-r-1}}{(s-r-1)!} + \tilde{\mathcal{K}}_{CA}((\xi,r),(\tau,s)),$$

where $\tilde{\mathcal{K}}_{CA}$ is given

(i) for $r,s\geqslant 0$, by

$$\tilde{\mathcal{K}}_{CA}((\xi,r),(\tau,s)) = \int_0^\infty A_s^-(\tau+\lambda)A_r^+(\xi+\lambda)\,d\lambda,$$

(ii) for $r\geqslant 0$, $s<0$, by

$$\tilde{\mathcal{K}}_{CA}((\xi,r),(\tau,s)) = (-1)^s\int_0^\infty A_{-s}^+(\tau+\lambda)A_r^+(\xi+\lambda)\,d\lambda,$$

(iii) for $r<0$, $s\geqslant 0$, by

$$\begin{aligned}\tilde{\mathcal{K}}_{CA}((\xi,r),(\tau,s)) = (-1)^r\int_0^\infty A_s^-(\tau+\lambda)A_{-r}^-(\xi+\lambda)\,d\lambda + (-1)^{s-r}\int_0^\infty p_{s-1}(\tau+\lambda)A_{-r}^-(\xi+\lambda)\,d\lambda\\ + (-1)^{s-r}\sum_{k=0}^{s-1}p_k(\tau)A_{-r+s-k}(\xi) + \sum_{k=0}^{s-r-1}(-1)^k p_k(\tau)p_{s-r-1-k}(\xi),\end{aligned}$$

(iv) and for $r,s<0$, by

$$\tilde{\mathcal{K}}_{CA}((\xi,r),(\tau,s)) = (-1)^{s-r}\int_0^\infty A_{-s}^+(\tau+\lambda)A_{-r}^-(\xi+\lambda)\,d\lambda.$$

Proof. From Definition 1.1 we have that

$$\tilde{\mathcal{K}}_{CA}((\xi,r),(\tau,s)) = \frac{1}{(2\pi i)^2}\int_{\mathscr{L}_L+\mathscr{C}_{out}}dz\int_{\mathscr{L}_R+\mathscr{C}_{in}}dw\frac{1}{w-z}\frac{w^r}{z^s}e^{\frac{1}{3}w^3-\frac{1}{3}z^3-\xi w+\tau z}.$$

Consider the case (i). If $r, s \geqslant 0$, then $\mathscr{C}_{in}$ does not contribute, and using $\mathscr{L}_L + \mathscr{C}_{out} = \mathscr{L}_L^*$, see figure 34, and the formula

$$\int_0^\infty e^{-\lambda(w-z)}\, d\lambda = \frac{1}{w-z} \tag{3.9}$$

valid if $\operatorname{Re}(w-z) > 0$, we find

$$\begin{aligned}\tilde{\mathcal{K}}_{CA}((\xi,r),(\tau,s)) &= \int_0^\infty \left(\frac{1}{2\pi i}\int_{\mathscr{L}_L^*} e^{-\frac{1}{3}z^3+(\tau+\lambda)z}\frac{1}{z^s}\,dz\right)\left(\frac{1}{2\pi i}\int_{\mathscr{L}_R^*} e^{\frac{1}{3}w^3-(\xi+\lambda)w}w^r\,dw\right)d\lambda \\ &= \int_0^\infty A_s^-(\tau+\lambda)A_r^+(\xi+\lambda)\,d\lambda,\end{aligned}$$

by (3.3) and (3.4). Here, we also used the fact that since $r \geqslant 0$, we can move $\mathscr{L}_R$ to $\mathscr{L}_R^*$.

In the case (ii) we have $r \geqslant 0$ and $s < 0$, and thus neither $\mathscr{C}_{in}$ nor $\mathscr{C}_{out}$ contribute. Using (3.9) and then moving $\mathscr{L}_L$ to $\mathscr{L}_L^*$ and $\mathscr{L}_R$ to $\mathscr{L}_R^*$, we obtain

$$\begin{aligned}\tilde{\mathcal{K}}_{CA}((\xi,r),(\tau,s)) &= \int_0^\infty \left(\frac{1}{2\pi i}\int_{\mathscr{L}_L^*} e^{-\frac{1}{3}z^3+(\tau+\lambda)z}z^{-s}\,dz\right)\left(\frac{1}{2\pi i}\int_{\mathscr{L}_R^*} e^{\frac{1}{3}w^3-(\xi+\lambda)w}w^r\,dw\right)d\lambda \\ &= (-1)^s\int_0^\infty A_{-s}^+(\tau+\lambda)A_r^+(\xi+\lambda)\,d\lambda.\end{aligned}$$

Next, consider the case (iii). If $r < 0$, $s \geqslant 0$, we can write

$$\begin{aligned}&\int_{\mathscr{L}_L+\mathscr{C}_{out}} dz \int_{\mathscr{L}_R+\mathscr{C}_{in}} dw = \int_{\mathscr{L}_L} dz \int_{\mathscr{L}_R+\mathscr{C}_{in}} dw + \int_{\mathscr{C}_{out}} dz \int_{\mathscr{L}_R+\mathscr{C}_{in}} dw \\ &= \int_{\mathscr{L}_L} dz \int_{\mathscr{L}_R} dw + \int_{\mathscr{C}_{out}} dz \int_{\mathscr{L}_R} dw + \int_{\mathscr{C}_{out}} dz \int_{\mathscr{C}_{in}} dw := I_1 + I_2 + I_3.\end{aligned}$$

Consider first I_1. By (3.4) and (3.8) we get

$$\begin{aligned}I_1 &= \int_0^\infty \left(\frac{1}{2\pi i}\int_{\mathscr{L}_L} e^{-\frac{1}{3}z^3+(\tau+\lambda)z}\frac{1}{z^s}\,dz\right)\left(\frac{1}{2\pi i}\int_{\mathscr{L}_R^*} e^{\frac{1}{3}w^3-(\xi+\lambda)w}\frac{1}{w^{-r}}\,dw\right)d\lambda \\ &= (-1)^s\int_0^\infty A_{-s}^+(\tau+\lambda)A_r^+(\xi+\lambda)\,d\lambda.\end{aligned} \tag{3.10}$$

Since $|w| > |z|$ if $z \in \mathscr{C}_{out}$ and $w \in \mathscr{L}_R$, we can use the identity

$$\frac{1}{w-z} = \sum_{k=0}^\infty \frac{z^k}{w^{k+1}}$$

to see that

$$\begin{aligned}I_2 &= \sum_{k=0}^{s-1}\left(\frac{1}{2\pi i}\int_{\mathscr{C}_{out}} e^{-\frac{1}{3}z^3+\tau z}\frac{1}{z^{s-k}}\,dz\right)\left(\frac{1}{2\pi i}\int_{\mathscr{L}_R} e^{\frac{1}{3}w^3-\xi w}\frac{1}{w^{-r+k+1}}\,dw\right) \\ &= \sum_{k=0}^{s-1} p_{s-k-1}(\tau)\Big((-1)^{-r+k+1}A_{-r+k+1}^-(\xi) + p_{-r+k}(\xi)\Big) \\ &= (-1)^{s-r}\sum_{k=0}^{s-1} p_k(\tau)A_{-r+s-k}^-(\xi) + \sum_{k=0}^{s-1}(-1)^k p_k(\tau)p_{-r+s-1-k}(\xi).\end{aligned} \tag{3.11}$$

If $z \in \mathscr{C}_{out}$ and $w \in \mathscr{C}_{in}$, then

$$\frac{1}{w-z} = -\sum_{k=0}^\infty \frac{w^k}{z^{k+1}}$$

and we see that, by (3.7), and the fact that $\mathscr{C}_{in}$ is negatively oriented, we have

$$I_3 = -\sum_{k=0}^{-r-1} \left(\frac{1}{2\pi i} \int_{\mathscr{C}_{out}} e^{-\frac{1}{3}z^3+\tau z} \frac{1}{z^{s+k+1}}\, dz \right) \left(\frac{1}{2\pi i} \int_{\mathscr{C}_{in}} e^{\frac{1}{3}w^3-\xi w} \frac{1}{w^{-r-k}}\, dw \right)$$
$$= \sum_{k=0}^{-r-1} p_{s+k}(\tau) p_{-r-k-1}(\xi) = \sum_{k=s}^{s-r-1} p_k(\tau) p_{-r+s-1-k}(\xi). \tag{3.12}$$

Adding up (3.10) - (3.12) we have proved (iii). The case (iv) follows from (i) by using Proposition 3.1. □

Note that if we take $r = s \geqslant 0$, then by (i),

$$\mathcal{K}_{CA}((\xi, r), (\tau, s)) = \int_0^\infty A_r^-(\tau + \lambda) A_r^+(\xi + \lambda)\, d\lambda := K^{(r)}(\tau, \xi),$$

which is called the *r-Airy kernel*. Note that when $r = 0$ we get the standard Airy kernel. The r-Airy kernel has appeared previously in the work [3] on largest eigenvalues of sample covariance matrices and in [1] on Dyson's Brownian motion with outliers. See also [2].

Though we do not show it in this paper using the results above and some further estimates it should be possible to prove that the scaling limit of the position of the last (red) particle on line r, close to the cusp point, has the distribution function $F_r(x) = \det(I - K^{(r)})_{L^2(x,\infty)}$. In particular, when $r = 0$ we should get the Tracy-Widom distribution.

Remark 3.1. It is instructive to compare the Cusp-Airy kernel to the GUE-corner kernel. Recall that the GUE-corner kernel is given by

$$K(n, x; n', x') = -1_{n>n'} 1_{x>x'} 2^{n-n'} \frac{(x - x')^{n-n'-1}}{(n - n' - 1)!} + \frac{2}{(2\pi i)^2} \int_{\Gamma_0} dz \int_L \frac{dw}{w - z} \frac{w^{n'}}{z^n} e^{w^2 - z^2 + 2zx - 2wx'}, \tag{3.13}$$

where $x, x' \in \mathbb{R}$ and $n, n' \in \mathbb{Z}$ and $n, n' \geqslant 0$, and where the contours are shown in figure 36.

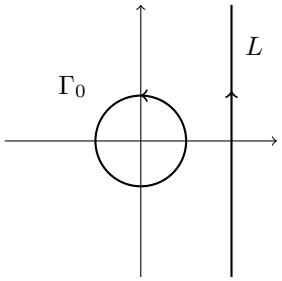

Figure 36: Contours for the GUE-corner kernel.

In a sense, one can regard the Cusp-Airy kernel as a double sided version of the GUE-corner kernel. If one changes the assumption that f'_{t_c} has a simple root at $t_c \in R_1 \bigcup R_2$, then a similar computation as in the Cusp-Airy case will yield the GUE-corner kernel for an appropriate scaling limit of $K_n((x_1^{(n)}, y_1^{(n)}), (x_2^{(n)}, y_2^{(n)}))$.

4 Derivation of the Correlation Kernel

4.1 Integral Representation of the Correlation Kernel for the Yellow Particles

In section A.1 in [8] it was shown that the correlation kernel for the interlacing particle system is given by

$$K_n((x_1,y_1),(x_2,y_2)) = \tilde{K}_n((x_1,y_1),(x_2,y_2)) - \phi^{(n)}_{(y_1,y_2)}(x_1,x_2), \tag{4.1}$$

where

$$\tilde{K}_n((x_1,y_1),(x_2,y_2)) = \frac{(n-y_1)!}{(n-y_2-1)!}\sum_{k=1}^{n} 1_{\beta_k^{(n)}\geqslant x_2} \sum_{l=x_1+y_1-n}^{x_1} \frac{\prod_{j=x_2+y_2-n+1}^{x_2-1}(\beta_k^{(n)}-j)}{\prod_{\substack{j=x_1+y_1-n\\ j\neq l}}^{x_1}(l-j)} \prod_{i\neq k}\frac{l-\beta_i^{(n)}}{\beta_k^{(n)}-\beta_i^{(n)}} \tag{4.2}$$

and

$$\phi^{(n)}_{(y_1,y_2)}(x_1,x_2) = 1_{x_1\geqslant x_2}\frac{(n-y_1)!}{(n-y_2-1)!}\sum_{k=1}^{n}\sum_{l=x_1+y_1-n}^{x_1} \frac{\prod_{j=x_2+y_2-n+1}^{x_2-1}(\beta_k^{(n)}-j)}{\prod_{\substack{j=x_1+y_1-n\\ j\neq l}}^{x_1}(l-j)} \prod_{i\neq k}\frac{l-\beta_i^{(n)}}{\beta_k^{(n)}-\beta_i^{(n)}}. \tag{4.3}$$

To arrive at an integral representation for the correlation kernel we now make use of the following corollary of the residue theorem:

Corollary 4.1. *Let $\Omega \in \mathbb{C}$ be an open simply connected bounded domain with positively oriented boundary Jordan curve γ, then for an analytic function $f(z)$ in Ω, we have for $\{z_1,...,z_n\}\in\Omega$ and $z_i\neq z_j$ if $i\neq j$*

$$\sum_{i=1}^{n} f(z_i)\prod_{\substack{k=1\\ i\neq k}}^{n}\frac{1}{z_i-z_k} = \frac{1}{2\pi i}\oint_{\gamma} f(z)\prod_{i=1}^{n}\frac{1}{z-z_i}dz.$$

Proposition 4.1. *The correlation kernel for the yellow tiles have the following integral representation*

$$\begin{aligned} K^{(n)}_{\mathcal{Y}}((x_1,y_1),(x_2,y_2)) &= 1_{x_1<x_2}\frac{(n-y_1)!}{(n-y_2-1)!}\frac{1}{(2\pi i)^2}\oint_{\mathscr{Z}_n}dz\oint_{\mathscr{W}_n}dw\frac{\prod_{k=x_2+y_2-n+1}^{x_2-1}(z-k)}{\prod_{k=x_1+y_1-n}^{x_1}(w-k)}\frac{1}{w-z}\prod_{i=1}^{n}\left(\frac{w-\beta_i^{(n)}}{z-\beta_i^{(n)}}\right)\\ &\quad - 1_{x_1\geqslant x_2}\frac{(n-y_1)!}{(n-y_2-1)!}\frac{1}{(2\pi i)^2}\oint_{\mathscr{Z}'_n}dz\oint_{\mathscr{W}_n}dw\frac{\prod_{k=x_2+y_2-n+1}^{x_2-1}(z-k)}{\prod_{k=x_1+y_1-n}^{x_1}(w-k)}\frac{1}{w-z}\prod_{i=1}^{n}\left(\frac{w-\beta_i^{(n)}}{z-\beta_i^{(n)}}\right), \end{aligned} \tag{4.4}$$

where $\mathscr{Z}_n$ is a counterclockwise oriented contour containing $\{\beta_j^{(n)}:\beta_j^{(n)}\geqslant x_2\}$ but not the set $\{\beta_j^{(n)}\leqslant x_2-1\}$ and $\mathscr{Z}'_n$ is a counterclockwise oriented contour containing $\{\beta_j^{(n)}:\beta_j^{(n)}<x_2\}$ but not the set $\{\beta_j^{(n)}\geqslant x_2+1\}$, and $\mathscr{W}_n$ contains the set $\{x_1+y_1-n,...,x_1\}$ and $\mathscr{Z}_n$ and $\mathscr{Z}'_n$.

Proof. The correlation kernel for the yellow tiles is the same as that for the interlacing particles, i.e. it is given by (4.1). From (4.1) to (4.3) we see that

$$\begin{aligned} \frac{(n-y_2-1)!}{n-y_1)}K^{(n)}_{\mathcal{Y}}((x_1,y_1),(x_2,y_2)) &= 1_{x_1<x_2}\sum_{k=1}^{n}1_{\beta_k^{(n)}\geqslant x_2}\sum_{l=x_1+y_1-n}^{x_1}\frac{\prod_{j=x_2+y_2-n+1}^{x_2-1}(\beta_k^{(n)}-j)}{\prod_{\substack{j=x_1+y_1-n\\ j\neq l}}^{x_1}(l-j)}\prod_{i\neq k}\frac{l-\beta_i^{(n)}}{\beta_k^{(n)}-\beta_i^{(n)}}\\ &\quad - 1_{x_1\geqslant x_2}\sum_{k=1}^{n}1_{\beta_k^{(n)}<x_2}\sum_{l=x_1+y_1-n}^{x_1}\frac{\prod_{j=x_2+y_2-n+1}^{x_2-1}(\beta_k^{(n)}-j)}{\prod_{\substack{j=x_1+y_1-n\\ j\neq l}}^{x_1}(l-j)}\prod_{i\neq k}\frac{l-\beta_i^{(n)}}{\beta_k^{(n)}-\beta_i^{(n)}}. \end{aligned} \tag{4.5}$$

Consider the first expression in the right hand side of (4.5). Using Corollary 4.1 we can rewrite the l-summation and we find

$$\begin{aligned} &1_{x_1<x_2}\sum_{k=1}^{n}1_{\beta_k^{(n)}\geqslant x_2}\frac{1}{2\pi i}\oint_{\mathscr{W}_n}dw\frac{\prod_{j=x_2+y_2-n+1}^{x_2-1}(\beta_k^{(n)}-j)}{\prod_{j=x_1+y_1-n}^{x_1}(w-j)}\prod_{i\neq k}\frac{w-\beta_i^{(n)}}{\beta_k^{(n)}-\beta_i^{(n)}}\\ &= 1_{x_1<x_2}\sum_{k=1}^{n}1_{\beta_k^{(n)}\geqslant x_2}\frac{1}{2\pi i}\oint_{\mathscr{W}_n}dw\frac{\prod_{j=x_2+y_2-n+1}^{x_2-1}(\beta_k^{(n)}-j)}{\prod_{j=x_1+y_1-n}^{x_1}(w-j)}\frac{1}{w-\beta_k^{(n)}}\frac{\prod_{i=1}^{n}(w-\beta_i^{(n)})}{\prod_{i\neq k}(\beta_k^{(n)}-\beta_i^{(n)})}. \end{aligned}$$

Since the w-contour is outside $\mathscr{Z}_n$ the sum over the $\beta_k^{(n)} \geqslant x_2$ can be rewritten using Corlollary 4.1 and we find

$$1_{x_1<x_2}\frac{1}{(2\pi i)^2}\oint_{\mathscr{W}_n} dw \oint_{\mathscr{Z}_n} dz \frac{\prod_{j=x_2+y_2-n+1}^{x_2-1}(z-j)}{\prod_{j=x_1+y_1-n}^{x_1}(w-j)}\frac{1}{w-z}\frac{\prod_{i=1}^{n}(w-\beta_i^{(n)})}{\prod_{i=1}^{n}(z-\beta_i^{(n)})}.$$

The second expression in the right hand side of (4.5) can be rewritten in exactly the same way and we have proved the proposition.

□

4.2 Particle Transformation

From knowledge of a correlation kernel for the yellow particles we now want to derive an expression for a correlation kernel for the red (and blue) particles.

Lemma 4.1. *Correlation kernels for the red and blue tiles (particles) are given by*

$$K_{\mathcal{R}}^{(n)}((x_1,y_1),(x_2,y_2)) = -K_{\mathcal{Y}}^{(n)}((x_1,y_1),(x_2,y_2-1))$$
$$K_{\mathcal{B}}^{(n)}((x_1,y_1),(x_2,y_2)) = K_{\mathcal{Y}}^{(n)}((x_1,y_1),(x_2+1,y_2-1)).$$

Proof. Let $K_{\mathcal{P}}$ be the Kasteleyn matrix of the adjacency matrix of the honeycomb graph $G_{\mathcal{P}}$ of the polygon $\mathcal{P}$. It is defined according to

$$K_{\mathcal{P}}((x,n);(y,m)) = \begin{cases} 1 & \text{if } (y,m)=(x,n) \\ 1 & \text{if } (y,m)=(x,n-1) \\ 1 & \text{if } (y,m)=(x+1,n-1) \\ 0 & \text{otherwise} \end{cases} \tag{4.6}$$

Recall that if $(y,m)=(x,n)$ we have a yellow particle (rhombi of shape) at position (x,n) in our lattice. Similarly, if $(y,m)=(x,n-1)$ we have a red particle at position (x,n) and if $(y,m)=(x+1,n-1)$ we have a blue particle at position (x,n).

It was shown in [20] Theorem 6.1 that inverse Kasteleyn matrix $K_{\mathcal{P}}^{-1}$ is related to the correlation kernel of the yellow particles $K_{\mathcal{Y}}$ according to

$$K_{\mathcal{P}}^{-1}((y,m);(x,n)) = (-1)^{y-x+m-n}K_{\mathcal{Y}}^{(n)}(x,n;y,m). \tag{4.7}$$

From Corollary 3 in [15] one has that the probability of finding a set of edges $\{b_1w_1,...b_kw_k\}$ is given by

$$\mathbb{P}[\text{edges at } \{w_1b_1,...,w_kb_k\}] = \left(\prod_i^k K_{\mathcal{P}}(w_i,b_i)\right)\det(K_{\mathcal{P}}^{-1}(b_i,w_j))_{i,j}^k$$

Now finding k red particles at positions $\{(x_i,n_i)\}_{i=1}^k$ is equivalent to finding the edges $\{((x_i,n_i),(x_i,n_i-1))\}_{i=1}^k$ Hence, the probability of finding k red particles at positions $\{(x_i,n_i)\}_{i=1}^k$ equals

$$\begin{aligned}\mathbb{P}[\text{red particles at positions } \{(x_i,n_i)\}_{i=1}^k] &= \mathbb{P}[\text{edges at positions } \{((x_i,n_i),(x_i,n_i-1))\}_{i=1}^k] \\ &= \det(K_{\mathcal{P}}^{-1}((x_i,n_i-1),(x_j,n_j))_{i,j}^k \\ &= \det((-1)^{x_i-x_j+n_i-n_j+1}K_{\mathcal{Y}}^{(n)}(x_j,n_j;x_i,n_i-1))_{i,j}^k \\ &= \det(-K_{\mathcal{Y}}^{(n)}(x_i,n_i;x_j,n_j-1))_{i,j}^k\end{aligned}$$

However, by definition

$$\begin{aligned}\rho_{\mathcal{R}}((x_1,n_1),(x_2,n_2),...,(x_k,n_k)) &= \mathbb{P}[\text{red particles at positions } \{(x_i,n_i)\}_{i=1}^k] \\ &= \det(K_{\mathcal{R}}^{(n)}(x_i,n_i;y_j,n_j))_{1\leqslant i,j\leqslant k}\end{aligned}$$

Hence, we find that as a correlation kernel for the red particles we can take

$$K_{\mathcal{R}}^{(n)}(x_i, n_i; y_j, n_j) = -K_{\mathcal{Y}}^{(n)}(x_i, n_i; x_j, n_j - 1).$$

Similarly, for the blue particles we can take

$$K_{\mathcal{B}}^{(n)}(x_i, n_i; y_j, n_j) = K_{\mathcal{Y}}^{(n)}(x_i, n_i; x_j + 1, n_j - 1).$$

This concludes the proof. □

We can now prove Proposition 1.1. Combining Lemma 4.1 with (4.4) we see that a correlation kernel for the red particles is given by

$$\begin{aligned} &- 1_{x_1<x_2} \frac{(n-y_1)!}{(n-y_2)!} \frac{1}{(2\pi i)^2} \oint_{\mathscr{Z}_n} dz \oint_{\mathscr{W}_n} dw \frac{\prod_{k=x_2+y_2-n}^{x_2-1}(z-k)}{\prod_{k=x_1+y_1-n}^{x_1}(w-k)} \frac{1}{w-z} \prod_{i=1}^{n} \left(\frac{w-\beta_i^{(n)}}{z-\beta_i^{(n)}} \right) \\ &+ 1_{x_1 \geqslant x_2} \frac{(n-y_1)!}{(n-y_2)!} \frac{1}{(2\pi i)^2} \oint_{\mathscr{Z}_n'} dz \oint_{\mathscr{W}_n} dw \frac{\prod_{k=x_2+y_2-n}^{x_2-1}(z-k)}{\prod_{k=x_1+y_1-n}^{x_1}(w-k)} \frac{1}{w-z} \prod_{i=1}^{n} \left(\frac{w-\beta_i^{(n)}}{z-\beta_i^{(n)}} \right) \end{aligned} \tag{4.8}$$

We can remove the prefactor $\frac{(n-y_1)!}{(n-y_2)!}$ since it cancels in the determinantal expression for the correlation functions. This proves Proposition 1.1.

5 Appendix. Determinantal Point Processes

In this appendix we give a brief introduction to determinantal random point processes that suffices for our purposes. See e.g. [13], for a more complete treatment.

Let Λ be a Polish space. Fix $N \in \mathbb{N} \cup \{\infty\}$ and $Y \subset \Lambda^N$, a space of configurations of N-particles of Λ. Denote each $y \in Y$ as $y = (y_1, \ldots, y_N)$. Assume, for all $y \in Y$ and compact Borel sets $B \subset \Lambda$, that the number of particles from y contained in B is finite, i.e., $\#\{y_i \in B\} < \infty$. Let $\mathcal{F}$ be the sigma-algebra generated by sets of the form $\{y \in Y : \#\{y_i \in B\} = m\}$ for all $m \leqslant N$ and Borel sets $B \subset \Lambda$. A probability space of the form $(Y, \mathcal{F}, \mathbb{P})$ is referred to as a *random point process*.

Given such a process, $m \leqslant N$, and $B \subset \Lambda^m$, define $N_B^m : Y \to \mathbb{N}$ by,

$$N_B^m(y) := \#\{(y_{i_1}, \ldots, y_{i_m}) \in B : i_1 \neq \cdots \neq i_m\},$$

for all $y \in Y$. In words, $N_B^m(y)$ is the number of distinct m-tuples of particles from y that are contained in B. Then define a measure on Λ^m by $B \mapsto \mathbb{E}[N_B^m]$ for all Borel subsets $B \subset \Lambda^m$. Assume that this is well-defined and finite whenever B is bounded. Then, given a reference measure λ on Λ, the density of the above measure with respect to λ^m, whenever it exists, is referred to as the m^{th} *correlation function*, ρ_m. That is,

$$\int_B \rho_m(x_1, \ldots, x_m) d\lambda[x_1] \ldots d\lambda[x_m] = \mathbb{E}[N_B^m],$$

for all Borel subset $B \subset \Lambda^m$.

A random point process is called *determinantal* if all correlation functions exist and there exists a function $K : \Lambda^2 \to \mathbb{C}$ for which

$$\rho_m(x_1, \ldots, x_m) = \det[K(x_i, x_j)]_{i,j=1}^m,$$

for all $x_1, \ldots, x_m \in \Lambda$ and $m \leqslant N$. K is called the *correlation kernel* of the process. Note, correlation kernels are not unique. For example, when $\Lambda = \mathbb{R}$, a new kernel $J : \mathbb{R}^2 \to \mathbb{C}$ can be defined by $J(u, v) := \frac{w(u)}{w(v)} K(u, v)$ for all $u, v \in \mathbb{R}$, where w is any non-zero complex function. Also, kernels can be viewed as integral operators on $L^2(\Lambda)$ by the relation,

$$Kf(u) := \int K(u, v) f(v) d\lambda[v],$$

whenever the right hand side is well-defined.

Finally consider a measurable function $\phi : \Lambda \to \mathbb{C}$ with bounded support, B, for which

$$\sum_{n=0}^{\infty} \frac{\|\phi\|_{\infty}^{n}}{n!} \int_{B^n} \det[K(x_i, x_j)]_{i,j=1}^{n} d\lambda[x_1] \dots d\lambda[x_n] < \infty.$$

Proposition 2.2 of [13], then gives,

$$\mathbb{E}[\prod_{j}(1 - \phi(x_j))] = \sum_{n=0}^{\infty} \frac{(-1)^n}{n!} \int_{B^n} \prod_{j=1}^{n} \phi(x_j) \det[K(x_i, x_j)]_{i,j=1}^{n} d\lambda[x_1] \dots d\lambda[x_n].$$

This quantity is referred to as the *Fredholm determinant*, denoted $\det[I - \phi K]_{L^2(B)}$.

References

[1] M. Adler, J. Delpine and P. van Moerbecke, Dyson's Nonintersecting Brownian Motions with a Few Outliers. *Communications on Pure and Applied Mathematics* 62 (2009), no. 3, 334–395

[2] J. Baik, Painlevé formulas of the limiting distributions for nonnull complex sample covariance matrices. *Duke Math. J.* 133 (2006), no. 2, 205–235.

[3] J. Baik, G. Ben Arous and S. Péché, Phase transition of the largest eigenvalue for non-null complex sample covariance matrices. *Ann. Probab.* 33 (2005), no. 5, 1643–1697

[4] J. Baik, T. Kriecherbauer, K.D.T-R. McLaughlin and P.D. Miller, Discrete Orthogonal Polynomials: Asymptotics and Applications. *Annals of Mathematics Studies* Princeton University Press, Princeton, NJ, 2007

[5] A. Borodin, V. Gorin and A. Guionnet, Gaussian asymptotics of discrete β-ensembles . arXiv:1505-03760v1

[6] J. Breuer and M. Duits, The Nevai condition and a local law of large numbers for orthogonal polynomial ensembles. *Adv. Math.* 265 (2014), 441–484

[7] P.D. Dragnev and E.B. Saff, Constrained Energy Problems with Applications to Orthogonal Polynomials of a Discrete Variable. *J. Anal. Math.* 72 (1997), 223–259

[8] E. Duse and A. Metcalfe, Asymptotic geometry of discrete interlaced patterns: Part I. arXiv: 1412.6653

[9] E. Duse and A. Metcalfe, Universal edge fluctuations of discrete interlaced particle systems. (In preparation).

[10] E. Duse, Constrained Equilibrium Measure in External Fields and Lozenge Tiling Models. (In preparation).

[11] D. Féral, On large deviations for the spectral measure of discrete Coulomb gas. *Séminaire de probabilités XLI, 19–49, Lecture Notes in Math.* 1934, Springer, Berlin, 2008

[12] K. Johansson, Discrete polynuclear growth and determinantal processes. *Communications in Mathematical Physics.* 242 (2003) 277–329.

[13] K. Johansson, Random matrices and determinantal processes. *Math. Stat. Phy, Session LXXXIII: Lecture Notes of the Les Houches Summer School, Elsevier Science.* Elsevier B. V., Amsterdam, 2006

[14] A. Metcalfe, Universality properties of Gelfand-Tsetlin patterns. *Probability Theory and Related Fields.* (2013), no. 1-2, 303–346

[15] R. Kenyon, Lectures on dimers. Statistical mechanics, 191–230, *IAS/Park City Math. Ser.*, 16, Amer. Math. Soc., Providence, RI, 2009.

[16] R. Kenyon and A. Okounkov, What is ... a dimer? *Notices Amer. Math. Soc.* 52 (2005), no. 3, 342–343

[17] R. Kenyon and A. Okounkov, Limit shapes and the complex Burgers equation. *Acta Mathematica.* 199,2 (2007) 263–302

[18] A. Okounkov and N. Reshetikhin, The birth of a random matrix. *Mosc. Math. J.* 6 (2006), no. 3, 553–566

[19] A. Okounkov and N. Reshetikhin, Random skew plane partitions and the Pearcey Process. *Comm. Math. Phys.* 269 (2007), no. 3, 571–609

[20] L. Petrov, Asymptotics of Random Lozenge Tilings via Gelfand-Tsetlin Schemes. *Probab. Theory Related Fields* 160 (2014), no. 3-4, 429–487

[21] L. Petrov, Asymptotics of uniformly random lozenge tilings of polygons. Gaussian free field. *Annals of Probability* Vol. 43 (2015), No. 1, 1–43.

[22] T. Ransford, Potential Theory in the Complex Plane. *London Mathematical Society Student Texts, 28* Cambridge University Press, Cambridge, 1995

[23] R. Remmert, Classical topics in complex function theory. *Graduate Texts in Mathematics* 172. Springer-Verlag, New York, 1998

[24] H. Weyl, The Classical Groups, Their Invariants and Representations. Princeton University Press, Princeton, NJ, 1997

Erik Duse, Department of Mathematics, KTH Royal Institute of Technology, Stockholm, Sweden, duse@kth.se

Kurt Johansson, Department of Mathematics, KTH Royal Institute of Technology, Stockholm, Sweden, kurtj@kth.se

Anthony Metcalfe, Department of Mathematics, Uppsala University, Uppsala, Sweden, anthony.metcalfe@math.uu.se